2011

Characterization Of Nanoparticle-Induced Airway Oxidant Stress And The Antioxidant Effects Of Sorrel (Hibiscus Sabdariffa): An Omics Approach

Christa Young Watson
North Carolina Agricultural and Technical State University

Characterization of Nanoparticle-Induced Airway Oxidant Stress and the Antioxidant Effects of Sorrel *(Hibiscus Sabdariffa*): An Omics Approach

Christa Young Watson

North Carolina Agricultural and Technical State University

A dissertation submitted to the graduate faculty

in partial fulfillment of the requirements for the degree of

DOCTOR OF PHILOSOPHY

Department: Energy & Environmental Systems

Major: Energy and Environmental Systems

Major Professor: Dr. Jenora T. Waterman

Greensboro, North Carolina

2011

School of Graduate Studies
North Carolina Agricultural and Technical State University

This is to certify that the Doctoral Dissertation of

Christa Young Watson

has met the dissertation requirements of
North Carolina Agricultural and Technical State University

Greensboro, North Carolina
2011

Approved by:

Jenora T. Waterman, Ph.D. Major Professor	Leonard L. Williams, Ph.D. Committee Member
Radiah C. Minor, Ph.D. Committee Member	Stephanie Luster-Teasley, Ph.D. Committee Member
Keith A. Schimmel, Ph.D. Department Chairperson	Sanjiv Sarin, Ph.D. Associate Vice Chancellor for Research and Graduate Dean

Biographical Sketch

Christa Young Watson was born February 3, 1977 in Memphis, Tennessee. She received her bachelor's of science in Biology from North Carolina A&T State University in 1999. After a brief stint in industry, Christa went back to graduate school in 2002 and completed her Master of Science degree in Biology, magna cum laude, from North Carolina A&T State University in 2004. She is a candidate for the Doctorate in Energy and Environmental Systems. Christa is a 2010-2011 Kannapolis Scholar and a 2011 American Thoracic Society Minority Trainee Travel Award recipient. Additionally, she is a National Science Foundation Engineering Research Center Revolutionizing Metallic Biomaterials (NSF-ERC-RMB) research fellow.

Acknowledgments

I would like to give thanks to my Lord and Savior, Jesus Christ, without Him I am nothing, but with Him I can do all things. Also, I give many thanks to my advisor, Jenora Waterman, for her guidance, persistence, and encouragement throughout this journey. Additionally, I would to thank my program director, Keith Schimmel for all his support and assistance in the Energy and Environmental Systems Program. Also, I would like to thank Dr. Minnie Holmes-McNary for her kindness and inspiration. This dissertation is dedicated to my mother and daughter, who kept me strong and loved me through all my trials and tribulations. To the love of my life, William T. Wright, thank you for being there for me throughout this process.

Table of Contents

List of Figures

List of Tables

List of Abbreviations

DE	Dust Extract
SE	Sorrel Extract
LPS	Lipopolysaccharide
NF- κB	Nuclear Factor kappa B
RPM	Revolutions per Minute
iNOS	inducible Nitric Oxide Synthase
COX-2	Cyclooxygenase-2
DUOX2	Dual Oxidase 2
GPX-2	Glutathione Peroxidase 2
Phospho-IκB	Phosphorylated Inhibitor kappa B
RT-PCR	Reverse Transcriptase- Polymerase Chain Reaction
TBS-T	Tris Buffered Saline-Tween
Kb	kilobases
kDa	kilodaltons
ECL	Enhanced Chemiluminescence
SDS-PAGE	Sodium Dodecyl Sulfate Polyacrylamide Gel Electrophoresis
κ	kappa
NHBE	Normal Human Bronchial Epithelial Cells
PTBE	Porcine Tracheobronchial Epithelial Cells
BPE	Bovine pituitary extract
ml	milliliter
µl	microliter

PBS	Phosphate Buffered Saline
hEGF	Human Epidermal Growth Factor
TGX	Tris Glycine
BEBM	Bronchial Epithelial Basal Media
DMEM	Dulbecco's Minimal Essential Media

Abstract

Nanotoxicology is the study of the potential toxic effects of anthropogenic and biogenic nanostructures on living organisms. The influence of nanostructures such as nanoparticles on the human airway has gained interest due to increased susceptibility of translocation into other regions of the body. Adverse effects such as oxidative stress and inflammation have been found after the inhalation of airborne nanoparticles in airway epithelial cells. Oxidative stress and inflammation in mice models have been attenuated through the consumption of antioxidant containing plant compounds called phytochemicals. In this dissertation, we have evaluated the hypothesis that nanoparticles regardless of origin can elicit oxidative stress and inflammation; however sorrel (*Hibiscus sabdariffa*) extract (rich in antioxidants) can minimize these effects. This study investigated markers of oxidative stress and inflammation through proteomic, genomic, and cytokine profile analyses following anthropogenic and biogenic nanoparticle exposure *in vitro* and the level of cellular response from antioxidant treatments. The overall goal of this study was to perform a comprehensive analysis of the molecular alterations mediated by nanoparticles on the human airway epithelium and substantiate a novel therapeutic antioxidant treatment. Results revealed that swine confinement facility dust upregulated expression of pro-inflammatory mediator genes in NHBE cells such as prostaglandin endoperoxide synthase 2 or COX-2 after 4hrs of exposure. Each of these genes was validated with Western blot immunoassay. Antioxidant treatments of sorrel (*Hibiscus sabdariffa*) attenuated the expression of GPX-2, PTGS2 or COX-2, and DUOX1 genes at 4hrs and 24hrs. In regards to the effect of magnesium biomaterials on normal human bronchial epithelial cells, no significant modulation of pro-inflammatory mediators such as COX-2 on IκBα were found in genomic profile or proteomic analysis using qPCR and Western blot respectively. Additionally, mucin and cytokine

production were unaffected and cell migration was enhanced by magnesium wire exposure for 24hr. Cellular assays of osteoblasts exposed to varying concentrations of different hydrophilic nanoclays induced high levels of cytotoxicity and interfered with the catalytic properties of assay reagents. Thus, nanoparticles from biogenic origins induced oxidative stress and inflammation in airway epithelium and anthropogenic nanoparticles imposed high cytotoxicity; however magnesium biomaterials did not encourage oxidative damage.

CHAPTER 1

Literature Review

1.1. Introduction

Respirable particles of either biogenic (natural) or anthropogenic (man-made) origin have become a major concern and health risk to our society. Individuals may be exposed to respirable nanoparticles in occupational settings from sources such as agricultural dusts, fossil fuel combustion and laboratory/industrial synthesis reactions. These respirable nanoparticles, with sizes ranging from 100nm to 1μm in diameter, have the ability to absorb in the upper, middle, and lower respiratory tract through particle deposition and Brownian diffusion; processes which depend upon various factors such as particle size, breathing force, and the structure of the lung (Hagens, 2007). Inhalation and absorption of biogenic or anthropogenic nanoparticles may ultimately lead to distribution to various organs and tissues through systemic circulation Studies have shown that these "environmental stressors" induce systemic oxidative stress and inflammation in the airways (Gomez-Mejiba, 2009). It has been well documented that oxidative stress occurring from exposure to nanoparticles stems from the overproduction of endogenous reactive oxygen species (ROS) and weakening of innate antioxidant defenses such as glutathione (Li, 2008). Further, the inadequate elimination of nanoparticles within the airway due to deposition produces chronic inflammation; which can lead to formation of granulomas, fibrosis, bronchial smooth muscle hypertrophy, and bronchoconstriction (Schluger, 2005). These previously mentioned conditions can induce tissue damage and airway remodeling, goblet cell metaplasia, mucus hypersecretion, loss of mucocillary clearance function. Thus, studies have shown that these occurrences are the precursors of respiratory diseases such as chronic obstructive pulmonary disease (COPD), and asthma, possibly even cancer (Robbins, 2010).

A number of studies have suggested that the aforementioned diseases and ailments are also influenced by dietary factors. Additionally in epidemiological studies, westernized diets consisting of high animal fat and protein were found to be detrimental to respiratory health (Woods &Gibson, 2009). For example, diets associated with high fat content found in fast foods and low in antioxidants, have been shown to increase asthma risk in children (Wickens, 2005). The consumption of foods high in antioxidants can provide reactive oxygen species scavenging thereby reducing oxidative stress and inhibiting inflammatory pathways found in chronic illnesses (Wood & Gibson, 2009). Fruits and vegetables possess abundant sources of antioxidants in the form of naturally occurring chemicals found in plants called phytochemicals. Phytochemicals impart color to fruits and vegetables as well as provide protection against insect attacks and plant diseases. When consumed by humans, phytochemicals such α-tocopherol or vitamin E have been found to prevent lipid peroxidation, a form of oxidative stress, by deactivating lipid peroxyl radicals (Mezzetti, 1995). Ascorbic acid or vitamin C also possess antioxidant properties by accepting free radical electrons, scavenging reactive oxygen species (ROS), reactive nitrous species (RNS), and regenerating other antioxidants such as uric acid and α-tocopherol. Thus, phytochemicals have the ability to prevent the overproduction of ROS thereby enhancing the endogenous oxidant defenses present in the airway by attenuating imbalances between antioxidants and oxidants (Essa, 2007).

Therefore, our central hypothesis is respirable nanoparticles elicit airway inflammation and oxidant stress, however phytochemicals can minimize these effects. The goal of this dissertation was to identify and quantify proteins, genes, and cytokines differentially expressed in airway epithelial cells after anthropogenic or biogenic nanoparticle exposure and determine if a novel source of antioxidants can be used as a therapeutic treatment to reduce said effects.

1.2. Anthropogenic Nanoparticles

Advances in technology and industry such as the evolution of the automobile, fossil fuel combustion, modernization of agriculture practices and increased manufacturing facilities have introduced pollutants such as particulate matter into our environment which have resulted in a decrease in our overall health and increased mortality rates (Radomski, 2007). Recently, the Environmental Protection Agency (EPA) declared that the "inhalation of fine particles is causally associated with premature death at concentrations near those experienced by most Americans on a daily basis" (EPA, 2009). Fine particles originating from biogenic and anthropogenic sources are a growing concern in regards to toxicity. In the last twenty years, new forms of engineered fine particles or nanoparticles have been included in this concern, as it remains unclear as to what threat these novel materials pose to our society. It is evident that the progression of technology brings about many advantages, but what will be the price for nanotechnology?

Nanotechnology has been defined by the United States Nanotechnology Initiative as the "understanding and control of matter at dimensions of 1-100 nanometers, where unique phenomena enable novel applications." Nanotechnology is a burgeoning realm in science that is making vast breakthroughs in medicine, industry, and commercial applications. These materials, commonly known as nanomaterials possess unique and attractive features, which are attributed to higher surface area to mass ratios as well as increased reactive sites on the surface. These properties can alter chemical reactivity, thermal and electrical conductivity, tensile strength, and change optical, magnetic, and electrical behavior (Owen & Depledge, 2005). Nanomaterials such as nanoparticles can be classified as either intentional or unintentional nanoparticles. Unintentional man-made nanoparticles are those produced as a consequence of different processes such as combustion, welding, cooking, or burning materials. Intentional nanoparticles

or engineered nanoparticles have a controlled shape and size, and are designed for functionality and applied uses. Applications in diagnostics and therapeutics have made intentional nanoparticles very useful in the development of lung disease treatments, due to their high retention rates in lung tissue. For example, Zara and coworkers studied the pharmacokinetics of doxorubicin loaded solid lipid nanoparticles after intravenous injection and compared the results with a doxorubicin solution (Zara, 2002). That study showed that the drug concentration in the lungs was higher in animals treated with doxorubicin nanoparticles compared to the doxorubicin solution. Nanoparticles have also been studied in pulmonary instillation evaluations in which dogs were instilled with iodinated nanoparticles intrabronichially. Their results showed that iodinated nanoparticles instilled into the small airways were transported to the tracheobronchial lymph nodes, where they resulted in higher imaging capabilities (Azarmi, 2008). Nanoparticles can also function as signal transducers in which the presence and location of these particles lead to changes in a biological system, thus creating a measureable signal. The use of nanoparticles in such a manner has provided an alternative to tagging biological samples thus providing a more cost efficient and productive means of testing. In short, the world of nanotechnology has revolutionized how we investigate and quantitate biological systems. However, introducing these particles into biological systems may pose some issues in the long run.

1.3. Biogenic Nanoparticles—Swine Confinement Facility Dusts

Naturally occurring or biogenic nanoparticles, also known as ultrafine particles, have been present in the ambient air since the evolution of man (Oberdorster, 2005). The origins of these nanoparticles have various sources such as gas to particle conversions, forest fires, volcanoes, biogenic magnetite, ferritin, and microparticles. In relationship to this study, another source of ultrafine particles has been correlated to dust generated from agricultural production

and operation. Studies have shown that exposure to organic dust stemming from the agricultural industry results in significant airway disease and lung function decline (Jill, 2007). More specifically, the dust associated with the swine production industry has been found to be harmful to swine workers and to pigs (Gerald, 2010; Hartung, 2003). The swine production industry utilizes two distinct swine management methods; confinement and pasture raising (Lebret, 2006). Swine confinement facilities provide higher efficiency in swine production than pasture raising, however this form of swine management has definite drawbacks. Due to the high number of swine and inadequate ventilation found in swine confinement facilities, high amounts of particulate matter or dust are commonly found (Gerald, 2010). This dust can contain endotoxins, food particles, epithelial cells, animal feces, fungi, ammonia gases, and chemicals such as disinfectants and pesticides (Nowak, 2007). Bioaerosols of these complex mixtures can be passively or actively released into the air due to swine housing sanitation levels and meteorological conditions (Singh, 2005). Airborne particulate matter or ultrafine particles generated from these swine confinement facilities could have a direct effect on the health of human caretakers, swine, and communities located near these facilities as these particles can be transmitted great distances through the air (Von Essen, 2005).

1.4 Respiratory Toxicity Induced by Anthropogenic and Biogenic Nanoparticles

As mentioned earlier, ultrafine particles, whether originating from biogenic or anthropogenic sources have been determined to cause serious health problems (Bystrzejewska-Piotrowska, 2009). In relation to the engineered nanoparticles, the properties that provide many of the advantages such as size, solubility, and large surface area, also are responsible for the potential health hazards (Sanvicens, 2008). These characteristics have been found to have a definite relationship in the level of toxicity imposed on cells, more specifically cells within the

airway. The fabrication and mass production of nanoparticles for commercial and research applications have resulted in increased occurrences of occupational and environmental exposures. About 1000 tons of nanomaterials were produced in 2004 (Maynard, 2006). Currently, there is an estimated 800 products containing nanomaterials on the market (Maynard, 2006). Increased use and production of these materials enhances the possibility of exposure at the cellular level.

Possible routes of exposure include inhalation of airborne nanoparticles, ingestion, dermal penetration, and injection of engineered nanoparticles (Choi, 2009). Airborne nanoparticles or particulate matter less than100nm in diameter can originate from various sources including combustion of fossil fuels, automobile exhaust, forest fires, aerosols and dust. Research has shown that due to the aerodynamic nature of particulate matter less than 100nm in size, there is a high probability of penetration and deposition of these particles into the lungs. Data from experimental and epidemiological studies show a correlation between nanosized particulate matter and the occurrence of asthma, chronic obstructive pulmonary disease, and cystic fibrosis (Carsten Schleh, 2009). In relationship, a recent study found a pro-inflammatory response after an exposure to bovine serum albumin coated 25nm gold nanoparticles in an epithelial airway model (Rothen-Rutishauser, 2007). Murine lungs exposed to titanium dioxide nanoparticles showed significant changes in morphology and histology including disruption of the alveolar septa, alveolar enlargement, type II pneumocyte proliferation, increased alveolar epithelial thickness, and the accumulation of particle-laden macrophages by a single instillation of titanium dioxide nanoparticles (Chen, 2006). In a separate inhalation study, the total number of macrophages was found to be significantly increased in the bronchoalveolar lavage (BAL) fluid collected from the treated mice (Grassian, 2007). Exposure to nanoparticles such as

titianium dioxide has also been found to induce cytotoxicity, oxidative stress, lung inflammation, cell proliferation, and histopathological responses (Park, 2009). Also pulmonary animal toxicity assessments of nickel oxide nanoparticle exposure are linked to the development of lung cancer, acute lung injury and inflammation (Oyabu, 2007). The use of the lactate dehydrogenase assay (LDH) is readily used to assess the cytotoxicity of nanoparticles. For example, in a study conducted on human lung epithelial cell line, 16HEB14o, LDH release analysis determined that polyalkylcyanoacrylate nanoparticles induced cytotoxicity. Hillegass and coworkers also routinely use the LDH assay in *in vitro* studies and on broncheolavage specimens to determine the amount of cytotoxicity following asbestos exposure (Hillegass, 2009). In a recent review article in which methods for evaluating the toxicity of nanomaterials on epithelium were discussed, the LDH cytotoxicity assay along with genomic and proteomic analysis were regarded as efficient and necessary assessments for determining the effects of nanoparticle exposure (Oberdorster, 2005).

1.5. Airway Inflammation

During respiration, environmental pollutants such as particulate matter comprised of carbon particles, spores, animal dander, and dusts enter into our bodies (Nel, 2005). Particles larger than 10μm are removed through mucociliary clearance and or phagocytosis, however smaller particles can travel freely within the airways which can result in alveolar deposition. This alveolar deposition is highly susceptible to initiate redox reactions with endogenous reactive constituents such as polyunsaturated fats, metals (i.e. iron), oxygen and inflammatory cells. These redox reactions are the precursors to inflammation. The primary objective of inflammation is to protect the host from infection and promote tissue repair. There are two main categories of inflammation—acute and chronic. Acute inflammation is usually immediate and short in

duration. Indicators of acute inflammation are the influx of neutrophils to the site of inflammation and swelling. If the acute inflammation is successful in eliminating the foreign components, the process subsides. However, in the event that the response is unable to eradicate the infection the inflammation progresses to chronic. Chronic inflammation is characterized by the presence of lymphocytes and macrophages, blood vessel proliferation, fibrosis and tissue destruction (Robbins, 2010).

Some common airway diseases associated with chronic inflammation are asthma and chronic bronchitis. Both of these airway diseases are governed by a host of mediators called chemokines and cytokines that are triggered by the inhalation of environmental stressors. For example in correlation to our proposed study, it is generally accepted that swine confinement workers have increased risks for developing respiratory tract diseases (Romberger, 2002). More importantly, workers exposed acutely to swine confinement facilities have airway inflammation characterized by neutrophilia and an increase in pro-inflammatory cytokines such as interleukin (IL)-8 and IL-6. Interleukin-8 is a potent attractor of inflammatory cells such as neutrophils and eosinophils to the airways (Thacker, 2006). Secreted by the airway epithelial cells, IL-8 is also used as a biomarker of environmentally induced pulmonary inflammation (Strieter, 2002). The expression of IL-8 is increased in airway epithelial cells exposed to hog barn dust (Wyatt, 2007) as well as bronchial biopsies from human subjects exposed to diesel exhaust particles or DEP (Inoue, 2010). More definitively in relationship to anthropogenic nanoparticles, gene expression analysis indicated that C-60 fullerenes induced the up-regulation of genes associated with inflammatory response, oxidative stress, apoptosis, and metalloendopeptidase activity after 1month post-inhalation exposure (Fujita, 2009). One of the main objectives in this proposed study is to elucidate the roles that important cytokines such as IL-6, IL-8, and IL-13 play in

inflammatory response initiated by inhalation of biogenic and anthropogenic nanoparticles. Additionally, characterizing proteins that are expressed differentially from the exposure of nanoparticles is essential to the validation of this study. In parallel, genomic profile analysis were performed to assess genes that are upregulated in response to nanoparticle exposure and to confirm our hypothesis that nanoparticles regardless of origin can elicit inflammatory response within the airway epithelium.

1.6. Proteomics

The science of proteomics involves the large-scale study of all proteins produced by the cell and the organism under specific conditions. Proteomics may be applied in the identification of proteins in the body and determination of their roles in physiological and pathophysiological functions. The field of proteomics has grown tremendously since the completion of the Human Genome Project. The interest in the protein compliment of the human organism has provided the momentum necessary to develop this burgeoning area of research at an astounding rate. The proteome, a term coined by a doctoral student in 1994, is unlike the genome in that proteins in any particular cell are subject to change dramatically as genes are turned on and off in response to the environment. The structure of the proteome is far more complicated than the genome. There are 30,000 to 40,000 potential genes encoding for 40,000 possible proteins in the human genome. RNA splicing and post translational modifications can increase the number of possible proteins to 2,000,000 (Kosak, 2004). To grasp the complexity of the proteome, an array of techniques has been developed.

Proteomics can be subdivided into two areas—qualitative and quantitative. Qualitative proteomics is a relative study of how protein patterns differ from control and experimental samples. The exact amount of how much the protein patterns differ are not determined but more

so examined. Gel electrophoresis is used to separate out the proteins based on molecular weight and silver or Coomassie stains are utilized to stain the differentiated proteins. Although this method clearly allows the observation of protein abundances, poor reproducibility plagues this technique. Thus, a more efficient and precise method of analyzing proteins has been created within quantitative proteomics.

Quantitative proteomics serves to not only distinguish proteins and visualize abundances but to quantitate the amounts of protein. This promising form of proteomics offers a wide range of techniques to determine accurate and reproducible quantification of proteins relative to each other. One method, difference gel electrophoresis (DIGE), utilizes fluorescent dyes for labeling in order to identify individual proteins. Cy-dyes are fluorescent tags that are designed to match each other in molecular weight and charge. Varying amounts of these dyes are combined to equal amounts of protein and consequently separated out on a two dimensional gel. The excitation and emission of the dyes allows for imaging of the fluorescently tagged proteins. This form of proteomic analysis was performed by Yang and coworkers to ascertain the protein altering potential of SiO_2 nanoparticle exposure on human epidermal kerotinocyte cell line HaCaT. The results from that study indicated that 16 proteins involved in oxidative stress, cytoskeleton development, molecular chaperones metabolism, apoptosis, and tumor regulation were differentially expressed by SiO_2 nanoparticles exposure.

In the past few years, these three prominent techniques have been combined with mass spectrometry to provide high throughput analysis of protein samples. In an experiment involving liquid chromatography tandem mass spectrometry (LC/MS-MS), an initial survey scan of a protein sample is performed, followed by three or four subsequent product ion scans, where the peptides from this sample are sequenced. However, the mass spectrometry approach to

quantitative proteomics provides good quantitative data in comparison to other proteomic approaches such as protein microarrays (Ong , 2003). Thus the unique applications of this field are ideal tools for characterizing the global effects of nanoparticles on the airway epithelium.

1.7. Antioxidant Treatments for Inflammation and Associated Ailments

In addition to understanding the effects of nanoparticle exposure on the human airways, we also intended to evaluate novel alternative therapeutic treatments to attenuate oxidative stress caused by nanoparticle exposure. Research has shown that oxidative stress is involved in the pathogenesis of airway obstructive diseases such as asthma and exposure to particulate matter enhances these occurrences as well as increases morbidity (EPA, 2009). One approach to combat oxidative stress would be to utilize antioxidant intervention. Considered to be an alternative or complementary therapy to traditional asthma medications, antioxidant treatment could be performed by increasing the endogenous antioxidant enzyme defenses or by enhancing the non-enzymatic defenses through dietary or pharmacological means (Kirkham, 2006). Several non-enzymatic antioxidant species exist within the lung including glutathione, ascorbic acid (vitamin C), uric acid, a-tocopherol (vitamin E), and albumin (Kirkham, 2006). In response to oxidative stress and inflammation the upregulation of protective antioxidant genes such as glutathione can be found. Research has shown that in both asthmatics and patients with COPD, glutathione is increased in the epithelial lining (Harju, 2007). The lung's enzymatic defenses are enzymes such as glutathione S transferase (GST), superoxide dismutase, and catalase. These enzymes work to neutralize and chemically detoxify free radical attacks on tissue. However, studies have revealed the levels of endogenous antioxidant defenses are altered in asthmatics (Kirkham, 2006).

Magnesium has been evaluated as a treatment for asthma due to the fact that asthmatics often have lower levels of magnesium. Some studies have shown that intravenous magnesium

can be an effective as an emergency treatment for asthma attacks (Mohammed, 2007). Moreover, inhaled magnesium has been shown to provide a mild broncho-protective effect for asthmatic patients (Grisanti, 2006). Epidemological studies have proven that high intake of food rich in antioxidants is related to higher FEV1 and forced vital capacity values, less frequent and milder asthmatic symptoms, and a lower incidence of asthma (Kirkham, 2006). Furthermore, some studies have reported that α-lipoic acid, a naturally occurring antioxidant, directly scavenges free radicals, recycles other antioxidants, accelerates glutathione synthesis, and modulates the activity of transcription factors, such as NF-kB (Cho, 2004).

1.8. Sorrel (*Hibiscus sabdariffa*)

The sorrel plant which is native to India, China, Thailand, Nigeria, and the West Indies has been found to contain several beneficial phytochemicals such as polyphenols which are comprised of phenolic acids, flavonoids, anthocyanins, lignans, and stillbenes. Studies involving animal and in vitro analysis have shown that flavonoids increase the activity of several detoxifying and antioxidant enzymes such as glutathione reductase, glutathione peroxidase, catalase, quinone reductase, and glutathione s-transferase (Valerio, 2001). The utilization of the sorrel extract as a drink and feed supplement to Fisher 344 rats provided protection against carcinogenic onslaught induced by azoxymethane, a potent carcinogen (Verghese, 2008). In a study conducted by Essa and coworkers (2006), the use of alcoholic extracts of sorrel resulted in anti-hyperammonemic and antioxidant effects in brain tissues of ammonium chloride-induced hyperammonemic rats. Within that study it was concluded that sorrel extracts could significantly reduce brain levels of lipid peroxidation products such as thiobarbituric acid and reactive substances (TBARS) and hydroperoxides (HP). Additionally, the administered extract significantly increased the levels of antioxidants such as catalase (CAT), superoxide dismutase

(SOD), glutathione peroxidase (GPx) and reduced glutathione (GSH) in brain tissues of hyperammonemic rats (Essa, 2006). Numerous studies have reported sorrel to be a potent oxidant scavenger as well as medicinal agent by providing anti-carcinogenic protection, hepatoprotection (Amin, 2006), cardioprotection (Olaleye, 2007) and antibacterial activity (Williams, 2010). We utilized the beneficial and therapeutic qualities of sorrel (*Hibiscus sabdariffa*) to attenuate the occurrence of oxidative stress induced by exposure to inhaled nanoparticles of biogenic and anthropogenic origins.

Thus, exposure to anthropogenic nanoparticles is on the rise due to increased usage and manufacturing of nanomaterials for commercial and industrial applications (Oberdorester, 2005). However, exposure of biogenic nanoparticles (i.e. dust) is affecting a growing population of workers and pigs in the swine production industry (Thacker, 2006). From these two different sources of exposure, similar consequences of oxidative stress and ensuing inflammation in the respiratory tract have been observed. Phytochemicals possess antioxidative properties that can restore the equilibrium between oxidants and antioxidants within biological systems. We hypothesized that nanoparticles regardless of origin could elicit the modulation of key oxidative stress and inflammatory genes and regulators, and the ensuing effects can be attenuated by antioxidant treatments. The following objectives were utilized to investigate and validate this hypothesis.

1.9. Objectives

Objective 1:

Characterize the proteomes of airway epithelial cells following stimulation with nanoparticles. Additionally, evaluate biogenic nanoparticle exposure proteome generation after sorrel treatment.

Working hypothesis: Pro-inflammatory and oxidant stress-related proteins will be differentially expressed in airway epithelial cells following exposure to anthropogenic and biogenic nanoparticles, however sorrel extracts will attenuate the effects of nanoparticles.

Objective 2:

Determine gene expression profiles of key pro-inflammatory and oxidant stress-related genes in airway epithelial cells in vitro following stimulation with nanoparticles and sorrel extracts.

Working hypothesis: Gene regulation patterns of pro-inflammatory and oxidative stress associated genes will be modulated by nanoparticle exposure and sorrel extracts will attenuate these occurrences.

Objective 3:

Characterize cytokines produced by airway epithelial cells following stimulation with nanoparticles and sorrel extracts.

Working hypothesis: Nanoparticles, regardless of origin, will elicit the release of pro-inflammatory cytokines in airway epithelial cells and sorrel extracts will reduce the production of cytokines associated with inflammation.

CHAPTER 2

Modulation of Pro-Inflammatory Genes by Swine Confinement Facility Dust and Phytochemical Treatments in Airway Epithelial Cells

2.1. Introduction

Certain populations are more susceptible to developing asthma-like symptoms and chronic bronchitis as they are routinely exposed to airborne oxidants in the form of biogenic nanoparticles. For example, agricultural workers who work in swine production/confinement facilities are exposed to biogenic nanoparticles namely dusts associated with the management of animals and feeds (Boschetto, 2006; Charavaryamath, 2006). In a recent study, swine barn dust extract was found to stimulate IL-6 and IL-8 release in human bronchial epithelial cells *in vitro* (Romberger, 2002). A single 3-5 hour exposure to swine barn air results in increases in IL-6 in serum, and increased levels of IL-6 and IL-8 in nasal lavage and inflammatory cells in bronchoavelolar lavage fluid (BALF), thus resulting in acute lung inflammation in healthy non-smoking workers (Charavaryamath, 2005).

Asthma and chronic bronchitis are complex airway diseases that can be initiated by various mechanisms. Airway hyperresponsiveness, broncho-constriction, and mucus hypersecretion are characteristic features of asthma. Chronic bronchitis is the result of chronic inflammation of the small and medium sized airways with clinical manifestations of airflow limitation, chronic cough, and sputum production (Sutherland, 2003). A key factor in the progression of both of these diseases is oxidative stress (Park, 2007). Oxidative stress is defined as an imbalance between antioxidants and oxidants within the airways. Oxidative stress has been found to be associated with the pathogenesis of asthma (Talati, 2006) by enhancing the production of T-helper cell type 2 (Th2) response cytokines such as IL-4, IL-5, and IL-13 (Park,

2007). To date, traditional treatments of asthma and bronchitis are formulated to treat the symptoms and not the root cause of these diseases.

Phytonutrient treatments containing known antioxidants such as flavonoids and anthocyanins have been used to prevent the accumulation of reactive oxygen species (ROS) *in vitro*. The consumption of functional foods such as fruits, vegetables, and spices have been found to provide a protective effect by deactivating or neutralizing the reactivity of ROS, thereby thwarting many pathophysiological conditions such as disease (Rice-Evans, 1996). In a recent study, anthocyanins were found to reduce inflammatory mediators in a lung inflammatory disease model (Rossi, 2003). Further, in an ovalbumin induced murine asthma model, anthocyanins were found to reduce mucus secretion, recruitment of inflammatory cells, and mRNA levels of various cytokine (Park, 2007).

Sorrel (*Hibiscus sabdariffa*), an edible medicinal plant native to India, Nigeria and China has been found to be a good source of antioxidants such as polyphenolic acids, flavonoids, and anthocyanins (Verghese, 2008). Researchers have reported that sorrel increased the levels of vital antioxidants such as catalase, superoxide dismutase, and glutathione peroxidase in brain tissues of hyperammoneic rats, which are subject to high levels of oxidative stress mediated-lipid peroxidation (Essa, 2007). In a study conducted by Christian and coworkers, red varieties of sorrel had the capability to inhibit COX-2 *in vitro* (Christian, 2006). In addition, aqueous extracts of sorrel have been shown to attenuate hypertension and reverse cardiac hypertrophy in 2K-1C hypertensive rats (Odigie, 2003). Further still, sorrel has the potential to reverse toxicity of chemicals such as sodium nitrate in Wistar rats by returning the haematological indices to the basal level (Bako, 2009). Toxicity studies have also revealed that sorrel is safe for human consumption (Okasha, 2008). Thus, we hypothesize that swine confinement facility dust can

modulate oxidative stress and inflammatory genes in human airway epithelial cells and sorrel can reduce dust-mediated oxidative stress and inflammation.

2.2. Materials and Methods

2.2.1. Chemicals and reagents. Normal human bronchial epithelial (NHBE) cells, bronchial epithelial cell basal media (BEBM), Singlequot supplement kits, DMEM and collagen were all purchased from Lonza (Walkersville, Maryland). Acetic acid was purchased from Sigma Aldrich (St. Louis, Missouri). Oxidative stress and antioxidant defense SuperArrays were purchased from Qiagen (PAHS-065A) (Valencia, California). TGX gels, nitrocellulose membranes and Western blot reagents were acquired from Biorad (Hercules, California). Lactate dehydrogenase kits were purchased from Roche (Indianapolis, Indiana). Phospho IκB, COX-2, and iNOS primary antibodies and anti-rabbit IgG secondary antibodies were purchased from Cell Signaling Technology (Beverly, Massachusetts). GPX-2, DUOX-2, and Beta actin secondary antibody was purchased from Santa Cruz Biotechnology (Santa Cruz, California). ECL kits for Western blotting were purchased from GE Healthcare Life Sciences Division (Fairfield, Connecticut).

2.2.2. Sorrel extract preparation. Aqueous extracts of sorrel were made by adding 2 grams of previously ground lyphollized sorrel calyces to 10ml of deionized and distilled water as described in previous literature. The solution was gently stirred at 10 rpm for 1hr at 4°C. After the stirring process was completed, the solution was evaporated at 40°C overnight. The sorrel aqueous extracts were then stored at 4°C until further use. Prior to use extracts were sterile filtered using a .22μm cellulose filter.

2.2.3. Preparation of dust extract (DE). Settled dust was acquired from raised surfaces at the North Carolina Agricultural and Technical State University Swine Confinement Facility.

Samples were collected from the same locations each time; gestation, farrowing, nursery and breeding rooms. Settled dust from the fixtures of the pig pens were brushed into a Ziploc bag using a cosmetic brush and transported immediately to the lab for further processing. Briefly, one gram of dust was then added to 10 milliliters of Hank's Buffered Saline salt (HBSS) and vortexed for one minute as described previously by Gerald. The dust suspension was left to stand at room temperature for one hour. The mixture was centrifuged for 10 minutes at 5,000 rpm at room temperature. The supernatant was transferred to a new 50 ml conical tube and centrifuged again at 5,000 rpm for 10 minutes. The final supernatant was sterilized via vacuum filtration by using 0.22 micrometer (μm) filter. The extracts were used immediately or aliquoted and stored at -80°C.

2.2.4. Cell culture and stimulation. Primary normal human bronchial epithelial cells (NHBE) (CC-2540) were expanded for a period of 7-10 days in T75 flasks until 70-80% confluency in high EGF BEBM expansion media containing 0.13mg/ml of bovine pituitary extract (BPE), 0.5μg/ml of hydrocortisone, 12.5ng/ml of human epithelial growth factor (hEGF), 0.5μg/ml of epinephrine, 10μg/ml of transferrin, 5μg/ml of insulin, 50nM of retinoic acid, 6.5ng/ml of triiodothyronine, and 50μg/ml of GA-1000. Confluent cultures were then trypsinized, centrifuged at 4000 rpm for 5 minutes at 4°C and resuspended in cryopreservation media, then stored in the vapor phase of liquid nitrogen at a density of $1x10^6$. For initial seeding, six-well plates were coated with collagen solution consisting of 13μg of collagen per ml of 0.02N acetic acid for 1hr. Plates were then washed with 1X phosphate buffered saline (PBS), pH 7.0 for 10 minutes. After seeding, NHBE cells were maintained in bronchial epithelial cell basal medium supplemented with 0.13mg/ml of bovine pituitary extract (BPE), 0.5μg/ml of hydrocortisone, 0.5ng/ml of human epithelial growth factor (hEGF), 0.5μg/ml of epinephrine,

10µg/ml of transferrin, 5µg/ml of insulin, 50nM of retinoic acid, 6.5ng/ml of triiodothyronine, and 50µg/ml of GA-1000. At 95-100% confluency cells were exposed to 1% dust extract, sorrel alone treatments, and concurrent dust exposure and sorrel treatments for 4hr and 24hr. For dust exposure experiments, dust extract (100 µl) was added to BEBM media (9.9 ml) for a final concentration of 1% (v/v) and added to NHBE monolayers for a period of 4hr and 24hr. For sorrel alone treatments, aqueous sorrel extracts were diluted in BEBM at 10%, 7.5%, 5%, and 2.5% concentrations (v/v). Concurrent experiments of dust extract (1%) and sorrel treatments (10, 7.5, 5, 2.5%) were conducted all in triplicate.

2.2.5. Quantitative reverse transcription PCR. The Human Oxidative Stress and Antioxidant Defense RT^2 Profiler PCR Array system (Qiagen) was utilized to evaluate the levels of oxidant and antioxidant defense genes in normal human bronchial epithelial cells (NHBE) following exposure to DE. A total of 84 genes were analyzed to determine the effect of DE exposure and subsequent phytochemical treatments. RNA (500ng) from each treatment group and control was reverse transcribed to produce cDNA using the First Strand cDNA Synthesis kit (SABiosciences/Qiagen, Frederick, MD). Real-time PCR detection was performed using the ABI 7500 Real Time Instrument (Applied Biosystems) and the cycle parameters were 95°C for 10 minutes, followed by 40 cycles at 95°C for 15 seconds and 60°C for 1 minute. A melt analysis was performed for all products to determine the specificity of the amplification using the ABI 7500 Fast System SDS Software. All values were normalized to the constitutive expression of the average of three housekeeping genes β-actin, GAPDH, and Ribosomal Protein L13A. SA Biosciences array analysis software was used to perform data analysis. Criteria for identifying differentially expressed genes included selection of candidates that had fold changes of greater than 2 and p-values of ≤ 0.05 were considered to be significant.

2.2.6. Western blot validation. Whole cell lysates were prepared from NHBE cells in control and treatment groups and quantitated using the Bradford assay. Samples (60μg) were boiled in 4x sample loading buffer at 100 °C for 5 min before gel loading. Lysates were then fractionated using 10% TGX gels (Biorad) by sodium dodecyl sulfate-polyacrylamide gel electrophoresis (SDS-PAGE) at 120 volts for 45 minutes at room temperature. Fractionated proteins were transferred to nitrocellulose membranes using a semi-dry method (Biorad) at 10V for 60 minutes in 1X tris glycine transfer buffer. After blocking in 5% milk for 1hr, nitrocellulose membranes were gently rocked three times for 10 minutes each with tris-buffered saline-tween (TBS-T). Membranes were probed with primary antibody in 5% bovine serum albumin solution (BSA) and gently rocked overnight at 4°C. Primary antibodies used were COX-2 (1:1000) (Cell Signaling), phospho-IκB (1:1000) (Cell Signaling), DUOX (1:200) (Santa Cruz), iNOS (1:1000) (Cell Signaling), GPX-2 (1:200) (Santa Cruz) and β-actin (1:1000) (Santa Cruz). Probed membranes were washed three times for 10 minutes each and HRP linked secondary antibody anti-rabbit and anti-goat IgG (1:2000) were used to detect primary antibodies. After washing, ECL detection reagents (1:1) were added (3ml) to probed membranes for one minute and subsequently exposed to film for automated development. Developed blots were then scanned and band densities were analyzed using Applied Biosystems FluorChem HD2 image acquisition and analysis software.

2.2.7. Glutathione peroxidase activity assay. To determine antioxidant levels after swine confinement facility dust exposures and sorrel treatments, a glutathione peroxidase assay kit (Caymen Chemical) was utilized. Glutathione peroxidase (GPx) catalyzes the reduction of hydrogen peroxides, by reduced glutathione and provides protection from oxidative stress. This assay is an indirect measurement of GPx activity by a coupled reaction with gluthathione

reductase (GR). Oxidized glutathione (GSSG), produced upon reduction of hydroperoxide by GPx, is recycled to its reduced state by GR and NADPH. The oxidation of NADPH to $NADP^+$ is accompanied by a decrease in absorbance at 340 nm. If the GPx activity is rate limiting, the rate of decrease in the absorbance at 340 nm is directly proportional to the GPx activity in the sample. Briefly, whole cell extracts were collected from control and experimental plates by using 1x cell lysis buffer and a rubber policeman. The collected cell lysates were then sonicated three times for 7 seconds each with intermittent ice baths for 1 minute. Sonicated samples were then centrifuged for 15min at 15,000rpm at 4°C. Supernatant was removed for assay and stored at -80°C until further use. Dilutions of 1:10, 1:5, and 1:2 were used to garner the best result. In a 96 well plate, for background, 120µl of assay buffer and 50µl of co-substrate mixture was added in triplicate. Positive controls of bovine erthyrocyte GPx were also added in triplicate consisting of 100 µl of assay buffer, 50 µl of co-substrate mixture, and 20µl of diluted GPx control. Each sample was assayed in triplicate and in each dilution by adding 100µl of assay buffer, 50 µl of co-substrate mixture, and 20 µl of sample. To initiate enzymatic reaction, 20 µl of cumene hydroperoxide were added to each well and mixed by slight tapping. Absorbances were read every minute at 340 nm for 5 minutes using the VersaMax plate reader (Molecular Devices).

2.2.8. Cytokine Analysis—ELISA. After experimentation, supernatants were removed and centrifuged at first at 250×g to remove floating cells, and then at 2500×g to remove remaining particles. The final supernatants were stored at −80°C. Cytokine protein levels for IL-8 were determined by ELISA (enzyme linked immunosorbent assay) according to the manufacturer's guidelines (ThermoScientific). The Human Cytokine ELISA for Profile 8 Cytokines (Signosis) was utilized for evaluating eight additional cytokines such as Vascular Endothelial Growth Factor (VEGF), Epidermal Growth Factor (EGF), IL-6, Resistin,

Plasminogen activator inhibitor-1 (PAI-1), IL-12, IL-13, and Eotaxin related to oxidative stress, airway inflammation and remodeling. Absorbance was measured and quantified using a VersaMax plate reader (Molecular Devices) and SoftPro Max software.

2.2.9. Statistical analysis. All results were expressed as means of $\pm$ SEM of at least three biological experiments. Statistical differences between the means were determined with one way analysis of variance (ANOVA) using Graphpad Prism software and a treatment effect with *P* value of $\leq$0.05 was considered significant. Individual groups were compared using the unpaired Student's *t*-test.

2.3. Results

2.3.1. Alteration and attenuation of oxidative stress and antioxidative defense genes due to dust and sorrel treatments. To investigate the effect of swine dust exposure and subsequent sorrel treatments on normal human bronchial epithelial (NHBE) cells, the human oxidative stress and antioxidant defense PCR array (PAHS-065) was utilized. Eighty-four genes were analyzed for modulation after exposure to 1% dust extract (DE) for 0hr, 4hr, and 24hr and subsequent treatments with 10% aqueous sorrel (*Hibiscus sabdariffa*). Initially, heatmap analysis was performed to evaluate the pattern of expression for each gene in each experimental group (Figure 2.1). Thirty-nine genes (46%) of the genes evaluated displayed upregulation during 4hr time exposures and were downregulated after 24hr exposure to 1% dust, 10% sorrel, and 1% dust and 10% sorrel. Conversely, the remaining 45 genes were downregulated after 4hr exposure of 1% dust, 10% sorrel alone, and 1% dust and sorrel treatments and upregulated after 24hr exposures and treatments.

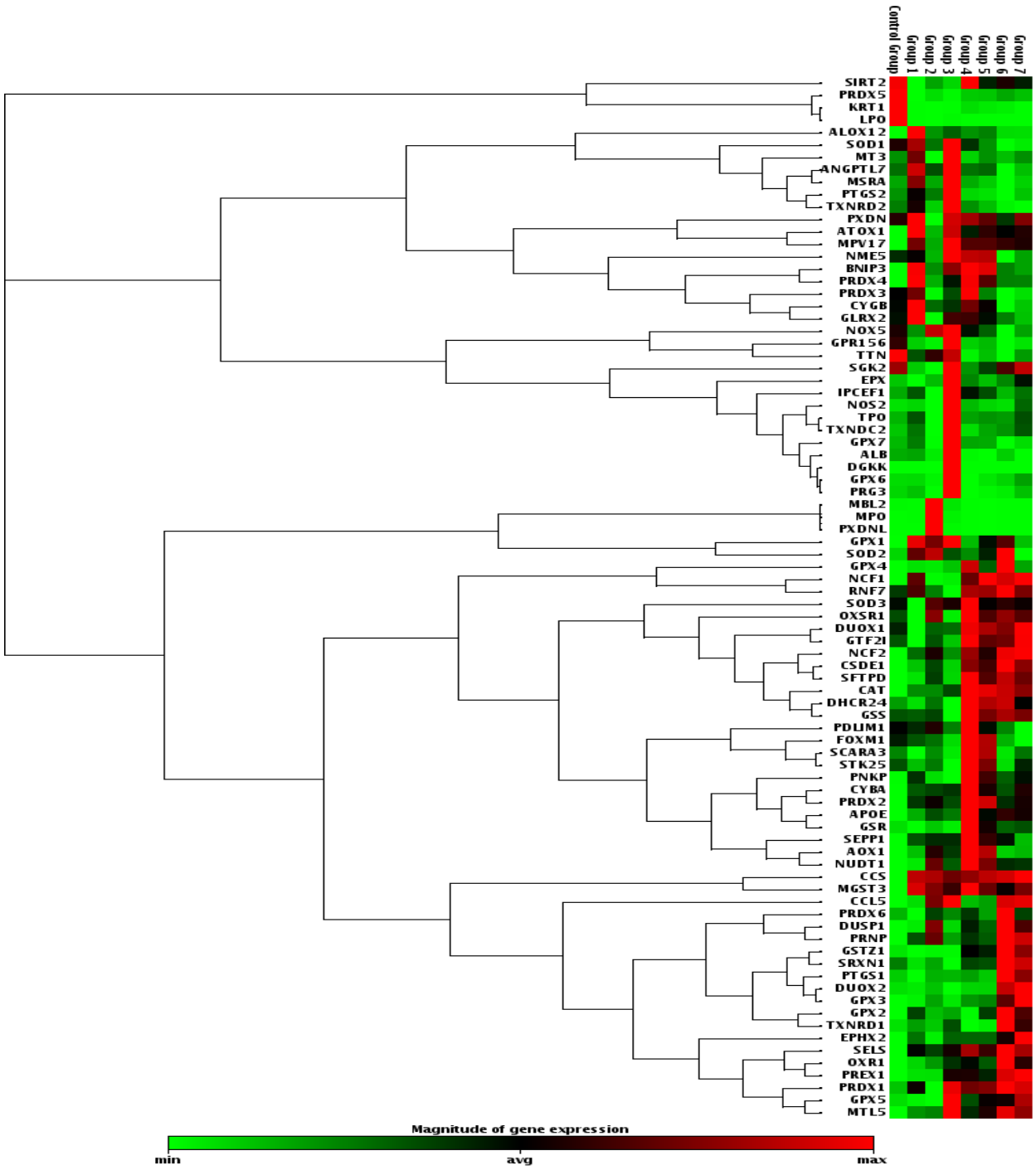

Figure 2.1. Heat map of antioxidant and oxidant stress genes in response to dust and sorrel. Control group= 4hr control, Group 1=4hr 1% dust exposure, Group 2=4hr 10% Sorrel, Group 3=4hr 1% Dust+4hr 10%Sorrel, Group 4=24hr control, Group 5=24hr 1% dust exposure, Group 6=24hr 1% dust exposure + 10% sorrel.

However, 12 genes in the second subset of genes revealed downregulation of expression due to sorrel antioxidant treatments after 24hr 1% dust exposure (Figure 2.2). Ten (80%) of these genes are related to oxidative stress, conversely two antioxidative genes were downregulated.

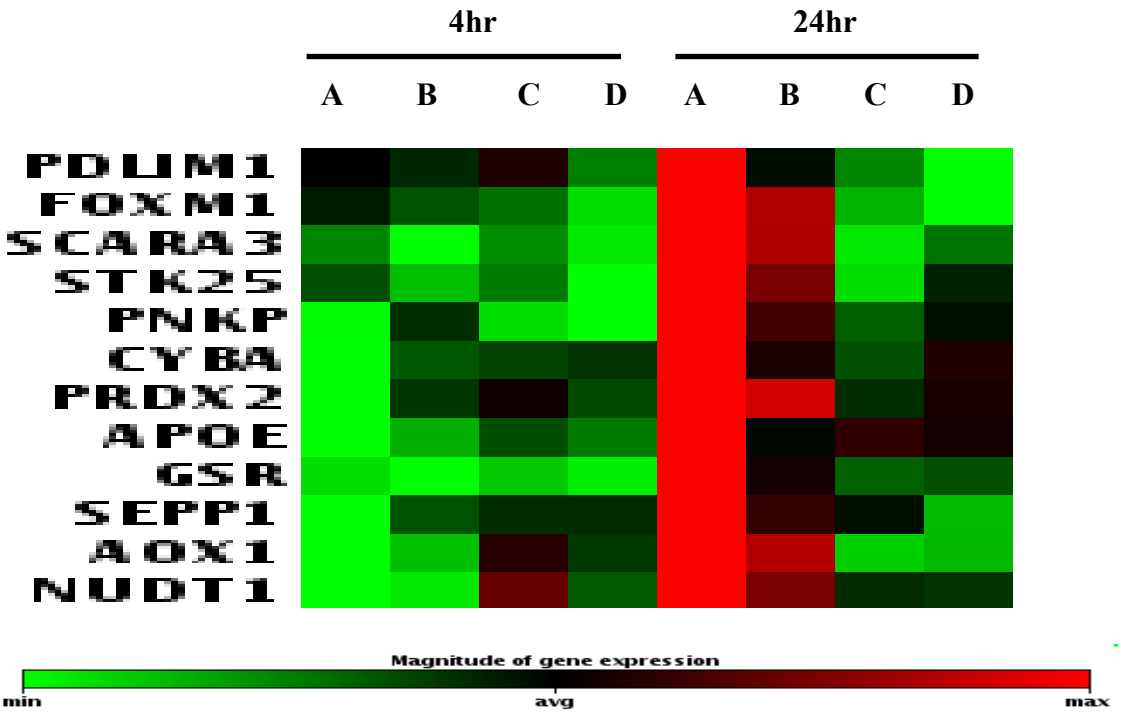

Figure 2.2. Dust and sorrel mediated time dependent gene modulation in NHBE cells. Magnified view of 12 genes related to oxidative stress which are upregulated after 24hr 1% dust exposure and downregulated with sorrel/antioxidant treatments. A= control, B=1% dust, C=10% sorrel alone, D=1% dust and sorrel treatments.

P-values and fold changes for genes of interest in NHBE cells exposed to 1% DE for 4hr are represented in Figure 2.3. The expression of GPX2 (glutathione peroxidase 2) and PTGS2 (prostaglandin endoperoxide) were significantly up-regulated by 2-fold and 1.75-fold respectively, which were validated with glutathione peroxidase activity analysis and Western blot. Conversely, GPR156 (G protein-coupled receptor) and DUOX1 (Dual oxidase 1) were down-regulated. Fold changes and p-values are summarized for 4hr dust exposures in Table 2.1.

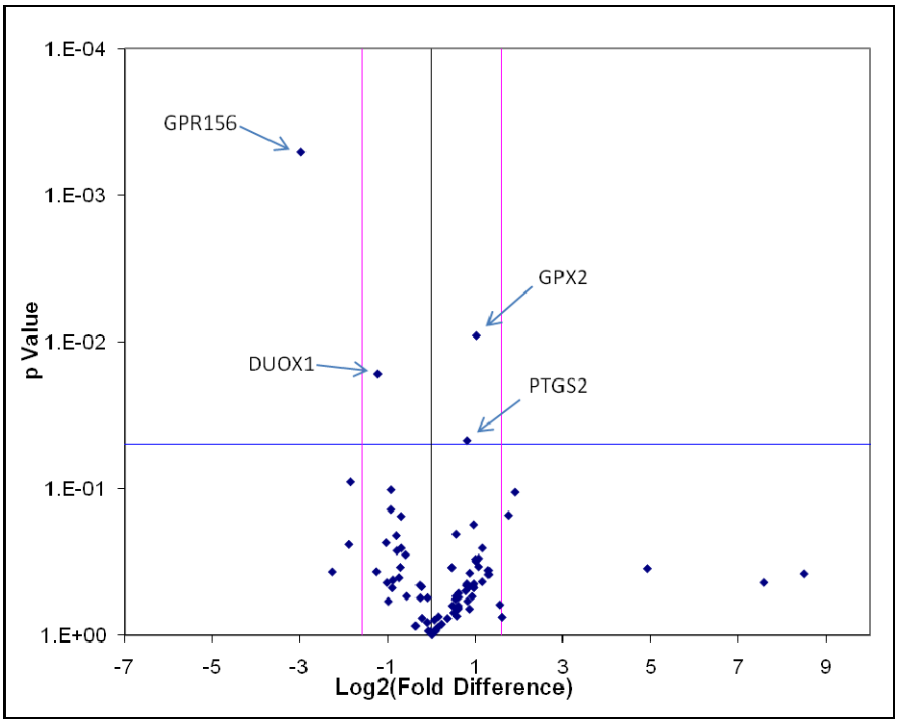

Figure 2.3. Gene expression patterns of NHBE cells treated with 1% dust extract for 4hr.

Table 2.1.

Modulation of oxidative stress and antioxidant defense related genes in NHBE cells exposed to 1% DE for 4hr.

Gene Name/RefSeq	Gene Symbol	Gene Function	*p*-value	Fold change
Glutathione peroxidase 2 (NM_002083)	GPX2	Peroxidase and Oxidoreductase activity	0.009	2.03
G protein-coupled receptor 156 (NM_153002)	GPR156	Peroxidase and Oxidoreductase activity	0.0005	-7.91
Prostaglandin endoperoxide (NM_000963)	PTGS2	Peroxidase activity	0.0472	1.75*
Dual Oxidase 1 (NM_175940)	DUOX1	Superoxide release and metabolism Peroxidase and Oxidoreductase activity	0.0167	-2.36

The expression of GPX2 (Glutathione peroxidase 2) and PTGS2 (prostaglandin endoperoxide) were significantly upregulated by 2-fold and 1.75-fold respectively, which were validated with glutathione peroxidase activity assessments and Western blot respectively. Conversely, GPR156 (G protein-coupled receptor) and DUOX1 (Dual oxidase 1) were downregulated. Figure 2.4 indicates an attenuation of the expression of three genes GPX2, PTGS2, DUOX1 mediated by 4hr post-treatment with 10% sorrel after a 4hr 1% dust exposure. GPR156 is modestly upregulated from a fold change of -7.91 after 4hr 1% DE exposure to -6.00 with 4hr sorrel treatment. Table 2.2 provides a summary of 4hr 1% DE exposure followed by 4hr 10% sorrel treatment.

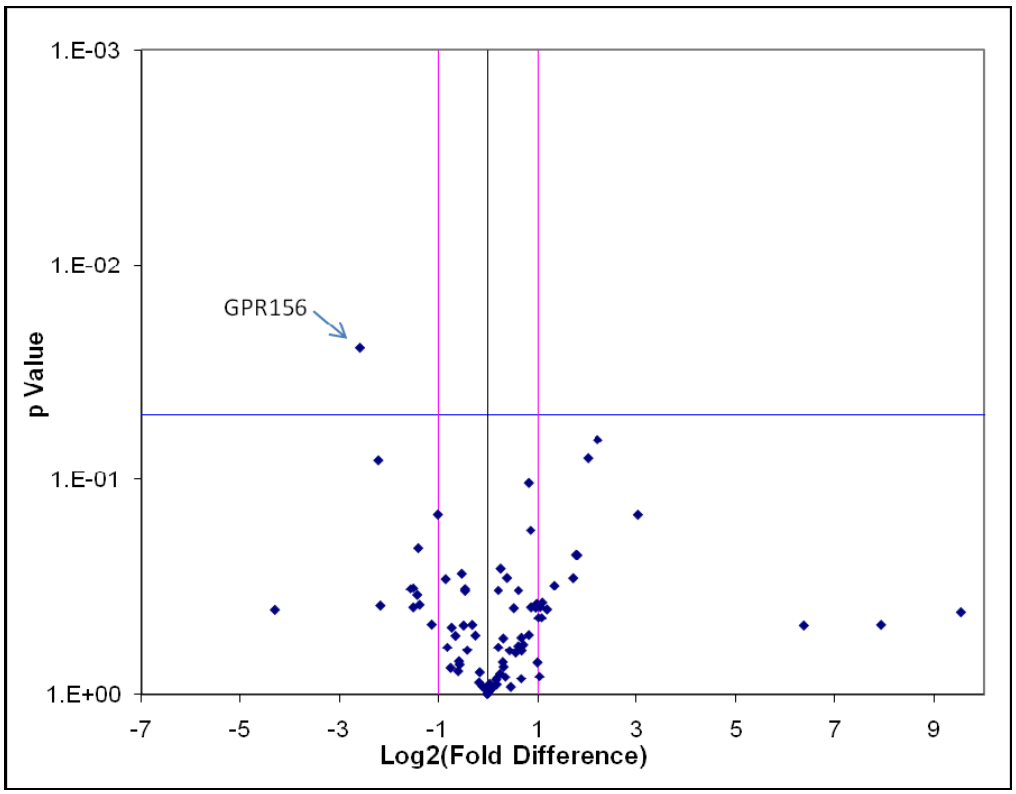

Figure 2.4. Gene expression in NHBE cells treated with 1% dust extract for 4hr and subsequently treated with 10% aqueous sorrel extract for 4hr.

Table 2.2.

Gene expression of dust exposed NHBE cells for 4hr followed by 4hr sorrel treatment.

Gene Name/RefSeq	Gene Symbol	Gene Function	*p*-value	Fold change
G protein-coupled receptor 156 (NM_153002)	GPR156	Peroxidase and Oxidoreductase activity	0.0243	-6.00

A sorrel only treatment group was evaluated to determine what effect this phytonutrient-rich extract had on oxidative stress and antioxidant defense related genes. Three genes, PTGS2 (Prostaglandin endoperoxide), EPX (eosinophil peroxidase), and NOS2 (inducible nitric oxide synthase 2) were upregulated due to the 4hr sorrel only treatment (see Appendix A - Figure 1). Inducible nitric oxide synthase 2 (NOS2/iNOS) sorrel mediated upregulation was validated by Western blot. Table 1 (see Appendix A) summarizes the p-values and fold changes related to the 4hr sorrel induced gene alteration. NHBE cells were exposed to 1% dust extract for 24hrs and gene expression levels are represented in Figure 2.5 and summarized in Table 2.3.

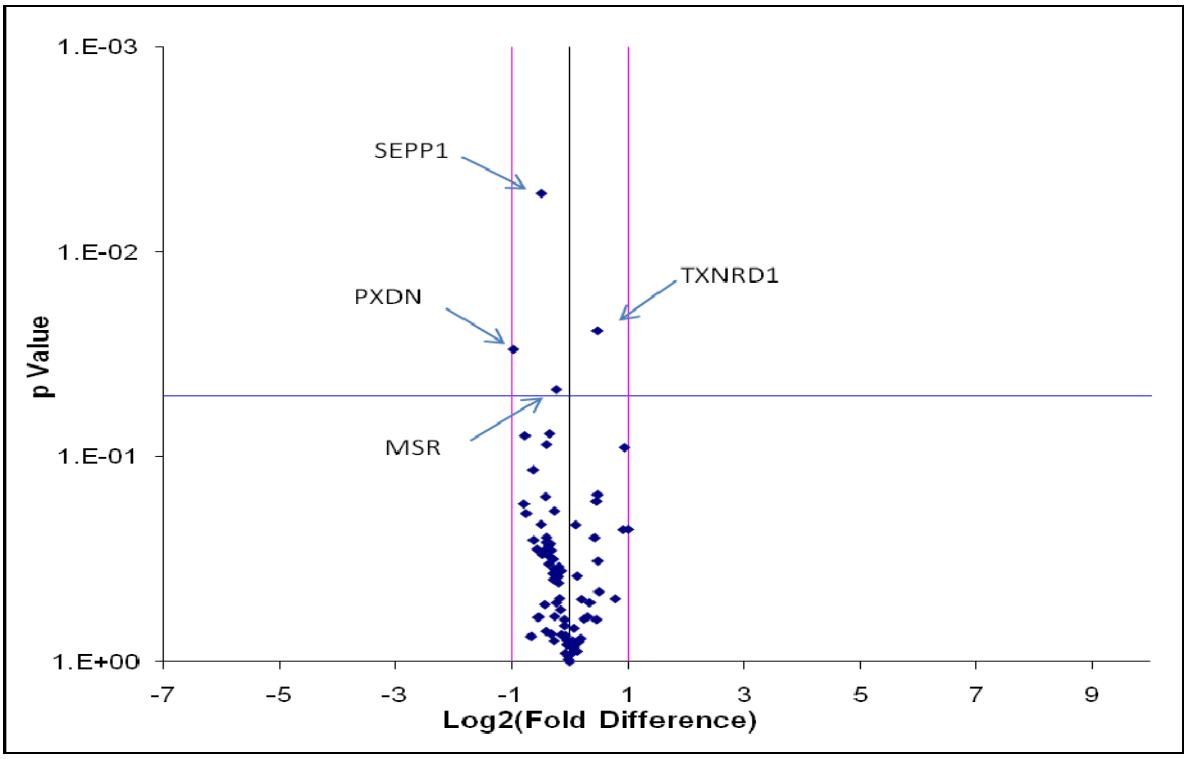

Figure 2.5. Gene expression patterns of NHBE cells exposed to 1% dust extract for 24hr.

Table 2.3.

Gene modulation of oxidative stress/antioxidant defense related genes in response to 24hr dust exposure

Gene Name/RefSeq	Gene Symbol	Gene Function	*p*-value	Fold change
Selenoprotein P,plasma, 1 (NM_005410)	SEPP1	Oxidoreductase activity	0.005	-1.41
Thioredoxin reductase 1 (NM_003330)	TXNRD1	Oxidoreductase activity	0.0243	1.39
Peroxidasin homolog (Drosophila)-like (NM_144651)	PXDNL	Peroxidase activity	0.0299	-1.96
Methionine sulfoxide reductase A (NM_012331)	MSRA	Oxidoreductase activity	0.0470	-1.18

TXNRD1 (Thioredoxin reductase 1) was upregulated by 1.39 fold in relation to the control due to 24hr dust exposure. SEPP1 (Selenoprotein P,plasma, 1), MSRA (Methionine sulfoxide reductase A), and PXDNL (Peroxidasin homolog (Drosophila)-like) were significantly downregulated by at least 1.4 fold. These four modulated genes at 24hrs were different from the four genes (PTGS2, GRP156, GPX, DUOX1) that were altered due to 4hr dust exposure, suggesting different pathways being initiated due to prolonged exposure to 1% dust. Dust exposure (1%) for 24hrs and subsequent sorrel treatments were analyzed in Figure 2.6. Table 2.4 summarizes the genes that were induced by the exposure of dust extract for 24hr and the subsequent antioxidant treatment for 24hr. Five genes associated with oxidative stress and cell division (KRT1, SCARA3, STK25, FOXM1, and NME5) were downregulated due to 1% dust extract exposure followed by 10% sorrel treatment. However, four genes associated with antioxidant activity (DUOX2, GPX3, PTGS1) were upregulated. An important antioxidant enzyme in the deactivation of free radicals in the human airway, thioredoxin reductase 1 (TXNRD1), was highly and significantly upregulated by 13-fold after 24hr exposure to dust and sorrel antioxidant treatments.

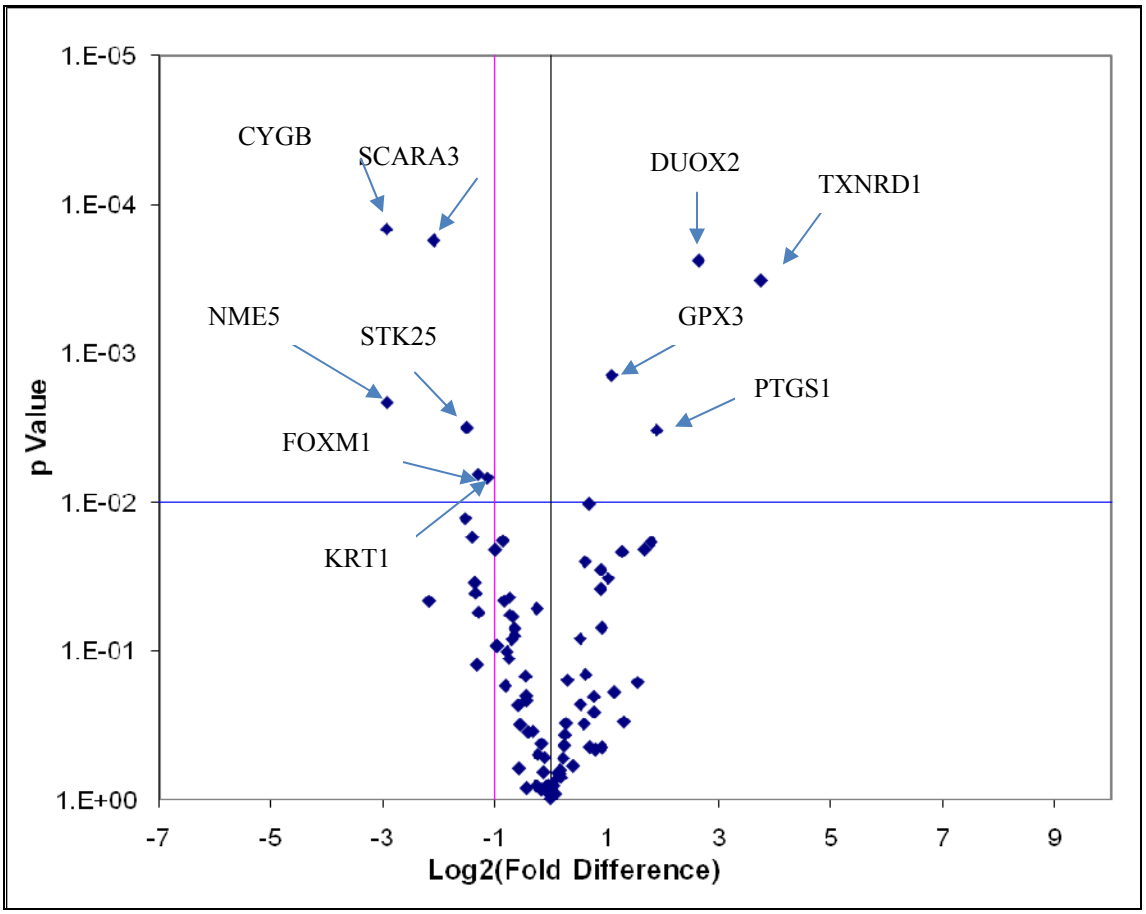

Figure 2.6. Gene expression in NHBE cells exposed to 1% dust extract for 24hr and post-treatment of 10% aqueous sorrel extract for 24hr.

Interestingly, after a 24hr sorrel alone treatment a myriad of genes were differentially expressed (see Appendix A-Figure 2). Six genes associated with antioxidant properties, dual oxidase (DUOX2), prostaglandin enderoperoxide synthase I (PTGS1/COX-1), sulfiredoxin 1 homolog (S.cerevisisae) (SRXN1), and thioredoxin reductase 1 (TXNRD1) were significantly upregulated at least by 2-fold. However, glutaredoxin 2 (GLRX2), glutathione reductase (GSR), genes associated with the glutathione antioxidant system, were significantly downregulated due to the presence of sorrel (10%) for 24hrs.

Table 2.4.

Gene modulation in NHBE cells after 24hr exposure to dust and subsequent sorrel antioxidant treatment.

Gene Name/RefSeq	Gene Symbol	Gene Function	*p*-value	Fold change
Cytoglobin (NM_134268)	CYGB	Superoxide release and metabolism	.0001	-7.66
Dual Oxidase 2 (NM_175940)	DUOX2	Superoxide release and metabolism Peroxidase/ Oxidoreductase activity	.0002	6.20
Forkhead box M1 (NM_021953)	FOXM1	Cell division	.006	-2.48
Glutathione peroxidase 3 (plasma) (NM_002084)	GPX3	Peroxidase / Oxidoreductase activity	.0014	2.12
Keratin 1 (NM_006121)	KRT1	Oxidative stress	.006	-2.19
Non-metastatic cells 5, protein expressed in (nucleoside-diphosphate kinase) (NM_003551)	NME5	Cell division	.002	-7.62
Prostaglandin-endoperoxide synthase 1 (prostaglandin G/H synthase and cyclooxygenase) (NM_000962)	PTGS1	Peroxidase activity	.003	3.70
Scavenger receptor class A, member 3 (NM_182826)	SCARA3	Oxidative stress	.0002	-4.28
Serine/threonine kinase 25 (STE20 homolog, yeast) (NM_006374)	STK25	Oxidative stress	.003	-2.83
Thioredoxin reductase 1 (NM_003330)	TXNRD1	Oxidoreductase activity	0.0003	13.42

Genes associated with oxidative stress and cell division (keratin 1 (KRT1), selenoprotein p, plasma, 1 (SEPP1), scavenger receptor class 1 (SCARA3) were decreased due to 24hr sorrel treatment. These genes and fold changes are summarized in Table 2 in Appendix A.

2.3.2. Western blot validation. Western blot analysis was utilized to validate prostaglandin endoperoxide, PTGS2 or COX-2, inducible nitric oxide (NOS2/iNOS), DUOX, and phospho-IκB genes that were significantly modulated from dust and sorrel experiments. Densitometry results reveal a significant increase of two fold in COX-2 expression due to 1% dust exposure at 4hr (Figure 2.7 and Figure 2.8). Sorrel only treatments induce only a modest amount of COX-2, which are equivalent to control values. An almost two-fold reduction in COX-2 expression after dust exposed NHBE cells were treated with sorrel (10%) for a total of 4hr, which correlates with genomic analysis. After 24hrs, COX-2 expression is increased from 10% sorrel, in relationship to the control. Dust exposure at 24hrs, also increases COX-2 expression but not significantly. However, after 24hr sorrel treatments, dust exposed NHBE cells exhibited a small reduction of COX-2 expression.

In regards to phospho-IκB expression in Figure 2.9, dust extract (1%) and sorrel treatments (10%) both generate higher levels of expression in comparison to the control at 4hrs. At the same time point, sorrel treatments on dust exposed NHBE cells had no effect on phospho-IκB expression. However at 24hrs, there was no difference in expression in phospho-IκB sorrel alone treatments and dust exposures. Dust exposed NHBE cells treated with 10% sorrel exhibited a modest reduction in phospho-IκB expression after a total of 24hrs.

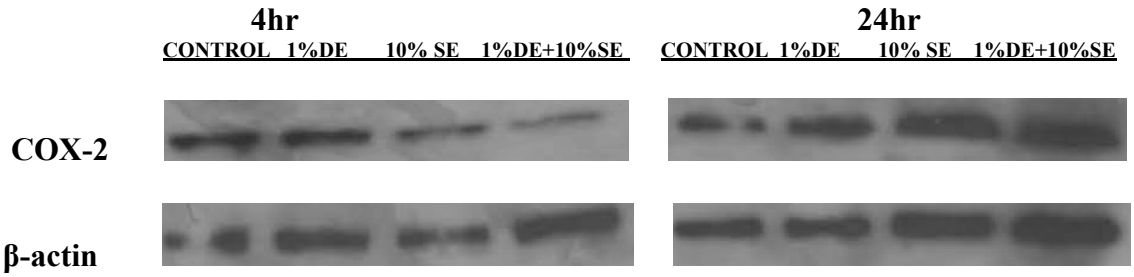

Figure 2.7. Modulation of COX-2 protein expression by dust and sorrel treatments. Immunoblots (a) and quantitative analysis (b) representing COX-2 response in NHBE cells treated with sorrel only (10% SE), dust only (1% DE), and dust exposed and sorrel treated (1% DE + 10% SE) at 4hr and 24hr. Mean ± SEM, n=3

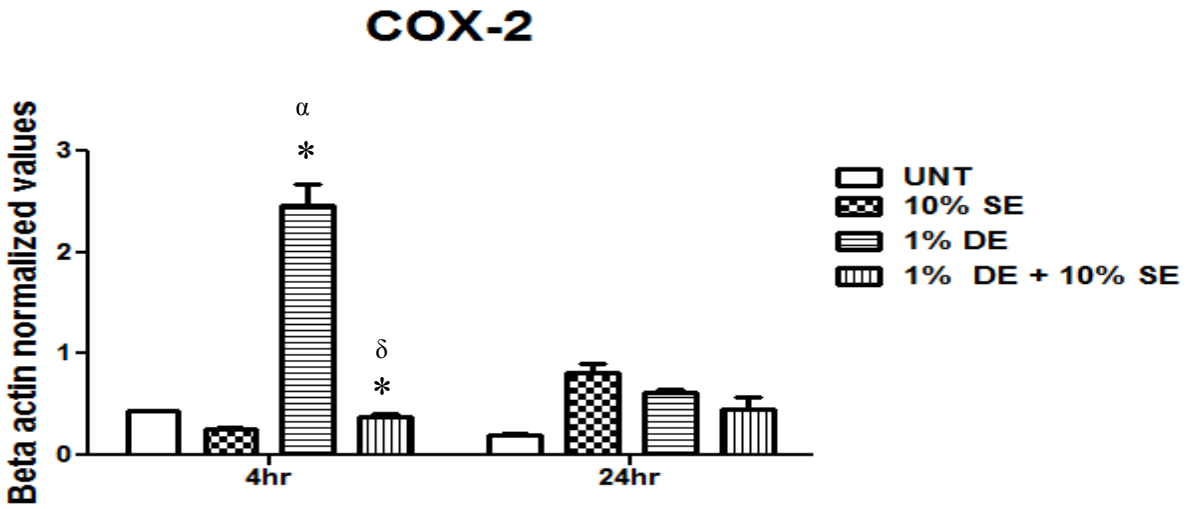

Figure 2.8. Quantitative analysis of COX-2 protein expression by dust and sorrel treatments. Densitometry analysis representing COX-2 response in NHBE cells treated with sorrel only (10% SE), dust only (1% DE), and dust exposed and sorrel treated (1% DE + 10% SE) at 4hr and 24hr.Mean ± SEM, n=3 (α=in respect to control, δ=in respect to 1%DE)

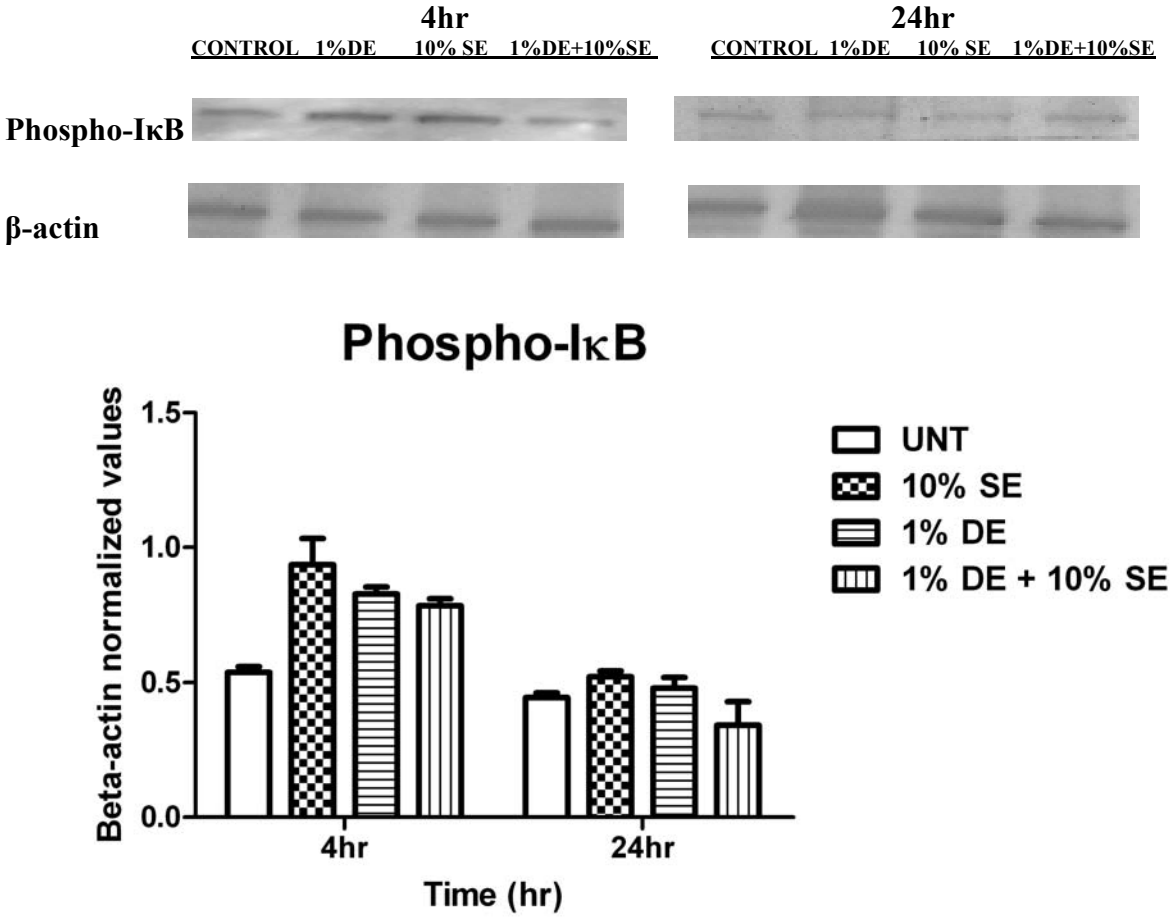

Figure 2.9. Phospho-IκB expression analysis at 4hr and 24hr. Immunoblots (top) of dust and sorrel mediated Phospho-IκB response in NHBE cells with quantitative measurements (bottom). Treatments include sorrel only (10% SE), dust only (1% DE), and dust exposed and sorrel treated (1% DE + 10% SE). Mean ± SEM, n=3

Inducible nitric oxide 2 (NOS2/iNOS) (Figure 2.10) protein levels for 10% sorrel alone remained equivalent to control values at 4hrs. However, 1% dust induced a 1-fold upregulation of iNOS, which were reduced below control levels with sorrel treatment. Dual oxidase protein evaluation (Figure 2.11) revealed slight reductions in DUOX levels at 4hrs due to 1% dust exposure. DUOX levels were also modulated due to the presence of 1% dust and 10% sorrel simultaneously but not significantly.

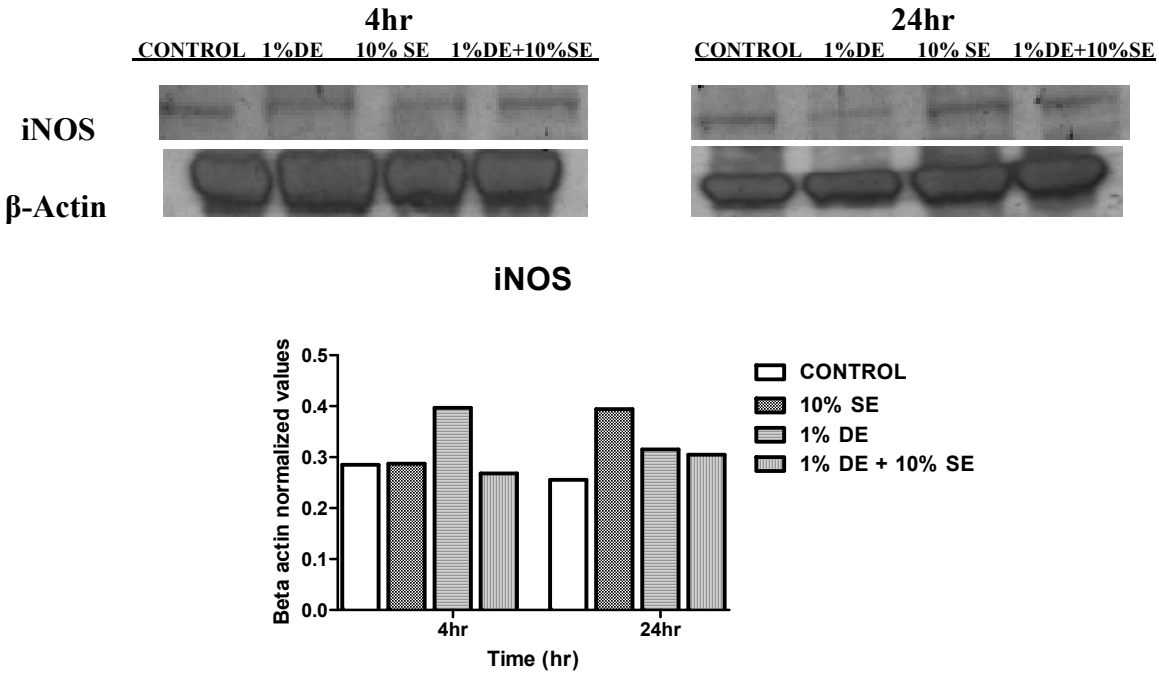

Figure 2.10. Inducible nitric oxide response in NHBE cells. Immunoblots (top) and densitometry analysis (bottom) of NHBE cells. iNOS expression after treatment with control, sorrel only (10% SE), dust only (1% DE), and dust exposed and sorrel treated (1% DE + 10% SE) at 4hr and 24hr. Mean ± SEM, n=3.

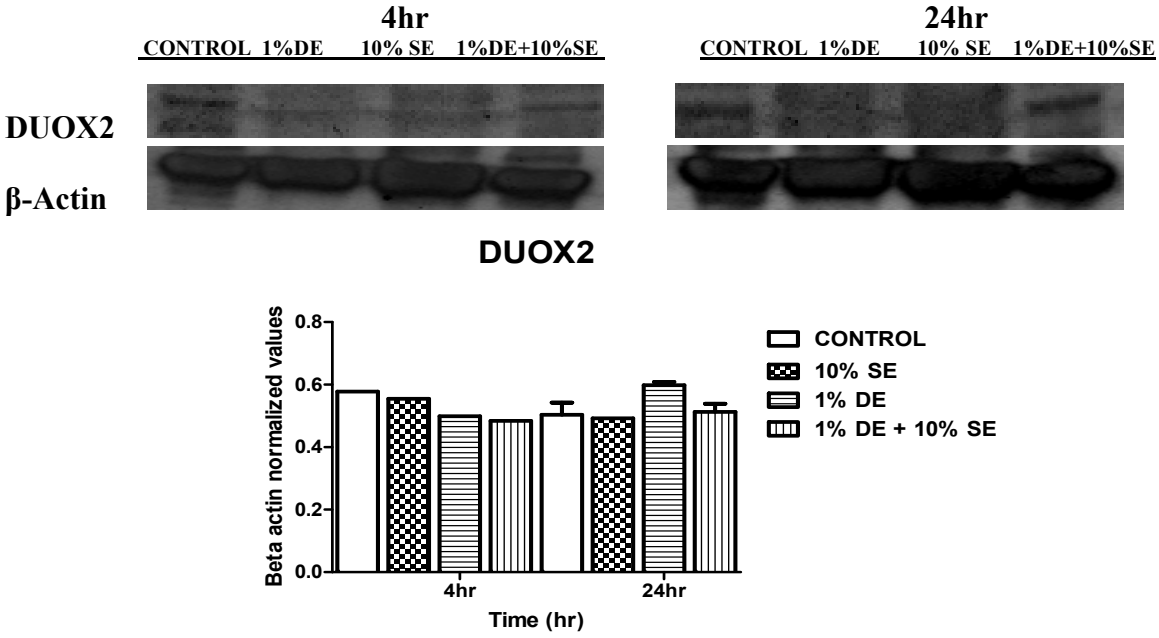

Figure 2.11. Quantitative analysis of dual oxidase 2 protein expression in NHBE cells.

Figure 2.11.(cont'd) Quantitative analysis of dual oxidase 2 protein expression in NHBE cells. Immunoblots (top) of NHBE cells treated with sorrel only (10% SE), dust only (1% DE), and dust exposed and sorrel treated (1% DE + 10% SE) at 4hr and 24hr. Densitometry analysis (bottom) of represented immunoblots of DUOX2. Mean ± SEM, n=3.

Additionally, protein expression for glutathione peroxidase 2 (GPX-2) was evaluated using Western blot analysis. In comparison to the control, 1% dust at 4hrs did not alter gene expression of GPX-2 (Figure 2.12).

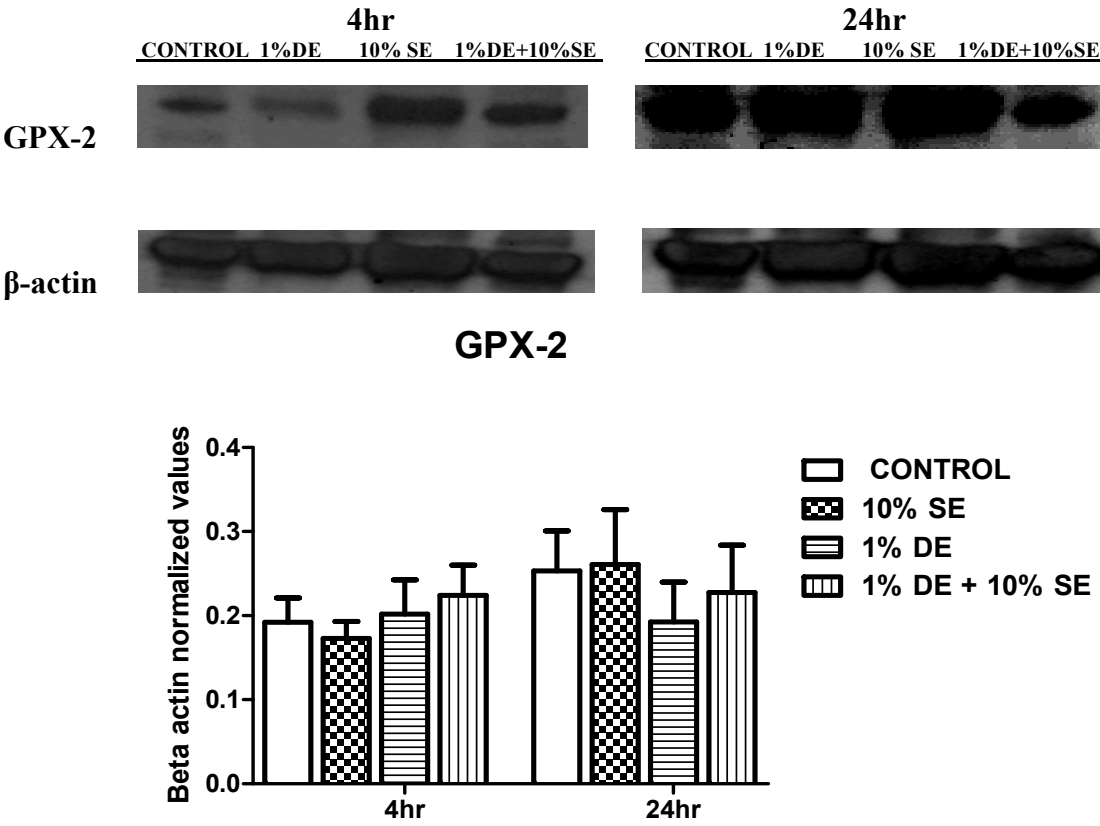

Figure 2.12. Glutathione peroxidase protein validation by Western Blot. Immunoblots (top) and quantitative analysis (bottom) of NHBE cell lysates at 4hr and 24hr with the following treatments: control (no treatment); 10% SE, Sorrel extract; 1% DE, Dust extract, and 1% DE + 10% SE, dust exposure with sorrel treatment. Data are presented as mean ± SEM, n=2.

Sorrel alone treatments for 4hrs encouraged a slight reduction in GPX-2 protein expression. For dust exposure and sorrel treatments, 4hr evaluations of glutathione peroxidase 2 protein expression revealed slightly higher levels than controls. GPX-2 expression after 24hrs of dust exposure was decreased in relation to controls. Sorrel alone treatments resembled control levels, however dust exposure and sorrel treatments exhibited lower levels of GPX-2 protein in comparison to control.

2.3.3. Glutathione peroxidase (GPx) activity. Glutathione peroxidases are responsible for the reduction of hydrogen peroxides by using reduced glutathione as an electron donor. These enzymes function to protect the cell from oxidative damage. We evaluated NHBE cell lysates exposed to dust and treated with sorrel for GPx activity to determine if sorrel enhanced GPx enzymes. Figure 2.13 represents data collected for 4hr and 24hr. At 4hr, there are significant increases in GPX activity in comparison to control due to 1% dust exposure. GPx activity remains constant with the treatment of sorrel on dust exposed cells. Sorrel alone treatments incite modest GPx activity at 4hr. Concentration gradients were also employed to determine if concentration could stimulate GPx activity. All four treatments (10, 7.5, 5, 2.5%) induced significantly enhanced GPx activity after 1% dust exposure. Interestingly, dust and sorrel GPx activity does not seem to be dose dependent however higher GPx activity was found when sorrel was at a concentration of 7.5% (v/v) at 4hr and 24hrs.

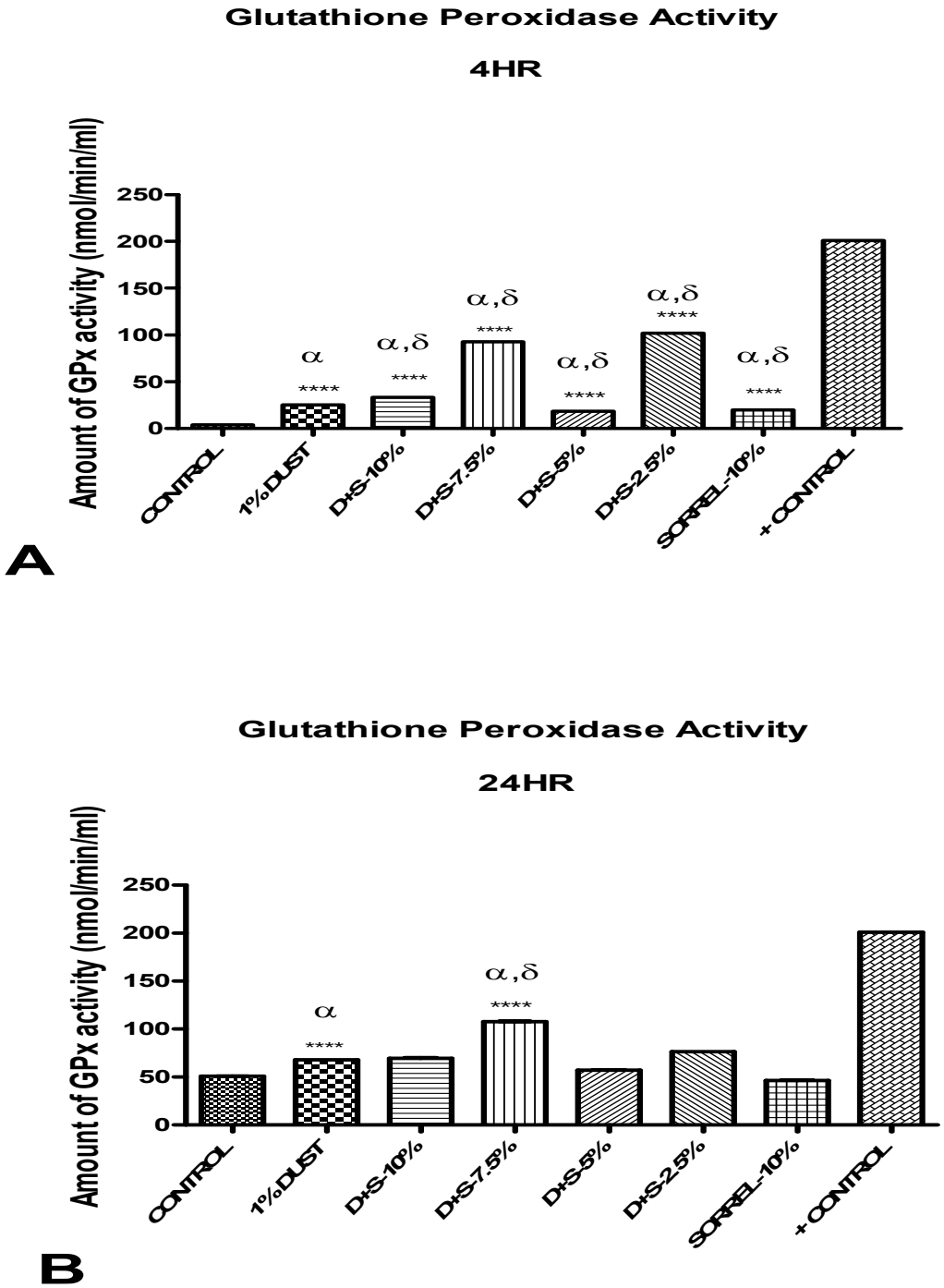

Figure 2.13. Glutathione peroxidase activity in NHBE cells at 4hr and 24hr in response to dust exposure and sorrel treatments. Measurement of glutathione–dependent peroxidases in cell lysates were determined by the rate of decrease in absorbance (340 nm). Data are presented as mean ± SEM, n=3. Asterisks indicate significance in comparison to α=control, δ= 1% dust

2.3.4. Modulation of IL-8 chemokine production. IL-8 is an important chemokine responsible for the induction of neutrophils into the airways and is a possible mediator in the neutrophilic response found in people that have had swine confinement dust exposure (Romberger, 2002). In this study, we found that there was an increase in dust mediated IL-8 production at 4hr (Figure 2.14). Sorrel alone treatments did not encourage IL-8 synthesis from NHBE cells. After a total of 4hr, dust exposed and sorrel treated NHBE cells showed a reduction in IL-8 production. At 24hr, NHBE cells exposed to 1% dust exhibited higher concentrations of IL-8, in relation to control. Sorrel alone, at 24hr, did not generate any higher production of IL-8 than found in control groups. Yet, due to sorrel treatment there is a reduction in IL-8 concentrations after dust exposure.

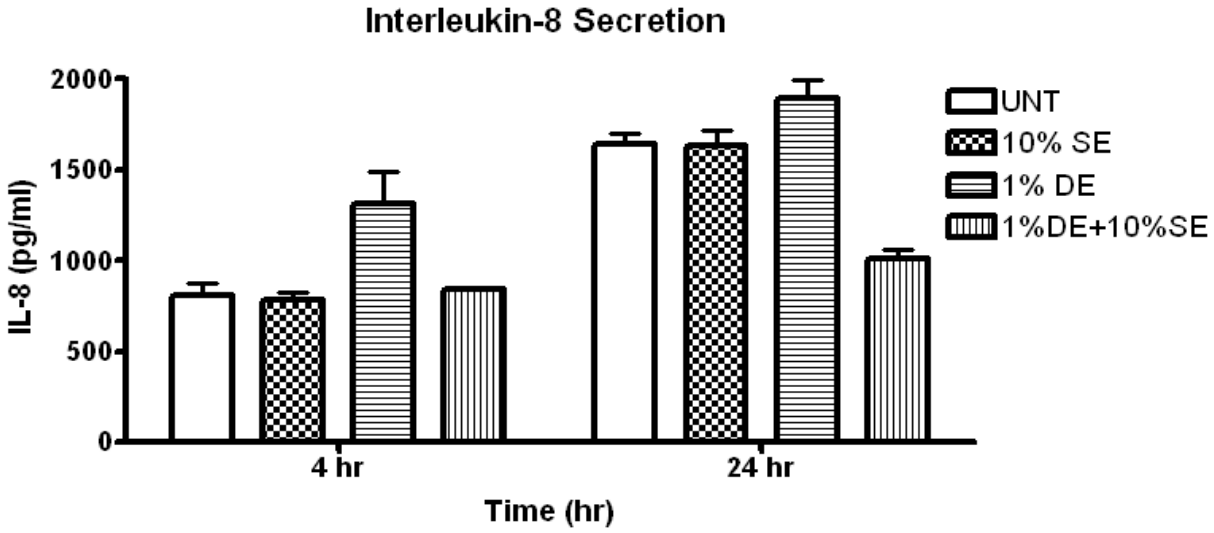

Figure 2.14. Chemokine secretion evaluation of IL-8 using ELISA in response to dust and sorrel. ELISA revealed a sorrel (10%) mediated-decrease in dust (1%)-induced IL-8 secretion in primary cultures of NHBE cells at 4hr and 24hr. UNT, Untreated; SE, Sorrell extract; DE, Dust extract. Data are presented as mean ± SEM, n=3.

2.3.5. Cytokine evaluation. A total of eight cytokines were measured in response to dust exposure and sorrel treatments. ELISA analysis (Figure 2.15) revealed that 24hr exposure to swine confinement facility dust did not induce elevated secretion of any of the eight cytokines.

However, control levels are higher than normal which could contribute to the reduced effect. Interestingly, sorrel (10% SE) alone produced a therapeutic effect by significantly reducing levels of IL-6 and PAI-1, which are both contributors of airway inflammation and tissue remodeling. Additionally, significant reductions of IL-6, PAI-1, and VEGF were found in dust exposure and sorrel treatment groups (1%DE+10%SE).

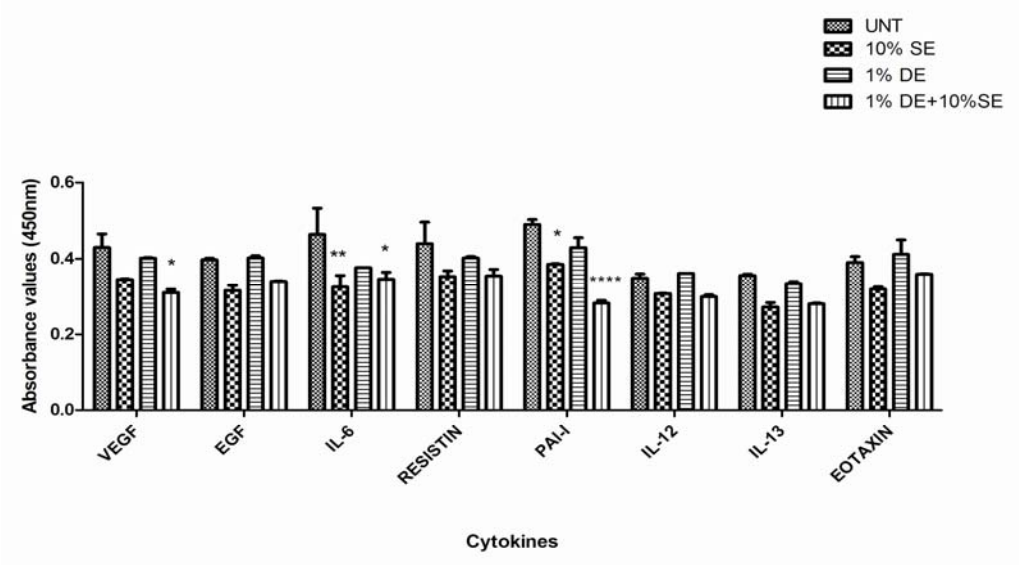

Figure 2.15. Human cytokine profile assessment in response to dust and sorrel.

2.4. Discussion

Swine confinement facility dust is a known contributor to respiratory illnesses for individuals who are exposed on an acute and chronic basis. The inhalation of such dusts have been found to generate a number of pro-inflammatory responses such as influxes of inflammatory cells like neutrophils, increases of cytokines such as IL-6, IL-8, and tumor necrosis factor alpha (TNFα) in nasal and bronchoaveolar lavage fluid and blood (Palmberg, 2002). Thus, particle inhalation has been linked to inflammation which can induce adverse health effects (Health Effects Institute, 2002). In this study, we used *in vitro* responses to evaluate the potential

of swine confinement facility dust to modulate the expression of pro-inflammatory and oxidative stress related genes in the human airway.

The innate host defense system in the respiratory tract is comprised of several different mechanisms (Thacker, 2006). The morphology of the upper respiratory system is structured to provide multiple layers of protection against foreign entities. These layers contain a tight layer of epithelial cells which lie in close proximity to one another to prevent contamination of its apical surface. The apical surface is coated with epithelial lining fluid that contains antimicrobial peptides and antioxidants for protection against bacterial and viral products. Resting on top of the epithelial lining fluid is a layer of mucus designed to capture bacteria and viruses. Through ciliary action of ciliated respiratory epithelial cells, captured bacteria and viruses are removed. However, if this primary line of defense is ineffective, high levels of antioxidants such as reduced glutathione are stored within the epithelial lining fluid to combat invaders. In addition to glutathione, dual oxidase and lactoperoxidase are responsible for bacterial defense through the generation of hydrogen peroxide. Hydrogen peroxide and thiocynate, also available in the epithelial lining fluid, are catalyzed by lactoperoxidase into a bactericidal product called hypothiocyanate. The above mentioned enzymes and many other antioxidants such as catalase, superoxide dismutase, and glutathione peroxidase are responsible for the protection of the airway epithelium and the elimination of all forms of environmental stressors (Comhair, 2002). The imbalance of antioxidants and oxidants, the reduction of antioxidants, and the inability to repair oxidative damage results in oxidative stress which can impair cellular components such as DNA, protein, membrane lipids, and carbohydrates (Comhair, 2002).

Using the Human Oxidative Stress and Antioxidant Defense RT^2 Profiler PCR array, genes that were involved in dust mediated oxidative stress were identified. Phytonutrient or

sorrel only profiles were also generated, providing insight into the potential of this novel source of antioxidants as a therapeutic agent. Genomic profiles generated revealed that 1% dust up-regulated inflammatory regulators such as prostaglandin 2 or COX-2. Interestingly, sorrel only treatments invoked the same genomic response as 1% dust; however this occurrence was not seen in the protein level. Conversely, in 4hr combinational experiments in which NHBE cells were exposed to 1% dust and 10% sorrel, COX-2 gene expression was attenuated. Various factors could have invoked this response, including the up-regulation of certain antioxidative enzymes at the gene and protein level such as glutathione peroxidase 2 (GPX-2) by two-fold. GPX-2 is involved in peroxidase and oxidoreductase activity and is responsible for free radical neutralization through redox reactions using glutathione. Studies have shown that GPX-2 has the ability to inhibit prostaglandin synthesis, which reduces the expression of pro-inflammatory mediators known to play a role in allergic asthma (Sakamoto, 2000). Protein expression at 4hr corresponds to this previous finding as COX-2 levels are reduced by almost 2-fold.

Western blot analysis also revealed no significant DUOX-2 protein expression divergence in control and sorrel alone treated NHBE cells at 4hrs. There was also an insignificant decrease in DUOX-2 protein expression for 1% dust exposed. Conversely, at 24hrs DUOX-2 protein expression was increased above controls due to 1% dust exposure. Studies have shown that DUOX-2 increases are related to host defense and hormone biosynthesis (Geiszt, 2006). DUOX isozymes have been highly expressed in the respiratory tract (Harper, 2008). Dust and dust extracts have been found to possess high quantities of lipopolysaccride (LPS), a known endotoxin (Poole, 2007). This increased response of DUOX-2 in relation to 1% dust exposure could be related to the presence of LPS in the dust extract sample.

In contrast, at the 24hr time point two genes were significantly modulated due to the presence of dust (1%) and sorrel (10%). Of the two genes, one gene related to oxidative stress was significantly downregulated by almost 3 fold with p-values of <0.01. One gene corresponding to antioxidant defense was significantly up-regulated. Thioredoxin reductase 1 (TXNRD1), which is involved in oxidoreductase activity, exhibited a 13 fold change with a p-value of less than 0.001. Studies indicate that increases in thioredoxin reductase expression are mechanisms of airway cells to counteract oxidant stress (Wisnewski, 2002). Recently, the thioredoxin reductase antioxidant system has also been correlated with IL-8 cytokine production (Oslund, 2002). In our study, dust mediated IL-8 secretion was reduced by almost 1 fold at both 4hr and 24hr due to sorrel treatment. Cytokine evaluation revealed significant reduction in important airway remodeling mediators such as IL-6, PAI-1, and VEGF in response to sorrel alone treatments. Recently, elevated IL-6 levels have been correlated to loss of lung function in mild-moderate asthmatic patients (Neveu, 2010). Studies have shown that bronchial epithelial cells release PAI-1 in response to allergen exposure (Kowal, 2008). In this study, we found that sorrel alone treatments could reduce relative abundances of PAI-1 after dust exposure. The reduction in secretion of the aforementioned cytokines (IL-8, IL-6, PAI-1, and VEGF) suggests that sorrel could possibly provide theraupeutic benefit to those who suffer from airway inflammation and remodeling, namely those afflicted with asthma and chronic bronchitis.

Further still, dust-mediated phospho-IκB protein expression levels were found to be less than control when supplemented with sorrel treatments for 24hr. At the genomic level, thioredoxin reductase 1 (TXNRD1) was significantly increased by thirteen fold. This possibly could indicate an increase in thioredoxin, which has been found to play an important role in the reduction of NFκB, an important step in the activation of this transcription factor. Studies

indicate that overexpression of thioredoxin in the cytoplasm suppresses degradation of IκBα thus inhibiting the activation of NFκB (Hirota, 1999). The evaluation of thioredoxin protein expression levels in dust exposed NHBE cells treated with sorrel extracts is a future direction in our lab.

2.5. Conclusions

In summary, we surmise that swine confinement facility dust can induce gene modulation in normal bronchial epithelial cells. *Hibiscus sabdariffa* or sorrel extract treatments encouraged reductions in genes/proteins associated with oxidative stress, increased antioxidant defense genes/proteins, and reduced relative amounts of pro-inflammatory cytokines. However, determining the appropriate dosage and concentration of sorrel extract is crucial for therapeutic benefits to be validated. Thus, this study shows that sorrel extract is a potential antioxidant treatment for swine confinement facility dust mediated oxidative stress and inflammation; yet additional investigations need to be performed.

CHAPTER 3

Proteomic Evaluation of Swine Confinement Facility Dust on Airway Epithelial Cells

3.1. Introduction

In understanding biological processes and cellular responses, determining which proteins are involved is as crucial as knowing their abundance over time (Krijgsveld, 2004). Over the past few years, proteomics has become a tool to assess protein expression patterns (Gavin, 2002), protein network interactions (Ho, 2002), and posttranslational modifications (Mann, 2003). In this study, two-dimensional electrophoresis was employed to evaluate changes in protein expression in normal human bronchial epithelial cells (NHBE) due to swine confinement facility dust exposure and phytochemical treatments. Swine confinement facility dust has been found to induce oxidative stress in airway epithelium (Gerald, 2010). Oxidative stress is a series of events that includes an increase in reactive oxygen species, a decrease in antioxidant protection, and a failure to repair oxidative damage (Smit-de Vries, 2007). Thus, oxidative stress and the reduction of antioxidant defenses have been linked to protein modifications; which results in loss or gain of function of the protein. Our goal in this study was to compare differentially expressed proteins in dust exposed NHBE cells and NHBE cells exposed to dust and treated with sorrel/phytochemical extracts.

3.2. Materials and Methods

3.2.1. Chemicals and reagents. Primary normal human bronchial and tracheal cells or NHBE cells (PCS-300-040), and primary bronchial basal media and epithelial supplemental growth kit (PCS-300-010) were purchased from ATCC (Manassas, VA). Dust samples were collected from swine confinement facility located on the North Carolina A&T State University farm. Sorrel extracts were a gift from Dr. Leonard Williams. 2-D Starter Kits, Criterion protein

gels, and SyproRuby fluorescent stain for 2D-DIGE analysis were purchased from BioRad (Hercules, CA). Acetic acid, methanol, and ethanol were purchased from Sigma Aldrich (St.Louis, MO). Protein sample buffer was purchased from Thermoscientific.

3.2.2. Normal human bronchial epithelial expansion and culture. Primary normal human bronchial/tracheal cells were seeded in T75 flasks at a density of 500 cells/cm^2 (or $3x10^4$ cells per flask) in bronchial basal media supplemented with human serum albumin (HSA) DU hydrocortisone, linoelic acid, lecithin, epinephrine, insulin, epidermal growth factor, transferrin, triiodothyronine (T3) bovine pituitary extract, L-glutamine, penicillin/streptomycin, amphotercin B, and nystatin in a 37°C incubator, with 5% CO_2 and humidified air overnight. Media was changed the following day to remove any non-adherent cells. Cells were allowed to proliferate for a maximum of two days before replacing the media; which was changed every other day thereafter. After cultures have reached 70-80% confluency, cells were then utilized in experiments or cryopreserved in freezing medium (80% expansion medium, 10% FBS, 10% DMSO) -80°C for one day and then placed in liquid nitrogen for long term storage.

3.2.3. Dust exposure and sorrel treatments. Airway epithelial cells were grown in collagen-coated culture vessels (100 mm dishes for proteomics work) to 90-95% confluency. After reaching confluency, NHBE cells were administered 1ml of bronchial epithelial basal (BEBM) media containing 1% dust extract. Time gradients consisting of 0 hr (unstimulated), 4hr, and 24hr time points were instituted. After time points were reached, the 1% dust extract media were removed and saved for further analysis. Post-treatment of sorrel extracts in concentrations of 10, 7.5,5, 2.5% for 4hr and 24hr were added to dust exposed NHBE cells. Each post treatment extract was collected at the end of the incubation to assess for cytotoxicity and cytokine analysis. Negative controls using NHBE cells cultured in bronchial basal media were

performed in triplicate. Hydrogen peroxide (100μM) in 1ml doses were used as positive controls. Dust (1%) only and sorrel (10, 7.5, 5, 2.5%) only controls were utilized as stimulation controls. All experiments were performed in triplicate.

3.2.4. Whole cell extraction preparation for proteome isolation. Following stimulation with swine confinement facility dust and sorrel treatments, NHBE cells were gently washed with 500ul of PBS containing phosphatase inhibitors (PBS-PI) to quench any further reactions. Ice-cold extraction buffer (lysis buffer, protease inhibitors, phosphatase inhibitor) was added on ice with gentle agitation. Cell scrapers were utilized to remove all the cells from the wells. The cell suspension was then collected in microcentrifuge tubes and placed horizontally on ice for 30 minutes. Cell suspensions were sonicated in three sequential seven second bursts interspersed with 1-minute incubations on ice. Cell lysates were centrifuged at 15,000 rpm at 4°C for 15 minutes. Supernatants were then collected and transferred to a new microcentrifuge tube. The Bradford assay was used to determine protein concentrations. Lysates were aliquoted (500-1000 μg/tube) and stored at -80^{o}C until further use.

3.2.5 One-dimensional gel electrophoresis. To survey differential expression of proteins, one dimensional gel electrophoresis was initially performed on pooled (4hr, 8hr and 24hr) control, 1% dust, 10% sorrel, dust + sorrel samples. Protein lysates (50μg) along with 2x sample buffer (Pierce) were loaded into individually into duplicate (side-by-side) lanes on a 4-15% TGX gradient gel (Biorad). The gel was then ran at 100 volts for 5 min, then 200 volts for 22 min. Gels were then rinsed 2-3 times with distilled water under low agitation for a duration of 10 minutes. After rinsing, gels were then stained with Gelcode blue stain (Thermo Fisher Scientific) and gently rocked at room temperature for 1hr. Stained gels were then washed and rocked in distilled water five times. Bands that were differentially expressed between control,

sorrel and dust groups were excised (using a clean razor blade to cut as close to bands as possible; then dicing gels slices into ~1 mm cubes) and saved for further analysis. Identical excised bands from lanes were pooled. A piece of empty gel was excised to use as a negative control for material interference.

Gel slices were placed into a Protein Lowbind tube (Eppendorf) and covered with 10 mM dithiothreitol (DTT) in 25 mM NH_4HCO_3 and incubated at 56^oC for 1 hour to reduce disulfide linkages and thus expose lysine and arginine residues for tryptic digestion. The reducing solution was removed and gel pieces were washed by adding 100 μL of 25 mM NH_4HCO_3, vortexing for 10 minutes and centrifugation (via pulsing in a personal microcentrifuge). The supernatant was removed by pipetting with gel loading tips and discarded. An alkylating solution, which consisted of 55mM iodoacetamide (IAA) in 25 mM NH_4HCO_3 (50 μL), was added to gels slices and samples were placed in complete darkness (i.e., steel can with secure lid) at room temperature for 1 hour. The alkylating solution was then removed and gel pieces were washed with 100 μL of 25 mM NH_4HCO_3, vortexed and centrifuged. The gel slices were then dehydrated by two washes with 100 μL of 25 mM NH_4HCO_3 containing 50% acetonitrile (ACN), vortexing for 5 minutes, centrifuging and pipet-removal of solution with gel loading tips. For trypsin digestion, 50 μL of trypsin solution (12.5 ng/μL trypsin in 25 mM NH_4HCO_3, prepared fresh no more than 1 hr prior to use and kept on ice) was added to just cover gel slices and reactions were left overnight (12-24 hours) at 37^oC using an Eppendorf thermomixer instrument. Tryptic peptide fragments were extracted by adding 50μL of a solution containing 5% formic acid in 50% ACN and the sample was vortexed, centrifuged and transferred to a clean tube. The extraction process was repeated twice to maximize the amount of peptides collected. Samples were cleaned prior to mass spectrometry analysis by passing the sample through a C18

column according to manufacturer instructions (Pierce). A 1:10 dilution of the sample in 50% ACN:1% TFA was prepared for analysis by MALDO-TOF. The remaining portion of the peptide fragments were placed in a refrigerated speed vac for 1 hour to evaporate to dryness. The resulting peptides were analyzed by MALDI-TOF and LC-MS/MS at the Proteomics and Mass Spectrometry Facility at the Huck Institutes for the Life Sciences (Pennsylvania State University).

3.2.6 Two-dimensional gel electrophoresis. Protein lysates were isoelectrically focused on the Protean IEF Cell (Biorad 165-400) using IPG Ready gel strips pH range (3-10). Initially, at least 500 µg of protein lysates dissolved in rehydration buffer was incubated with the IPG Ready gel strips overnite at 4 -8°C in rehydration trays to rehydrate and saturate the protein onto the gel strips. Protein gel strips were then isoelectrically focused using 50A per protein strip for 5.5 hours. The focused gels were then ran in the second dimension using Criterion 10% polyacrylamide protein gels (BioRad). Protein strips were embedded and conjugated to the 10% gels using melted agarose. A standard Tris/Glycine/SDS (TGS) buffer was used as the running buffer and gel electrophoresis was performed for 65 minutes at 200V. After fractionation of isoelectrically focused proteins lysates, gels were fixed using a 40% methanol and 10% acetic acid solution. Sypro Ruby (Biorad) was used for fluorescent staining and images were taking with a Gel Doc Imager 2000 (Biorad).

3.2.7 Oxyblot. Protein oxidation (protein carbonyl formation) was detected using an OxyBlot Oxidized Protein Detection Kit. Briefly, proteins were denatured by adding an equal volume of 12% SDS to a 5 µl-volume containing 15-20 µg of protein. Protein-bound carbonyl groups were derivatized at room temperature for 15 minutes with 10 µl of 1X dinitrophenylhydrazine (DNPH) solution per manufacturer's instructions. Following 2,4-dinitro

phenyl hydrazine derivitization proteins were separated using 4-15% or 10% SDS-PAGE gels. Proteins were immobilized on nitrocellulose membranes and blocked with 5% bovine serum albumin. They were then probed with an anti-4-dinitro phenyl hydrazine antibody, followed by visualization using chemiluminescent detection and automated film processing using a Hope Autoprocessor.

3.3 Results

3.3.1 Dust mediated differential expression of proteins in NHBE cells. One dimensional gel electrophoresis analysis revealed divergent patterns of protein expression between dust exposed NHBE cells and NHBE cells exposed to dust and treated with sorrel. In Figure 3.1, control samples (Lane 2 and 3) were compared to 1% dust samples (Lane 6 and 7), 10% sorrel samples (Lane 4 and 5), and dust and sorrel treatments (Lane 8 and 9). Bands of interest which were differently expressed are highlighted in red. These bands were excised or cut from the gel and trypsinized and analyzed via LC/MS. However, LC/MS was confounded due to polyethylene glycol signal generated through the use of cell lysis buffer (Cell Signaling) which contains high levels of the polymer (see Appendix A-Figure 4).

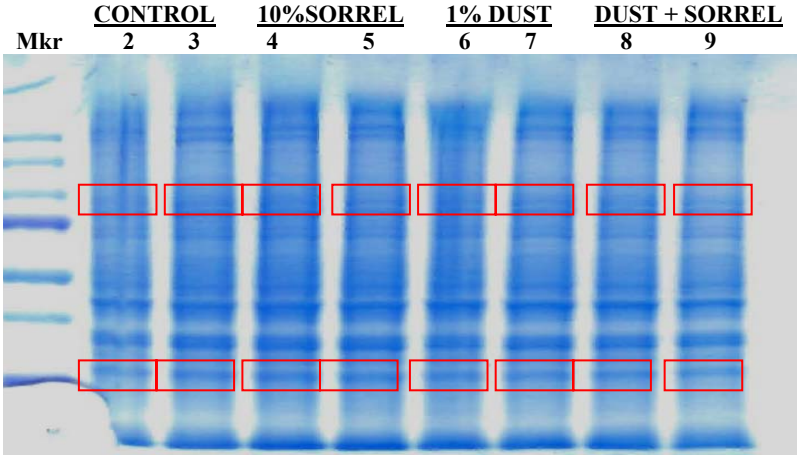

Figure 3.1. One-dimensional (1-D) gel electrophoresis of NHBE protein lysates exposed to dust and sorrel treatments for 4hr and 24hr.

Figure 3.1. (cont'd) One-dimensional (1-D) gel electrophoresis of NHBE protein lysates exposed to dust and sorrel treatments for 4hr and 24hr. Pooled samples of 4hr and 24hr control (Lanes 2 and 3), 10% sorrel (Lanes 4 and 5), 1% dust (Lanes 6 and 7), and dust + sorrel (Lanes 8 and 9), Mkr = molecular weight ladder. Bands with red outline indicate differentially expressed proteins that were excised for LC/MS.

3.3.2. Oxyblot-protein carbonylation confirmation. Verification of protein modulation via confirmation of protein carbonylation was performed using the Oxyblot Oxidized Protein Kit (Millipore). In previous studies, our lab determined that 1% dust exposure could induce oxidative stress and protein carbonylation on porcine tracheobronchial epithelial cells in vitro. This study was to demonstrate similar results in normal human bronchial epithelial cells. In Figure 3.2, analysis of oxyblot revealed modulation of dust mediated protein modification in relation to the control. Darker areas in the representative lanes indicate higher levels of protein carbonylation thus protein modification. However, through densitometry analysis (Figure 3.3), no significant modulation of proteins was found between experimental groups. For relative analysis the entire lane of each duplicated sample (Control, 1% dust, 10% sorrel, and 1% dust and 10% sorrel) was analyzed using densitometry software Alpha FluoroImager HD2.

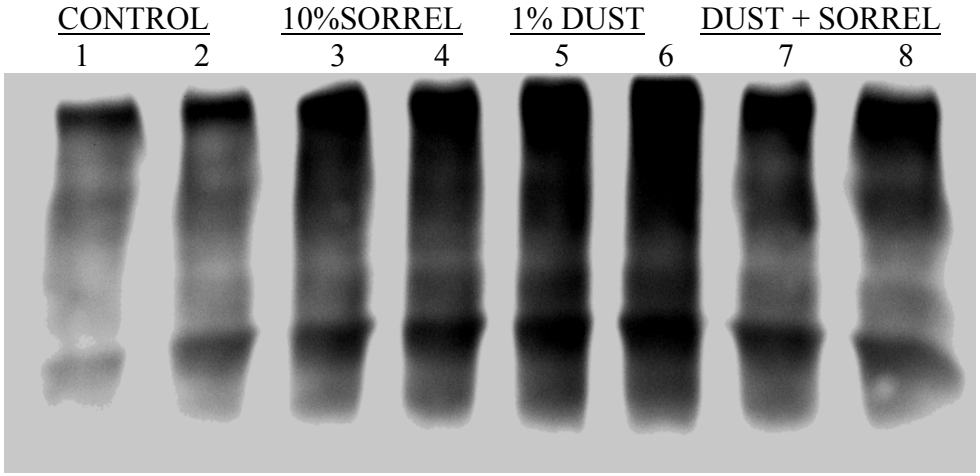

Figure 3.2. Protein carbonylation evaluation.

Figure 3.2. (cont'd) Protein carbonylation evaluation. Oxyblot analysis of 4hr, 8hr, and 24hr combined protein lysates of NHBE cells exposed to 1% Dust, 10% sorrel, and 1% dust +10% sorrel in duplicate.

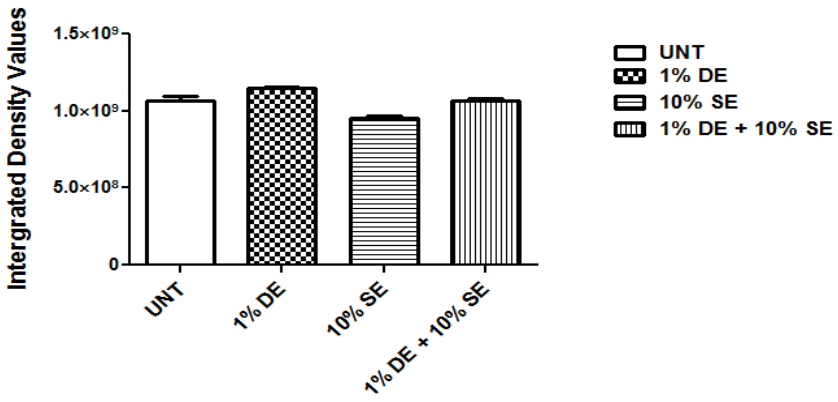

Figure 3.3. Oxyblot Analysis. Densitometry results of Oxyblot of 4hr, 8hr, and 24hr combined protein lysates of NHBE cells exposed to 1% Dust, 10% sorrel, and 1% dust +10% sorrel. *n*=2

3.3.3. 2-D gel electrophoresis of dust mediated modulation in PTBE proteomes.

Two-dimension gel electrophoresis was used to determine proteomic differences generated by 1% dust exposure on porcine tracheobronchial epithelial cells. Two-dimensional analysis allows for separation of proteins/amino acids by two dimensions, by pH via isoelectric point and molecular weight. If the pH is above an amino acids designated isoelectric point, the amino acid will carry a negative charge. However, the pH enforced is lower than the isoelectric point, the amino acid will carry a positive charge. Using a pH gradient of 3-10, complex samples of proteins can be separated before being fractionated using the SDS-PAGE method. In Figure 3.4, untreated or control porcine tracheobronchial epithelial cell lysates were analyzed via 2-D gel electrophoresis. Protein spots circled in green were considered to be prominent and denoted the proteome of untreated PTBE cell lysates.

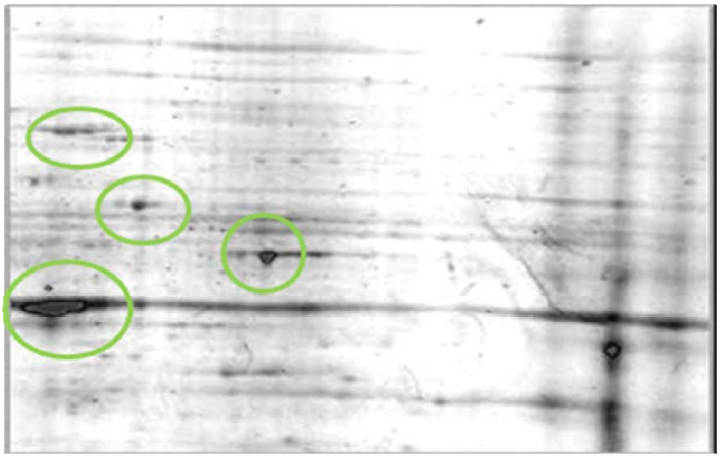

Figure 3.4. Proteome expression in untreated PTBE cells. Whole cell protein extracts of control PTBE cells were extracted and evaluated via 2-D gel electrophoresis. Representative of n=3.

In Figure 3.5, PTBE cell lysates treated with 1% dust extract for 24hr were analyzed via 2-D gel electrophoresis and revealed modulation of protein expression. In addition to previously identified control protein spots (circled in green), additional protein expression or spots (circled in red) were observed.

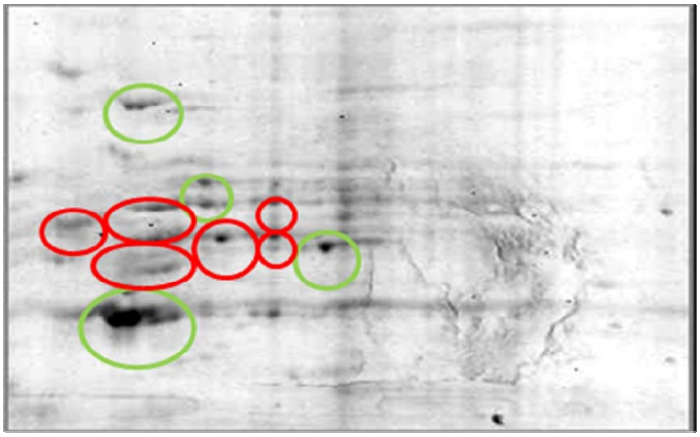

Figure 3.5. Differential proteome expression in DE-stimulated PTBE cells. PTBE cells were stimulated 24 hours with 1% DE. Dust extract induced differential expression in the proteomes of PTBE cells. Representative of n=3.

3.4. Discussion

Differential proteomic expression was observed due to the presence of 1% dust exposure using 1-D and 2-D gel electrophoresis. In previous experiments conducted in our lab, the occurrence of differential proteomes was found not only in human airway epithelium but also in porcine airway epithelium (Gerald, 2010). These differences in protein expression were produced by increases in reactive oxygen species which were determined by carbonylated protein regions deduced by Oxyblot analysis. Research has shown that during oxidative stress cellular components such as DNA, lipids, carbohydrates, and proteins can be modified through redox reactions. Proteins in particular are subject to many posttranslational modifications due to direct oxidation of amino acid residues or by the formation of reactive intermediates of carbohydrates (Grimsrud, 2008). Protein modification via carbonylation has been found to deactivate protein targets in most cases; however in some instances carbonylation can result in gain of function for some metabolic signaling systems. For example, transcriptional activation of antioxidant response genes can be upregulated by protein carbonylation (Grimsrud, 2008). In our genomic profile analyses found in Chapter 2, several antioxidant response genes were found to be upregulated due to the presence of 1% swine confinement facility dust. Conversely, sorrel (10%) treatments modulated antioxidant response genes also. Our initial hypothesis of protein modification via protein carbonylation was verified via Oxyblot analysis, yet the intensity and significance of these modifications due to 1% dust exposure were not found. This indicates that other methods of protein modification may be involved in addition to protein carbonlyation. However, through the use of 2D gel electrophoresis, variations of protein modifications mediated by 1% dust exposure were confirmed.

3.5. Conclusions

In summary, initial evaluations of protein modifications and expression were performed using 1-D gel electrophoresis. This provided an economical alternative to identifying proteins of interest which may contain carbonyl or other protein modifications. Differentially expressed proteins or bands were excised, trypsinized and analyzed via LC/MS. Due to high levels of polyethylene glycol within lysis buffer solutions, protein signals were quenched. Further analysis, using Oxyblot Protein Modification Kit, revealed protein carbonylation but not to the extent that was expected. However, 2-D gel electrophoresis confirmed the presence of different proteomes induced by exposure to 1% dust for 24hr.

CHAPTER 4

In Vitro Evaluation of Magnesium Biomaterials Exposed to Airway Epithelial Cells in Air Liquid Interface (ALI)

4.1. Introduction

Airway obstruction, caused by tracheal stenosis or tracheomalacia, is a challenging problem especially in children and infants. Traditional surgical treatments for these ailments have included the stabilization of airway lumen through metal stent implantation. The use of metal stent implants has been met with controversy due to physiological and technical difficulties associated with toxicity and inflammation; however some benefits have been attained (Weinberg, 2005). The development of obstructive granulation tissue (Vinograd, 2005), possible toxicity due to corrosion or leaching (Vearick, 2007), recovery difficulties (Noppen, 2005) and lack of biocompatibility (Pietak, 2005) have been reported as the major issues encountered with the use of metallic stents. Although the disadvantages of metallic stent use seem great, their benefits outweigh their shortcomings. Metallic stents have been found to provide smaller migration rates, conformity to abnormal airways, increased cross-sectional airway diameters, and inner stent epithelialization enabling mucociliary clearance (Noppen, 2005). Thus it is evident that metallic stents are valuable tools in the treatment of airway strictures, but so far, the ideal stent has yet to be designed.

The field of tissue engineering and regenerative medicine has increased greatly due to the development and incorporation of biocompatible and bioactive materials. More specifically, biomaterials have contributed to this growth due to their dynamic properties useful in various applications such as wound healing (Chu, 2010), drug delivery (Reis, 2006) and tissue scaffolds (Bowlin, 2010). However, in order for this revolution to continue, the safety and toxicity of these

novel materials must be properly investigated. This study evaluated the efficacy of magnesium wires as a material for scaffolding in the development of biodegradeable tracheal stents.

Magnesium (Mg^{++}) is an essential divalent intracellular cation that plays a pivotal role in daily physiological functions within the body. In fact, magnesium is necessary for the synthesis of nucleic acids and proteins, and is critical in the production and function of various enzymes and transporters (Saris, 2000). There is approximately 22-26 grams (1 mol) of magnesium within the adult human body and it is the fourth most abundant cation (Vormann, 2003). Magnesium also has important effects on the cardiovascular system (Seo, 2008) and modulates neuromuscular transmissions (Gourgoulianis, 2001). Magnesium along with calcium act in concert within the human airway to control smooth airway muscle (Gourgoulianis, 2001). The vast properties of magnesium can also be seen in the bulk material of this diverse element. Although magnesium is subject to corrosion, its corrosion resistance has been improved by alloying it with other metals such as titanium or zinc. Currently, degradable magnesium alloys are being held as promising biomaterials for applications in orthopedic and trauma surgery (Mueller, 2007). Research suggests that magnesium oxide (MgO), in the form of nanoparticles, are soluble in the epithelial lining fluid of the lungs providing some therapeutic benefit by reducing irritation. Magnesium alloys containing calcium polyphosphate particles have been found to have good mechanical properties and controlled degradation (Feng, 2011). Additionally, Mg^{++} did not inhibit cell growth and enhanced bone cell adhesion (Staiger, 2006).

The goal in this study was to examine the toxicity and cell migratory potential of normal human bronchial epithelial cells in response to magnesium wires. The air-liquid interface (ALI) cell culturing system was used as a model because NHBE cells maintained in this manner are essentially identical to tracheal epithelial cells *in vivo* with respect to structure and function. In

addition, this model reduces the occurrence of magnesium corrosion due to the lack of submersion of the magnesium in the growth medium. The genomic and proteomic analysis of NHBE cells exposed to magnesium wires revealed no substantial modulation of genes associated with oxidative stress and inflammation such as NFκB and COX-2. Low levels of lactate dehydrogenase were also exhibited suggesting minimal cytotoxicity. Thus, magnesium could be a potential substrate for the development of resorpable metallic stents for the treatment of airway obstruction.

4.2. Materials and Methods

4.2.1. Chemicals and reagents. Pure magnesium was purchased from Goodfellow (Oakdale, PA). Air liquid trans-well inserts and 6 well plates were purchased from Corning (Corning, New York). Normal human bronchial epithelial (NHBE) cells, bronchial epithelial cell basal media (BEBM), Singlequot supplement kits, and collagen were all purchased from Lonza (Walkersville, Maryland). Acetic acid was purchased from Sigma Aldrich (St. Louis, Missouri). Oxidative stress and antioxidant defense SuperArrays were purchased from Qiagen (Valencia, California). TGX gels and Western blot reagents were acquired from Biorad (Hercules, California). Lactate dehydrogenase kits were purchased from Roche (Indianapolis, Indiana). IκB and COX-2 primary antibodies and anti-rabbit IgG secondary antibodies were purchased from Cell Signaling Technology (Beverly, Massachusetts). Beta actin secondary antibody was purchased from Santa Cruz Biotechnology (Santa Cruz, California). ECL kits for Western blotting were purchased from GE Healthcare Life Sciences Division (Fairfield, Connecticut).

4.2.2. Cell culture and exposure. Primary normal human bronchial epithelial cells (NHBE) (CC-2540) were purchased mycoplasma free and source verified. NHBE cells were expanded for a period of 7-10 days in flasks until 70-80% confluency in high EGF BEBM

expansion media containing 0.13 mg/ml of bovine pituitary extract (BPE), 0.5 µg/ml of hydrocortisone, 12.5 ng/ml of human epithelial growth factor (hEGF), 0.5 µg/ml of epinephrine, 10µg/ml of transferrin, 5 µg/ml of insulin, 50nM of retinoic acid, 6.5 ng/ml of triiodothyronine, and 50 µg/ml of GA-1000. Confluent cultures were then trypsinized, spun down, pelleted, and cryopreserved in the vapor phase of liquid nitrogen at a density of $1x10^6$. For initial seeding, trans-well inserts contained in six-well plates were coated with collagen solution consisting of 13µg of collagen per ml of acetic acid for 1hr. Plates were then washed with 1x phosphate buffered saline (PBS) for 10 minutes. After aspiration of PBS, adherent cells were seeded onto collagen coated trans-well inserts and fed every two days for a period of 7 days with 2ml of bronchial epithelial cell basal growth medium (BEBM) supplemented with 0.13 mg/ml of bovine pituitary extract (BPE), 0.5 µg/ml of hydrocortisone, 5 ng/ml of human epithelial growth factor (hEGF), 0.5µg/ml of epinephrine, 10 µg/ml of transferrin, 5 µg/ml of insulin, 50nM of retinoic acid, 6.5 ng/ml of triiodothyronine, and 50 µg/ml of GA-1000. After 7 days, cells were taking to air liquid interface by aspirating media off the apical surface of the NHBE cell monolayer. Cells were then fed daily with 2ml of BEBM growth media for 14days and until mucus layer was present. Magnesium wires were manually placed on the apical surface of the cell/mucus monolayer for a time period of (0-48hrs). Microscopic observation was obtained 0, 4hr, 24hr, and 48hrs using an EVOS digital inverted light microscope (Advanced Microscopy Group) (Bothell, Washington).

4.2.3. ELISA—Pan mucin production. To examine the effect of magnesium wires on mucin production enzyme linked immunosorbent (ELISA) assay was used. Magnesium nanowires were placed in the cell/mucus monolayer for 24hrs. After exposure, NHBE cells were then rinsed with 500 µl of 1x PBS containing 100 µM ditriethylthiol (DTT) followed by a second

rinse of 500 µl of 1x PBS. Each rinse was collected and pooled for mucin ELISA analysis. β-mercaptoethanol (12.5M/5µl) was added to each sample for a final concentration of 50mM and mixed well. Mucin samples were then centrifuged at 8,000rpm for 5 minutes. Dilutions of each sample (1:10) were made in triplicate using 1x PBS, pH 7.4 and added to 96 well plate. Undiluted standards in duplicate were also added and incubated at room temperature for 2hrs and then overnight at 4°C. After incubation, contents of each well were discarded and washed twice with 1xPBS, pH 7.4. Blocking solution (200ul) containing 3% bovine serum albumin in 1x PBS, pH 7.4 was added to each well and incubated at room temperature for 2hrs. Wells were then washed twice with 1x PBS, pH 7.4. Diluted primary antibody (1:1000/50µl) in 0.3% BSA/PBS, pH 7.4 was added to the entire 96-well plate and incubated at room temperature for 1hr. Subsequently, wells were washed three times with 1x PBS, pH 7.4 and probed with 50µl of secondary antibody, anti-human IgG-HRP linked (1:2000)(Santa Cruz) and incubated at room temperature for 1hr. Well contents were discarded and washed five times with PBS, pH 7.4. For detection, a 1:1 dilution of TMB substrate solution (KPL, catalog#50-76-02) and TMB peroxidase solution (KPL, catalog#50-65-02) were added to each well (50 µl) and incubated for 30 minutes. Following 50 µl of stop solution (1M H_2SO_4), absorbance was read at 450 nm using a VersaMax microplate reader (Molecular Devices).

4.2.4. Cytokine evaluation. The secretion of eight cytokines related to oxidative stress, airway remodeling, and airway inflammation were assessed using the Human Cytokine ELISA Panel (EA-1081) by Signosis (Sunnyvale, CA). After culturing NHBE cells in the presence of pure magnesium wires for 24hr, supernatants from experimental groups and control groups were collected in 1ml aliquots in stored at -80^0 C until further use. For cytokine analysis, triplicate dilutions (1:10) of each sample were added (100 µl) and spread across the cytokine antibody

conjugated 96 well plate. Samples were incubated for 1hr at room temperature and subsequently washed three times with 1x assay wash buffer. After washing, 100 µl of biotin labeled human cytokine antibody mixture was added to each well and incubated for 1hr at room temperature with gentle shaking. Wells were aspirated and washed three times, and 100 µl of streptavidin-HRP conjugate was added to each well and was incubated for 45 minutes at room temperature with gentle shaking. After aspiration and washing, substrate (100 µl) was added to each well for 15 minutes and stop solution (50 µl) was added. Optical densities were acquired using the VersaMax microplate reader at 450nm.

4.2.5. Lactate dehydrogenase assay (LDH) – Cytotoxicity assay. To determine the cytotoxic effect of magnesium wires on NHBE cell line, the lactate dehydrogenase assay was used by Roche. Lactate dehydrogenase (LDH) is a ubiquitous enzyme located in the cytoplasm of all mammalian cells. The release of this enzyme indicates a disruption of the plasma membrane thus a reduction in cell vitality. The spent media of NHBE cells cultured in air-liquid interface was collected from the basal compartment after 24hr and 48hr exposure to magnesium nanowires. The low and high controls as well as experimental wells were collected and then spun down to eliminate cell contamination. The supernatant was then placed in fresh 96 well plates and LDH was detected according to manufacturer's instructions using a Molecular Devices VersaMax microplate (Sunnyvale, California) reader at 490 nm.

4.2.6. Reverse transcription polymerase chain reaction. Total RNA was isolated using an RNeasy mini kit and an RNase-free DNase set (Qiagen, Valencia, CA). RNA (800ng) from each treatment group and control was reversed transcribed to produce cDNA using the iScript synthesis cDNA kit (BioRad, Hercules, CA). The iScript Reverse Transcriptase Kit was used to generate cDNA according to manufacturer instructions. Briefly, the total RNA (800ng) was

combined with 5X iScript Reaction mix, nuclease-free water and iScript Reverse Transcriptase in a 25 µl reaction. The samples were incubated in a iCycler thermal cycler (BioRad) using the following reaction protocol: 5 minutes at 25°C, 30 minutes at 42°C, 5 minutes at 85°C and held at 4°C. The generated cDNA was then probed for pro-inflammatory mediators such as NF-κB and COX-2 using the primers described in Table 4.1 produced from Invitrogen software. For the amplication of cDNA, GoTaq® Green Mastermix and protocol were used according to manufacturer's instructions. For a 25ul reaction, 12.5µl of 2x GoTaq® Green Mastermix, 1µl of forward primer, 1µl of reverse primer, 4µl of template DNA, and 6.5µl of nuclease free water were combined and added to a RNase free and sterile PCR plate for each gene and sample. The samples were incubated in a preheated (95°C) iCycler thermal cycler (BioRad) using the following reaction protocol: 4 minutes at 94°C; 35 cycles of 95°C for 30 seconds, 60°C for 30 seconds, 72°C for 1 minute; and post-extension for 4 minutes at 72°C; and hold at 4°C. PCR products were resolved on 1% agarose gel in 1X Tris-Borate-EDTA buffer , pH 8.0 (Boston Biologicals, Wellesley, MA) at 160 volts (V) and visualized using ethidium bromide.

Table 4.1.

Primers used for pro-inflammatory gene modulation evaluation.

Primer	Sequence 5'-3'	T_m (°C)	Amplicon Length (bp)
NF-κB chr4:103884954-103885650	(F)CACCTAGCTGCCAAAGAAGG	60.0	657
	(R)GCCAATGAGATGTTGTCGTG	60.1	
COX-2 chr1:183377409-183378512	(F) CAGCACTTCACGCATCAGTT	60.1	1064
	(R)CAGCAAACCGTAGATGCTCA	60.0	

4.2.7. Western blot analysis. Whole cell lysates were extracted from NHBE cells in control and magnesium wire exposed groups and quantitated using the Bradford assay. Equal amounts of protein were loaded in each lane with 4x sample loading buffer. Samples were boiled at 100 °C for 5 min before gel loading. Lysates (50μg) were then fractionated using 10% TGX gels (Biorad) by sodium dodecyl sulfate-polyacrylamide gel electrophoresis (SDS-PAGE) at 150 volts for 45 minutes. Fractionated proteins were transferred to nitrocellulose membranes using a semi-dry method at 10V for 60 minutes. After blocking in 5% milk, nitrocellulose membranes were washed twice with tris-buffered saline-tween (TBS-T). Membranes were probed with primary antibody in 0.5% bovine serum albumin solution (BSA) and gently rocked overnight at 4°C. Primary antibodies used were anti-human rabbit IκB (Cell Signaling), anti-human rabbit COX-2 (Cell Signaling), and goat β-actin (Santa Cruz) at a concentration of 1:1000. Probed membranes were washed and secondary antibody anti-rabbit IgG (Cell Signaling) (1:2000) was used to detect primary antibodies. After washing, ECL detection reagents were added (3ml) to probed membranes for one minute and subsequently exposed to film for automated development. Developed blots were then scanned and band densities were analyzed using Applied Biosystems FluorChem HD2 image acquisition and analysis software.

4.2.8. Wound repair. Cellular interaction and migration potential in response to magnesium wires was evaluated by utilizing the wound repair method. After 21days, the NHBE cell monolayer including mucus layer was cut using a sterile blade. One magnesium wire was inserted into the wound for a period of 24hrs and 48hrs. Phase contrast microscopy images were taken 0hr, 4hr, 24hr, and 48hrs to monitor the progression of wound healing and cellular migration.

4.2.9. Scanning electron microscopy (SEM). After incubation with NHBE cells in air liquid interface for 24hrs, magnesium wires were examined by SEM (Shimadzu) to characterize the surface morphology of the recovered wires.

4.2.10. Statistical analysis. Statistical differences between the means were determined with ANOVA software and a treatment effect with *P* value of <0.05 was considered significant. Individual groups were compared with the unpaired Student's *t*-test. All results were expressed as means of ± standard deviation of at least three biological experiments.

4.3. Results

4.3.1. ELISA evaluation of mucin secretion. Enzyme linked immunosorbent assay (ELISA) was utilized to determine if magnesium wires inhibited or increased mucin production in NHBE cells. At 24hrs, a reduction in magnesium wires-mediated mucin production was found in relationship to the control (Figure 4.1).

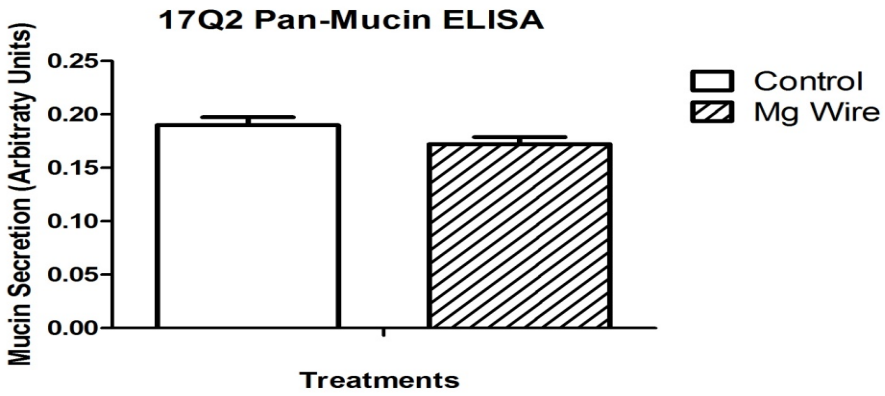

Figure 4.1. Assessment of airway mucus secretion due to magnesium wire exposure of 24hr. *In vitro* evaluation of global mucin production in NHBE cells, where mucin was collected following 24 hr exposure to Mg wires. Pan-Mucin ELISA was performed. Data are presented as mean ± SEM, n=9.

4.3.2. Cytokine profile assessment. To assess cytokine secretion in response to the presence of magnesium wires in culture with NHBE cells for 24hrs, a panel of cytokines related

to oxidative stress, airway inflammation, and airway remodeling were evaluated. In relationship to control, relative abundances of each cytokine (VEGF, EGF, IL-6, Resistin, Plasminogen activator inhibitor-1 (PAI-1), IL-12, IL-13, and Eotaxin) were obtained, however no significant increases in secretion were found through ELISA analysis shown in Figure 4.2.

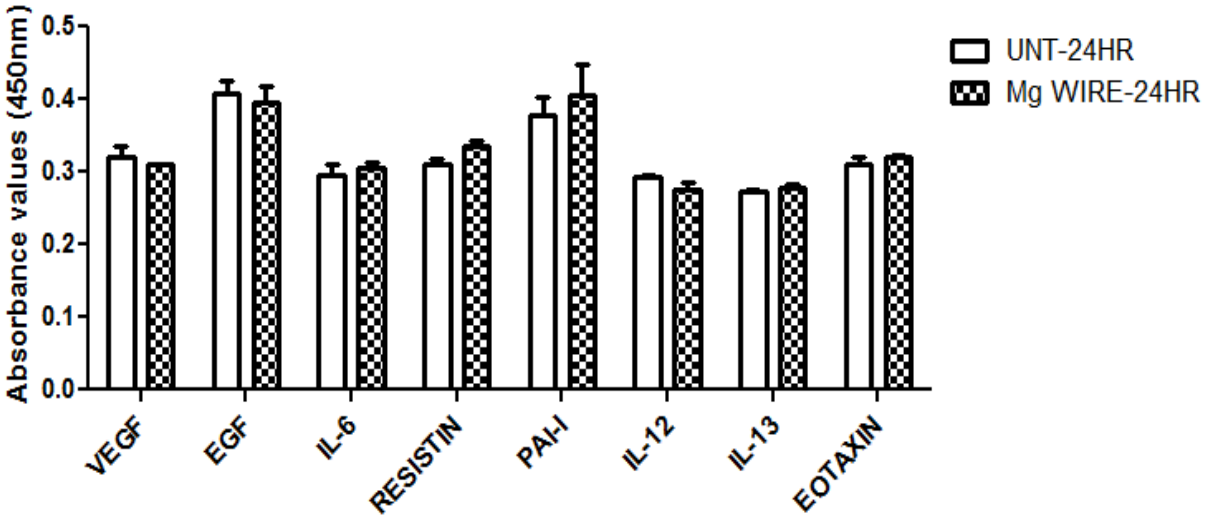

Figure 4.2. Human cytokine profile assessment in response to magnesium wire. ELISA analysis revealed no significant modulation in cytokines involved in airway remodeling, airway inflammation, and oxidative stress.

4.3.3. Cytotoxicity of magnesium wires. In recent studies, magnesium ions produced by the interaction of cells with magnesium materials have caused serious problems when using cellular based assays such as MTT and LDH. False negatives or positives and interference with dye stability have been an issue when analyzing the biocompatibility of metal alloys *in vitro* (Witte, 2006). However, within this study, our experimental design which employs a technique that enables complete cellular interaction with our magnesium substrate without media submersion which prevented Mg ion interference. LDH was monitored at 24hr and 48hrs for control and Mg wire exposed NHBE cells. Magnesium wire only controls were also incorporated. In Figure 4.3, in relation to the control, magnesium wires induced 18% cytotoxicity

after 24hrs and 36% after 48hrs. It should be noted that fully differentiated NHBE cells demonstrate high levels of lactate dehydrogenase release, thus levels in control cells are normally high.

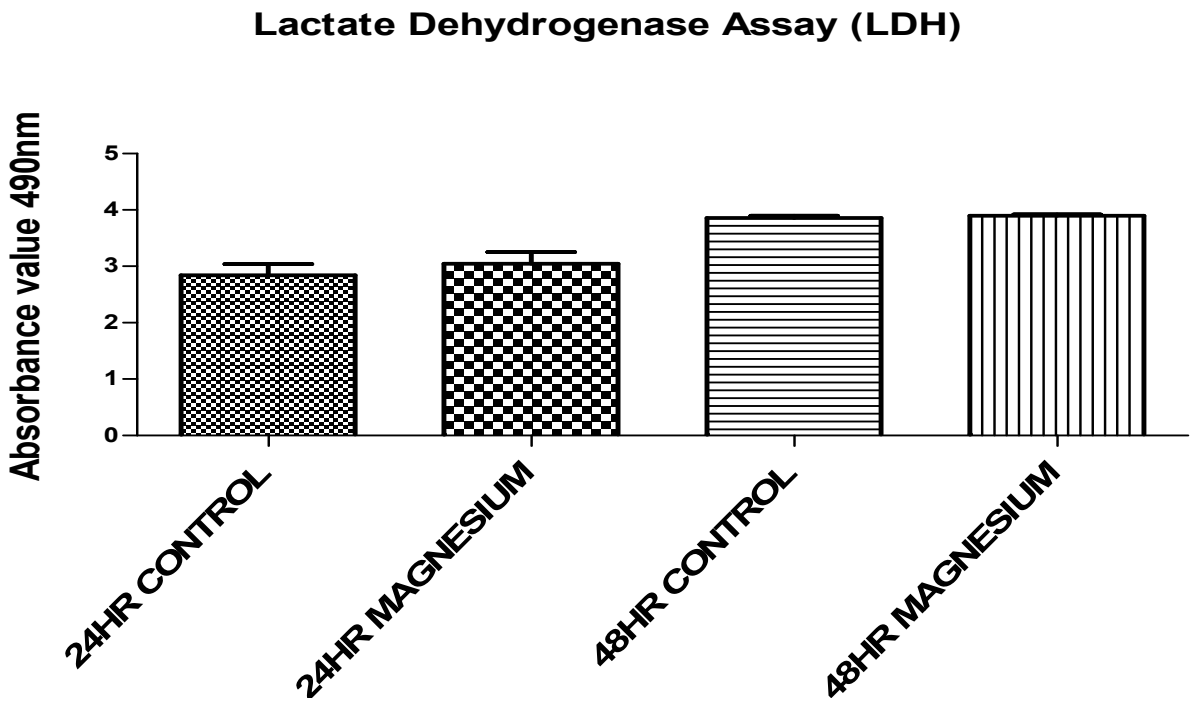

Figure 4.3. Cytotoxicity analysis of magnesium wire in NHBE cells at 24hr and 48hr. Lactate dehydrogenase assessment to determine plasma membrane damage of NHBE cells in air-liquid interface exposed to magnesium wires for 24hr and 48hr. Data are presented as mean ± SEM, *n*=9.

4.3.4. Pro-inflammatory genes unmodulated in response to magnesium wire exposure. The evaluation of gene modulation is a necessary assessment that gives insight of molecular changes induced by cellular interaction with biomaterial substrates. Genomic profiles of NHBE cells exposed to magnesium wires for 24hr were obtained for NFκB and COX-2 using polymerase chain reaction kit provided by BioRad. In Figure 4.4, less than 0.5 fold change can be seen in NFκB gene expression indicating that no inflammatory processes were upregulated

due to the presence of magnesium. The same trend can be seen in COX-2 gene expression (Figure 4.5).

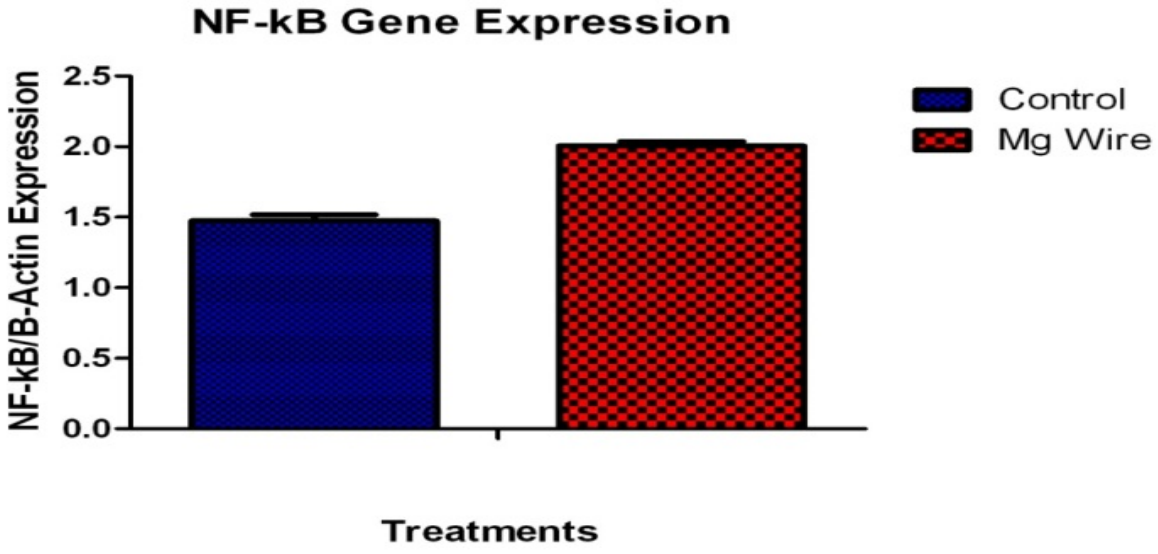

Figure 4.4. Quantitative polymerase chain reaction assessment of NFκB gene modulation in NHBE cells at 24hr. qPCR reveals no significant modulation of transcription factor NF-κB in NHBE cells after 24hr exposure to magnesium wires. Data are presented as mean ± SEM, n=6.

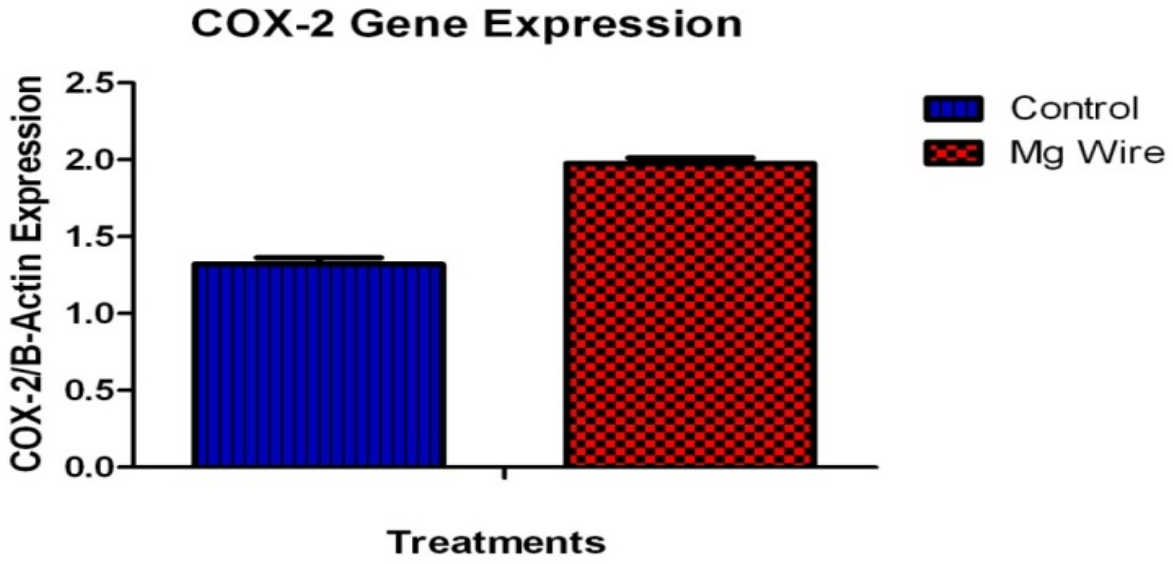

Figure 4.5. Quantitative polymerase chain reaction assessment of COX-2 gene modulation in NHBE cells at 24hr. qPCR reveals slight modulation of COX-2 in NHBE cells after 24hr exposure to magnesium wires. Data are presented as mean ± SEM, n=6.

4.3.5. Western blot analysis. Using the Western blot method to validate genomic profiles of NHBE cells exposed to magnesium wire for 24hr, IκB-α, a regulator of NFκB, was found to be protected from phosphorylation. The phosphorylation and degradation of IκB-α symbolizes the inactivation of the inhibitory complex composed of IκB-β and IκB-α. This complex prevents NFκB, which is normally sequestered in the cytoplasm, from entering into the nucleus and transcribing pro-inflammatory genes such as cyclooxygenase 2 or COX-2. We found in Figure 4.6a that in relationship to the control, there was no degradation of IκB-α suggesting that the presence of the magnesium nanowire for 24hr did not induce oxidative stress. In similar studies, the generation of free radicals i.e. oxidative stress from the presence of metal alloys, were found to induce the phosphorylation of IκB encouraging the transcription of key pro-inflammatory proteins (Valko, 2006). COX-2 expression was not significantly increased due to the presence of magnesium nanowire after 24hr in Figure 4.6b. Figure 4.6c represents beta-actin loading controls.

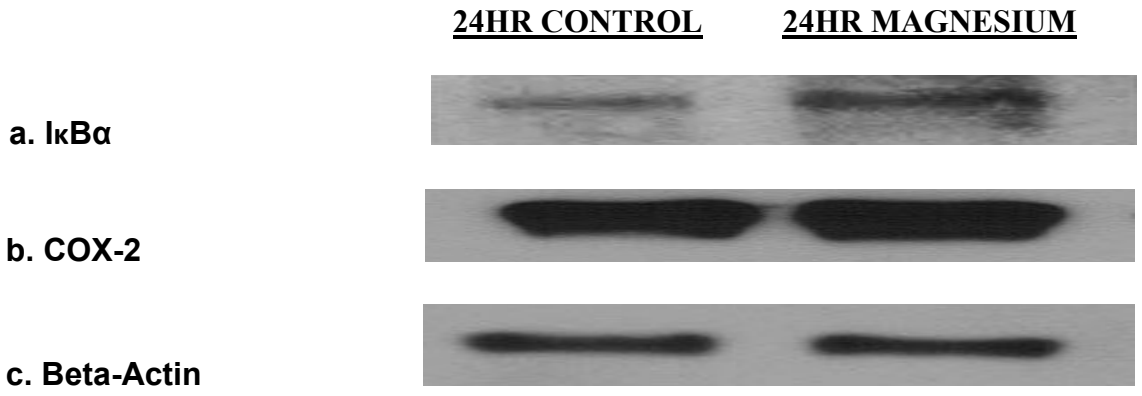

Figure 4.6. Western blot analyses of key inflammatory and oxidative stress mediators in NHBE cells at 24hrs of exposure. Immunoassay of Inhibitor of kappa B, Iκ-Bα (a), and cyclooxygenase-2, COX-2(b) revealed that there was no detectable inflammation caused by Mg wires. Beta-actin (c) expression was used as loading control.

IκBα protein analysis is quantitatively evaluated through densitometry in Figure 4.7. COX-2 protein expression was expressed quantitatively in Figure 4.8 and indicates no upregulation due to 24hr exposure to magnesium.

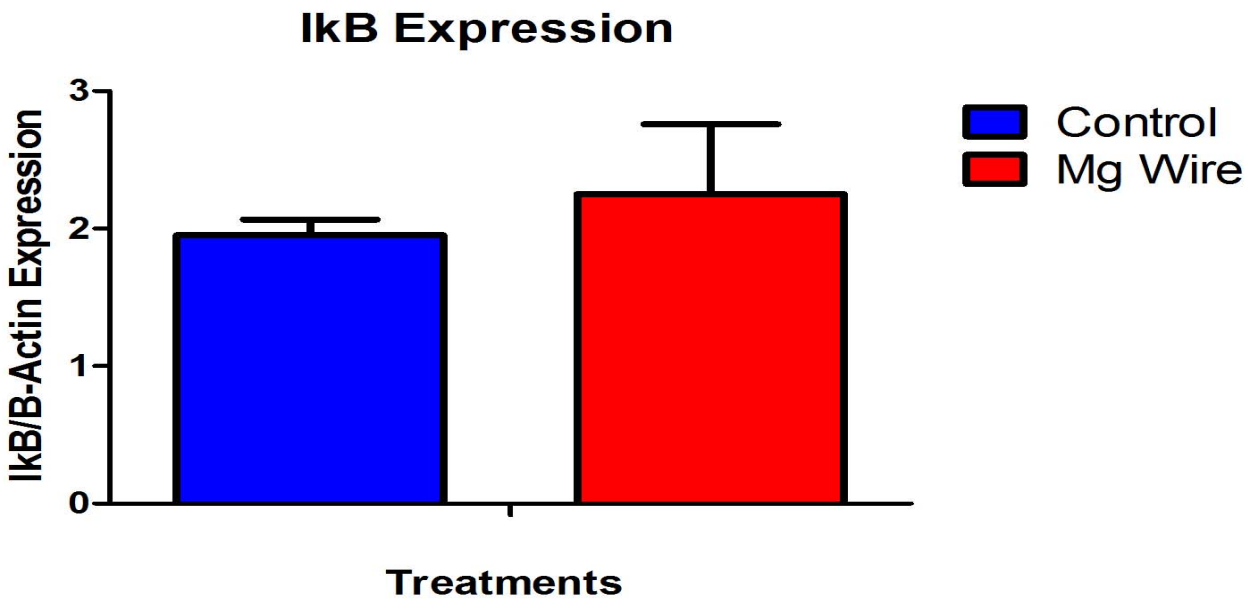

Figure 4.7. Densitometry analysis of IκBα protein expression in NHBE cells after 24hr of exposure to Mg wires. No significant upregulation of IκBα in NHBE due to presence of magnesium wires for 24hr as determined by one-way analysis of variance (ANOVA). Data represents the mean ± SEM, n=6.

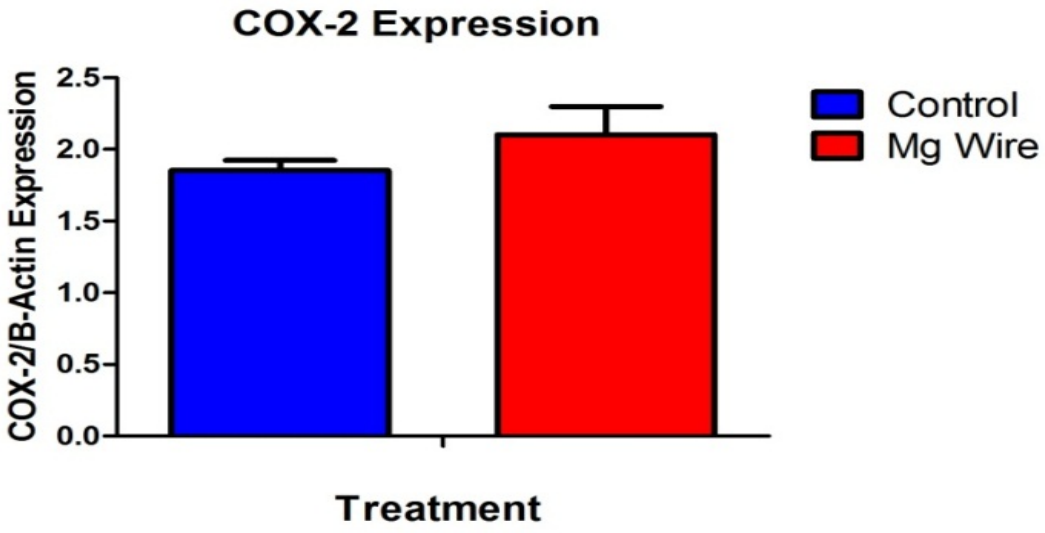

Figure 4.8. Densitometry analysis of COX-2 protein expression in NHBE cells after 24hr exposure to Mg wires. No significant differences between COX-2 protein expression levels as determined by one-way analysis of variance (ANOVA). Data represents the mean ± SEM, n=6.

4.3.6. Wound repair. The wound repair assay has been used to evaluate the potential of various agents to close manually or chemically induced wounds for many years. Magnesium has been found to be a prevalent ion in many processes within the body. To determine the impact of magnesium on wound repair, magnesium wires were placed in a NHBE cell monolayer wound for 24hr and 48hrs. The progress of wound healing as depicted in Figure 4.9 was recorded at (A.) 0hr (B.) 4hr (C.) 24hr and (D.) 48hr. The white arrow in Figure 4.9B indicates the location of the magnesium wire. Hydrogen bubble formation can be seen at 4hrs, which increase over time. After 48hrs, the Mg wire was degraded by 75%. Cell migration can be seen in the upper left corner of the wound as cell formations move towards the magnesium wire to initiate wound healing.

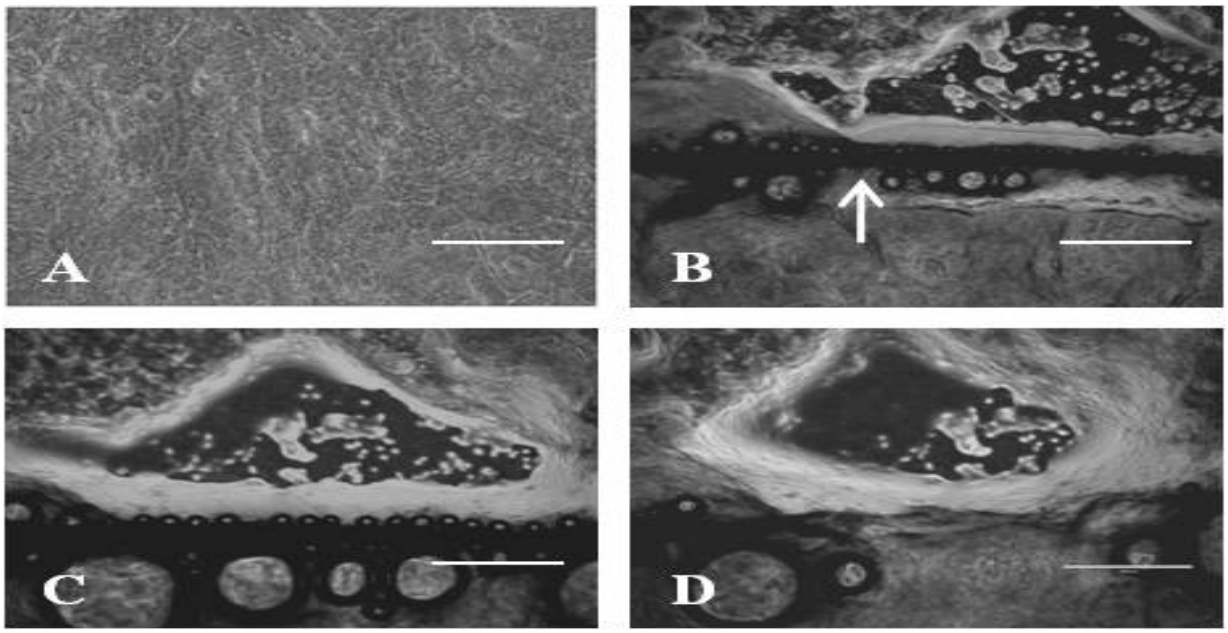

Figure 4.9. Phase contrast images of wound repair assay. Images (left) of fully differentiated NHBE monolayer (A) prior to injury and Mg wire (arrow) exposure and (B) 4 hr with migrating NHBE cells in upper left region, (C) 24 hr, NHBE cells have migrated to the center of wound and (D) 48 hr post-injury NHBE cells have migrated and repaired right hand portion of wound and wound area is decreasing. Scale bar, 1000 μm.

4.3.7. Minimal degradation of Mg wire after 24hrs using SEM. The degradation of magnesium wires was evaluated after in vitro exposure using scanning electron microscopy. The width of control and experimental wires were determined using imaging analysis software. A negligible reduction in width was found of 4μm in Figure 4.10. Some cracking and corrosion can be seen 4.10b in comparison to the control in 4.10a, demonstrating moderate dissolution of the magnesium wire into the epithelial lining fluid.

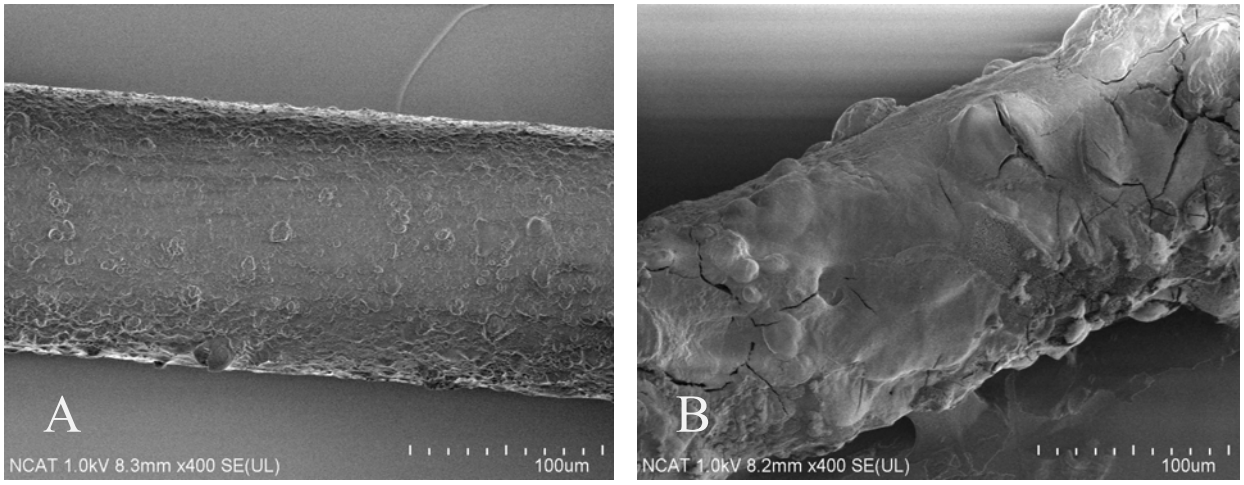

Figure 4.10. Scanning electron microscopy images of Mg wires after 24hr of NHBE/ALI culture**.** (A) Mg wire (0hr of exposure) and (B) 24hr of NHBE/Mg wire exposure. Average rates of degradation were 4μm after 24hr, (n=3).

4.4. Discussion

The development of the ideal metallic stent for the treatment of malignant or benign tracheal obstructions has been met with many challenges. For example, metallic tracheal stents have been associated with various complications such as mucus plugging and granulation formation (Lemaire, 2005), stent fracture and migration (Chung, 2008), difficult recovery (Brietenbucher, 2008), and fistula development (Sihvo, 2006). To alleviate many of these obstacles, the optimization of the stent material has been implemented. In this study we evaluated the use of magnesium wires as a biodegradeable tracheal stent material. The use of magnesium alloys as biomaterials is a relatively new concept but has gained some momentum in orthopedic and osteogenic applications. Recently in a study to compare magnesium alloys to titanium alloys that are currently in clinical bone implant use, magnesium alloys did not provoke any systemic inflammatory response or generate fibrotic tissue. This study also revealed that the magnesium alloy enhanced bone response, which was a result of significantly higher bone-implant contact and bone volume per tissue volume (Castellani, 2011).

Additionally, the benefits of magnesium biomaterials have been found in cardiovascular applications. For example, the magnesium alloy, AE21, has been used in cardiovascular stents to provide predictable degradation kinetics, and negligible thrombogenic and inflammatory responses in porcine models (Heublein, 2003). It has also been theorized that magnesium may have therapeutic value due to its role as a cofactor of ATPase and calcium antagonist thus possibly preventing ischemic complications caused by intracellular calcium overload and platelet aggregation (Erne, 2006).

To date, there have been few studies evaluating the efficacy of magnesium alloys as a core material for tracheal stenting. To determine the value of pure magnesium as a potential tracheal stent material initial cytotoxicity assays were conducted. The occurrence of cytotoxicity in relationship to cell/material interaction can be caused by many factors. One main factor is the influx of metal ions from the degradation of implanted biomaterials. Increases in systemic levels of metal alloying ions such as manganese have been found to induce neurotoxicity (Crossgrove, 2004) and zirconium ions have been found to be associated with liver, lung, breast and nasopharyngeal cancers (Song, 2007). Within this study, we concluded that pure magnesium posed no significant cytotoxicity to normal human bronchial epithelial cells. Lactate dehydrogenase (LDH) assay revealed low levels of LDH release in relationship to the controls after 24hr and 48hr. Similar findings have been found in studies exposing pure magnesium biomaterials to mouse bone marrow cells (Li, 2004). Additionally, the generation of metal ions from degraded metal biomaterials has been thought to promote oxidative stress (Purnama, 2010).

Oxidative stress, which is the imbalance of free radicals and antioxidants, can activate important pro-inflammatory transcription factors such as nuclear factor kappa B or NF-κB. NF-

κB not only plays a role in initial inflammatory response but also in cell cycle progression, cell growth, and neoplastic transformation (Chen, 2002). In our genomic evaluation of normal human bronchial epithelial cells exposed to pure magnesium for 24hrs, no significant modulation of NF-κB was found. However, at 24hrs of exposure there was some degradation of the magnesium wire and gas bubble formation. In comparison to the control, NF-κB was not upregulated due to these occurrences suggesting that the metal ions produced from the interaction of epithelial lining fluid and cells with Mg did not induce oxidative stress.

Prostaglandin II or COX-2, an essential pro-inflammatory mediator, was not found to be substantially modulated due to the presence of magnesium as well. Yet, some studies involving metal ion exposures have suggested the possibility that these ions are blocking the expression of these regulatory genes (Roussel, 2000). One study used to assess the possible mechanism of action of chromium (VI) and arsenic (III) ions, found that NF-κB activation was inhibited through the interference of inhibitory molecule, IKK and NF-κB DNA binding or from impeding the activity of cAMP-responsive element binding protein or (CREB) (Shumilla, 1999). These scenarios could be occurring within our magnesium studies, however more work needs to be performed. Conversely, if transcriptional activity of NF-κB is being inhibited from the presence of magnesium ions, then all of its regulatory functions would be offset including cell growth. This is not the case due to the high level of cell migration seen in our wound repair assays. Additionally, mucin production was not affected by magnesium wires suggesting that differential normal human bronchial epithelial cells maintained functionality and cell cycle progression.

4.5 Conclusion

We have determined that pure magnesium had no modulatory effect on pro-inflammatory genes (NF-κB or COX-2) in normal human bronchial epithelial cells after 24hrs in air liquid interface (ALI) culturing system. No differential expression of IκB-α or COX-2 proteins was exhibited in Western blot analysis, which validates genomic analysis. Cytotoxicity analysis correlated with genomic and proteomic evaluations in that no relevant increases of lactate dehydrogenase were found after exposure time points of 24hr and 48hrs. Mucin production and cell migration were unaffected due to magnesium interaction suggesting that cell cycle progression, cell growth and functionality were maintained. The above tests support the efficacy of using magnesium biomaterials in tracheal stent development and fabrication. However, further testing of possible alloying elements needs to be performed.

CHAPTER 5

The Cytotoxic Potential of Bioremediation Nanomaterials on Osteoblasts

5.1. Introduction

Environmental remediation is a growing field of research as the list of current or ongoing remediation projects now stands at an estimated 294,000 sites within the United States (Watlington, 2005). These projects range from Superfunds to Underground Storage Tanks (USTs), each having momentous tasks of cost effective and efficient cleanup due to vast levels of soil and water contamination. To date the gold standard in groundwater remediation is the "pump and treat" method. The pump and treat method utilizes the system of collecting contaminated water downstream from the site of contamination and treating the water before returning it to the ground. This remediation technique has been found to be not highly effective, expensive, and time intensive according to a USEPA 2004 report. However, pump and treat systems still account for 67% of all ground water remedies in current or proposed remediation projects (USEPA, 2004). However, there are continuing efforts to improve and develop remediation technologies within this industry.

In recent years, the emergence of nanotechnology has found great application in the field of remediation. It has been theorized that the three categories in which nanotechnology could influence environmental remediation are treatment and remediation, sensing and detection, and pollution prevention (Masciangoli, 2003). Nanomaterials such as nanoparticles, due to their novel properties such as robust surface area, self-assembly potential, high reactivity and specificity, make excellent candidates for water treatment applications (Hristovski, 2007). For example, nanopowders, consisting of metal oxides, were incorporated into fixed bed columns for the removal of arsenic in drinking water during municipal treatment (Hristovski, 2007). Other

endeavors using the diverse nanoclays include oil and grease removal from water (Sancha, 2010), uptake of heavy metals and endocrine disrupting chemicals (Churchman, 2006), and inhibition of organic leachates from waste disposal sites (Theng, 2006). Additionally, metal nanoparticles such as zero valent iron (nZVI) have been used for the removal of highly volatile chemicals and arsenic from groundwater (Krajanpan, 2007).

Many advantages and benefits have been found with the utilization of nanoclays in environmental remediation. However, the consequences on human health through the use of these materials must be investigated as well. Some studies have shown that nanoclays have no genotoxic effect and slight cytotoxicity on Chinese Hamster Ovary (CHO) cells (Li, 2010). However, various forms of iron nanoparticles have been associated with inflammation (Veranth, 2007), the formation of apoptotic bodies (Stroh, 2004), impaired membrane function, and lactate dehydrogenase leakage. Within this study, derivatives of montmorillonite clay (Cloisite 10A, Cloisite 20A, Cloisite 25A, 93A) were evaluated for their cytotoxicity on osteoblastoma cell line, hFOB 1.19 via MTT [3-(4,5-dimethylthiazol-2-yl)-2,5-diphenyltetrazolium bromide, a tetrazole] and LDH (lactate dehydrogenase) assays.

5.2. Materials and Methods

5.2.1. Reagents. Cloisite 10A, 20A, and 25A were purchased from Southern Clay Products. Dulbecco's Minimal Essential Media (DMEM) and fetal bovine serum (FBS) was purchased from ATCC (Manassas, VA). MTT and LDH kits were purchased from Roche (San Franscisco, CA). Osteoblasts (hFOB 1.19) (catalog# CRL-11372) were purchased from ATCC (Manassas, VA).

5.2.2. Cell culture. Osteoblasts (hFOB 1.19) (ATCC) were cultured in Dubcellco's Minimum Essential Media (DMEM) with 10% fetal bovine serum and gentamacin in 37°C at 5%

CO^2 in T75 flasks. After aspiration of old media, cell monolayers were rinsed with 1xPBS (phosphate buffered saline) every 2 days and 15ml of new media was added. At 80-90% confluency, cells were subcultured to a density of $1x10^6$/ml and cryopreserved in liquid nitrogen until further use.

5.2.3. Lactate dehydrogenase assay (LDH)- plasma membrane damage. To determine the effect of nanomaterials on hFOB1.19 osteoblast cell line, the lactate dehydrogenase assay was used. Lactate dehydrogenase (LDH) is a ubiquitous enzyme located in the cytoplasm of all mammalian cells. The release of this enzyme indicates a disruption of the plasma membrane thus a reduction in cell vitality. One vial of $1x10^6$ OST-1 cells were subcultured into a 96 well plate and allowed to adhere for 24hrs. After seeding, media was aspirated and a gradient (0.5, 1, 2.5, and 5%) (w/v) of nanomaterials diluted in DMEM (9ml) was added to the cells across the plate in triplicate. No treatment (negative control), positive control of 300mM of hydrogen peroxide (H_2O_2), and high control (1x cell lysis buffer-Cell Signaling) plates were also performed. LDH levels were evaluated at 0hr, 4hr, and 24hr time points according to manufacturer's instructions (Roche). Supernatant of all control and experimental wells were collected and placed in fresh 96 well plates, then spun down to eliminate cell contamination. LDH was detected according to manufacturer's instructions and absorbance was measured using the Versamax microplate reader (Molecular Devices) at 490 nm.

5.2.4. MTT Assay—Inhibition of cell proliferation. MTT or (3-(4,5-Dimethylthiazol-2-yl)-2,5-diphenyltetrazolium bromide is a tetrazolium salt that when added to the cell culture of viable cells, is metabolically reduced into insoluble purple crystals called formazan. After solubilization, formazan can be optically detected and thus give an indication of the vitality of treated cells. In a 96 well format, OST-1 cells were subcultured to a density of $3x10^5$ per well

and allowed to adhere overnite. Spent media and nonviable cells were aspirated and a gradient (0.5, 1, 2.5, and 5%) of nanomaterials diluted in DMEM (9ml/100µl per well) was added to the cells across the plate in triplicate rows. Cells were incubated with the nanomaterials for 0hr, 4hr, and 24hr then aspirated off and fresh media (100µl/well) was applied. 10µl of MTT reagent (Roche) was then added to culture media and incubated for 4hrs at 37°C in 5% CO_2. After incubation, 100µl of solubilization solution was added and formazan crystals were allowed to dissolve. Absorbance readings were taken using the Versamax microplate reader (Molecular Devices) at 490 nm.

5.2.5. Statistical analysis. Each experiment was replicated three times and data are presented as mean $\pm$ SEM (standard error of mean). Statistical analysis of the data was carried out using GraphPad. Differences were analyzed with the student's *t*-test and considered significant at the *P*-value <0.05.

5.3. Results

5.3.1. Lactate dehydrogenase assay—Cytotoxicity assessment. The lactate dehydrogenase assay is utilized in cytotoxicity assays to determine the amount of membrane damage that is imposed to mammalian cells due to the presence of toxic agents. Within this assay, standard gradient concentrations of nanoclays 10A, 20A, 25A, and 93A were interacted with osteoblastoma cell line, hFOB 1.19 (ATCC) after cells were seeded for 24hrs. Figure 5.1A-D represents data collected for each nanoclay at 4hrs. Cloisite 10A nanoclay at 0.5% induced a significant increase of absorbance, which directly correlates with the increase in the presence of LDH in the media. At 1%, Cloisite 10A exhibited significantly higher (*p*-value <0.05) absorbance values in relationship to the control. Higher concentrations of Cloisite 10A produced lower amounts of LDH than lower concentrations. Interestingly at Cloisite at 5%, LDH levels

were below control values. Cloisite 25A (0.5% and 1%) (Figure 5.1C) exhibited significantly higher LDH production in relation to the control.

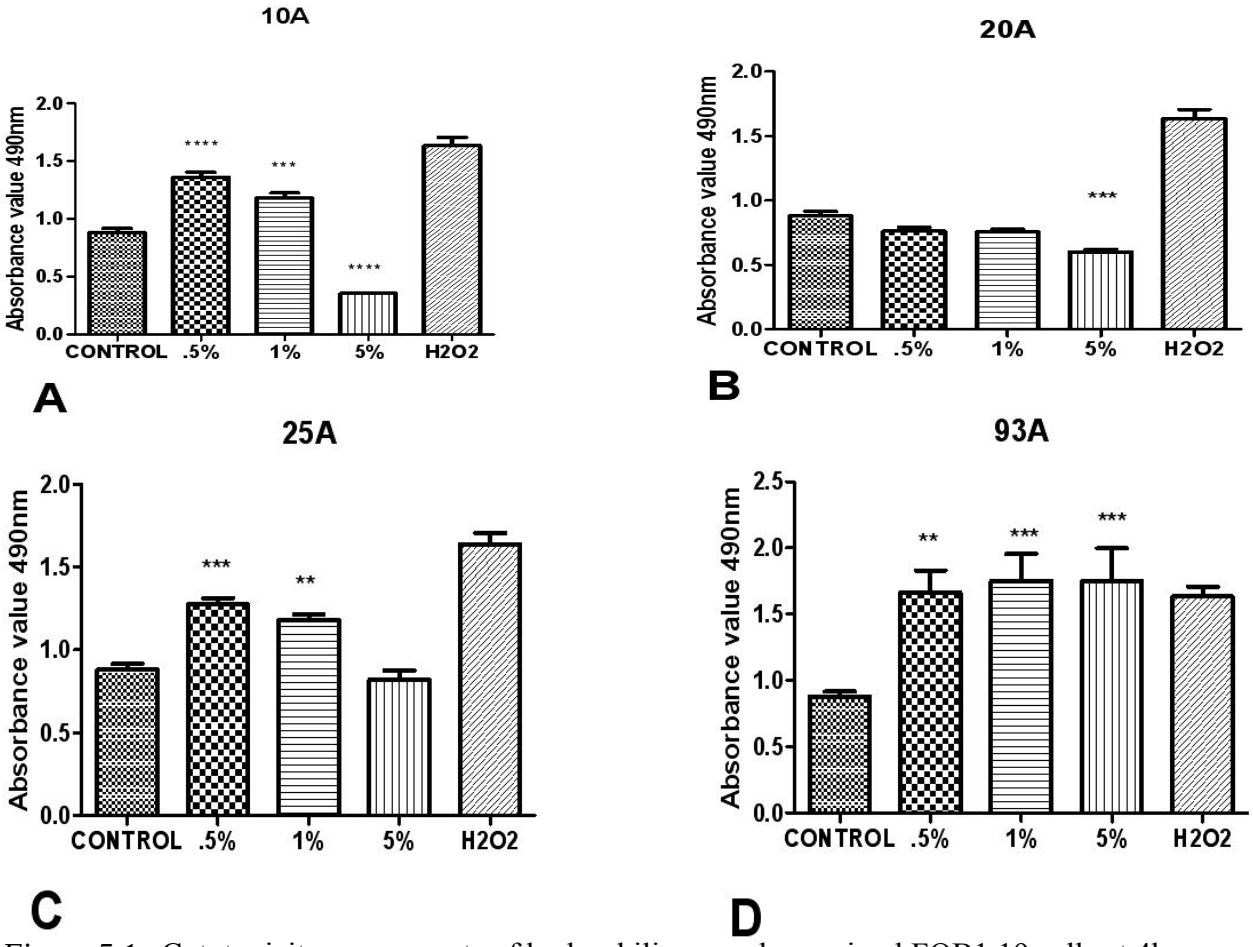

Figure 5.1. Cytotoxicity assessments of hydrophilic nanoclays using hFOB1.19 cells at 4hr. Lactate dehydrogenase assay on osteoblast cells exposed to 10A, 20A, 25A, and 93A nanoclays for 4hrs showing differences in cytotoxicity for each nanoclay.

Cloisite 25A at 5% did not encourage a significant production of LDH in relationship to the control. Cloisite 93A (Figure 5.1D) induced significantly (p-value <0.05) higher leakage of LDH, as absorbance values were equivalent to our high control of 100µM hydrogen peroxide (H_2O_2). At 24hrs (Figure 5.2A-D), all four nanoclays (10A, 20A, 25A, 93A) encouraged high levels of LDH leakage similar to the high control of hydrogen peroxide (100µM).

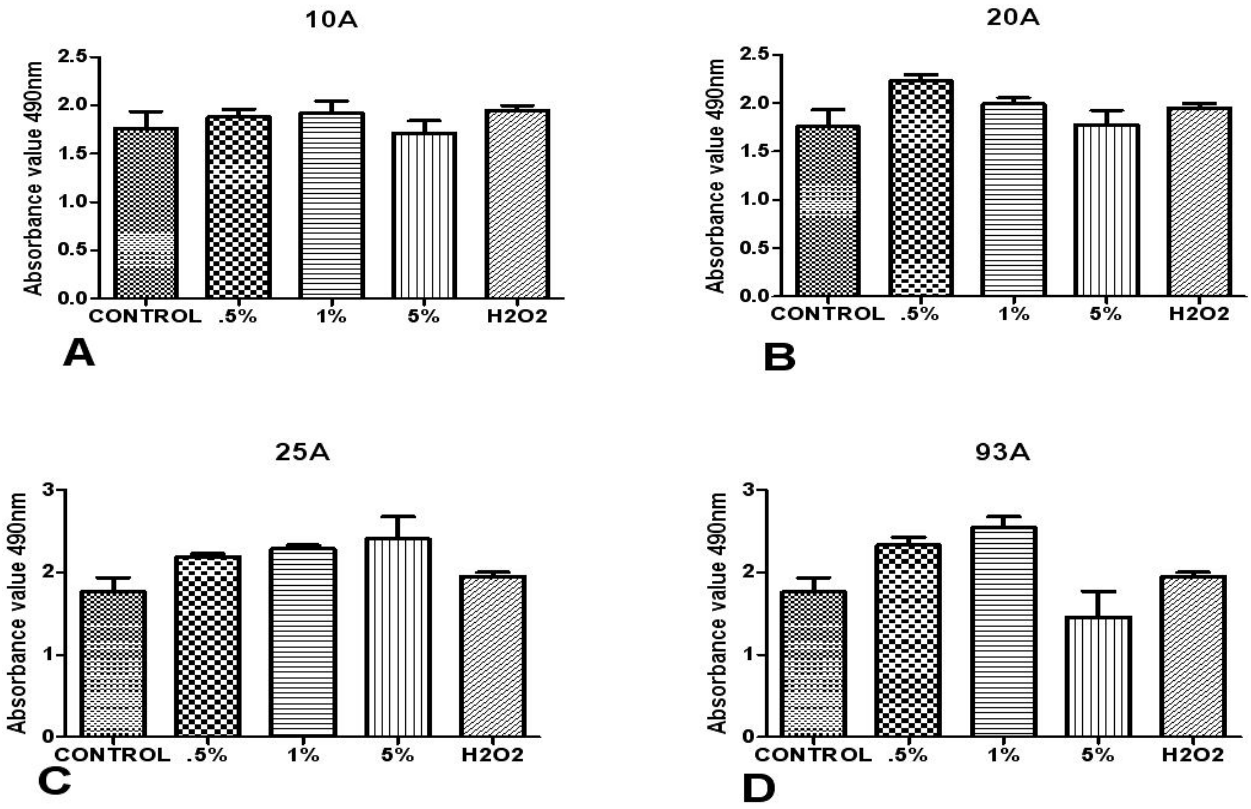

Figure 5.2. Cytotoxicity assessments of hydrophilic nanoclays using hFOB 1.19 cells at 24hr. Lactate dehydrogenase assay on osteoblast cells exposed to 10A, 20A, 25A, and 93A nanoclays for 24hrs reveal fluctuation of LDH leakage between different forms of nanoclays.

However, to ensure that the nanoclays had no impact or interference on the catalytic reagents used to detect LDH, simultaneous experiments using nanoclays, media only, and no cells (reagents only) were performed (data not shown). This cell free experiment helped determine that nanoclays contain surfactants that are capable of reducing formazan as mammalian cells, thus the results found in the LDH and MTT analysis are invalid. Data for invalid experiments are represented as Figures 5 and 6 in Appendix A: Supplemental Data.

5.4. Discussion

Nanoclays are used in manufacturing as an additive for plastic to improve various plastic physical properties such as reinforcement. Cloisite is a natural montmorillonite, or nanoclay, that is modified with a quaternary ammonium salt. In the field of bioremediation, Cloisite has found a use as a material to treat contaminated and waste water (Sancha, 2010), uptake of heavy metals and endocrine disrupting chemicals (Churchman, 2006), and inhibition of organic leachates from waste disposal sites (Theng, 2006). The evaluation of this nanomaterial as a potential cytotoxic reagent is necessary because of its possible release into the environment during bioremediation processes and the manufacturing of the material.

The data collected in this study was confounded due to the highly reactive nature of the modified structure and surface components of Cloisite. Cloisite 10A, 20A, 25A, 93A are chemically modified to ensure hydrophillicity. However, the surfactants used to provide the hydrophilic properties interfered with reagents used to measure metabolic activity and the presence of enzymes such as lactate dehydrogenase. Actions were taking to reduce this interference such as reducing concentrations to 0.0001% using titrations of the nanoclays, however, these lower concentrations proved lethal for the hFOB 1.19 cell line. This enhanced lethality could be due to higher particle dispersal and less aggregation, thus reducing particle size. Cell proliferation inhibition caused by particle size has been reported in HepG2 cells exposed to 70nm SiO_2 (Chen, 2005). It has also been noted that particle size plays a role in cellular uptake and bioactivity (Chithrani, 2006), (Jang, 2008). Additionally, wash steps were used to prevent buildup of nanoclays on the surface of the cells, however residual nanoclays were still present which were confirmed by light microscopy.

5.5. Conclusions

In summary, determining the cytotoxic potential of Cloisite nanoclays is necessary to classify these diverse materials as safe for use in the environment. However, other methods of analysis or assays need to be utilized which do not use reagents that can be easily reacted with. Future directions of this study would be to identify other means of analysis or use molecular techniques to evaluate toxicity.

CHAPTER 6

Conclusions

In summary, the airway epithelium is exposed to an onslaught of environmental stressors on a daily basis. These environmental stressors can include bacteria, viruses, and air pollutants consisting of chemicals and particulate matter. Once inhaled, adaptive and innate immune responses generate counter active measures such as antioxidants and oxidants to combat and prevent further contamination. However, imbalances in antioxidants and oxidants can lead to oxidative stress, the precursor to many diseases such as asthma, COPD, and chronic bronchitis. Evaluating the toxicity of different forms of environmental pollutants has now become a nationwide initiative due to the increase in asthma in America. The CDC reports that in 2009 24.6 million people (8.2%) in America have asthma, which is an increase of 4.3 million people since 2001. Thus, delineating what factors can initiate disease states in the respiratory system is an important step in reducing the prevalence of these issues.

In this dissertation, we have determined that swine confinement facility dust can induce gene modulation of oxidative stress and antioxidant genes in normal bronchial epithelial (NHBE) cells. Novel phytonutrient treatments such as *Hibiscus sabdariffa* or sorrel encouraged reductions in genes associated with oxidative stress and increased antioxidant defense genes. However, determining the appropriate dosage and concentration of sorrel extract is crucial for therapeutic benefits to be validated.

In addition to evaluating biogenic nanoparticles, we evaluated metals that are potential biomaterials used for applications in regenerative medicine. We have concluded that pure magnesium had no modulatory effect on pro-inflammatory genes (NF-κB or COX-2) in normal human bronchial epithelial cells after 24hrs in air liquid interface (ALI) culturing system. No

differential expression of IκBα or COX-2 proteins was exhibited in Western blot analysis, which validates genomic analysis. Cytotoxicity analysis correlated with genomic and proteomic evaluations in that no relevant increases of lactate dehydrogenase were found after exposure time points of 24hr and 48hrs. Mucin production, cytokine secretion, and cell migration were unaffected due to magnesium interaction suggesting that cell cycle progression, cell growth and functionality were maintained. The above tests support the efficacy of using magnesium biomaterials in tracheal stent development and fabrication. However, further testing of possible alloying elements needs to be performed.

As a final point of evaluation, we evaluated the toxicity of nanoclays that are used in environmental bioremediation processes. The cytotoxic potential of Cloisite nanoclays is a necessary measure to classify these diverse materials as safe for use in the environment. Cell viability and cytotoxicity assays revealed that these nanoclays are highly toxic and reactive with reagents in solution. Different methods of analysis need to be utilized which do not use reagents that can be easily compromised. Future directions of this study would be to identify other assays to evaluate toxicity levels and maximal inhibitory concentrations.

Thus our hypothesis of nanoparticles, regardless of origin, can elicit oxidative stress and inflammation was validated however magnesium metals are a viable biomaterial to use within the airway.

References

Amin A, A. A. Hamza. (2006). Hepatoprotective effects of Hibiscus, Rosmarinus and Salvia on azathioprine-induced toxicity in rats. *Life Sciences, 77*, 266-78.

Azarmi, S., W. H. Roa (2008). Targeted delivery of nanoparticles for the treatment of lung diseases. *Advanced Drug Delivery Reviews, 60*, 863-875.

Bako, I. G., M. Mabrouk, and A. Abubakar. (2009). Antioxidant Effect of Ethanolic Seed Extract of Hibiscus sabdariffa linn (Malvaceae) Alleviate the Toxicity Induced by Chronic Administration of Sodium Nitrate on Some Haematological Parameters in Wistars Rats. *Advance Journal of Food Science and Technology, 1*,39-42.

Boschetto P., S. Quintavalle, D. Miotto, N. Lo Cascio, E. Zeni, C. E. Mapp. (2006). Chronic obstructive pulmonary disease (COPD) and occupational exposures. *J Occup Med Toxicol, 1*,11.

Bowlin, G. L. (2010). Nanotechnology in the design of soft tissue scaffolds: innovation in structure and function. *WIREs Nanomedicine and Nanobiotechnology,2*,20-35.

Breitenbücher, A., P. N. Chhajed, M. H. Brutsche, C. Mordasini, D. Schilter, and M. Tamm. (2008). Long-term follow-up and survival after Ultraflex stent insertion in the management of complex malignant airway stenoses. *Respiration, 75*,443-449.

Bystrzejewska-Piotrowska, G., J. Golimowski, et al. (2009). Nanoparticles: Their potential toxicity, waste and environmental management. *Waste Management, 29*, 2587-2595.

Carsten Schleh, C. M., Karin Pulskamp, Andreas Schmiedl, H. D. L. Matthias Nassimi, Armin Braun, Norbert Krug, et al. (2009). The effect of titanium dioxide nanoparticles on pulmonary surfactant function and ultrastructure. *Respiratory Research, 10*,90.

Castellani, C. (2011). Bone implant interface strength and osseointergration: Biodegradable magnesium alloy versus standard titanium control. *Acta Biomaterialia***,** 7,432-440.

Charavaryamath, C. (2005). Multiple exposures to swine barn air induce lung inflammation and airway hyper-responsiveness. *Respiratory Research,* 6,50-63.

Charavaryamath, C. and B. Singh. (2006). Pulmonary effects of exposure to pig barn air. *J Occup Med Toxicol*., *1*,10.

Chen, F., and X. Shi. (2002). Intracellular signal transduction of cells in response to carcinogenic metals. *Critical Reviews in Oncology and Hematology, 42*,105-121.

Chen, H.-W., S.-F. Su, et al. (2006). Titanium dioxide nanoparticles induce emphysema-like lung injury in mice. *FASEB J***.,** *20*, 2393-2395.

Cho, Y. S., J. Lee, T. H. Lee, E. Y. Lee, K. U. Lee, J. Y. Park, H. B. Moon. (2004). alpha-Lipoic acid inhibits airway inflammation and hyperresponsiveness in a mouse model of asthma. *Basic and Clinical Immunology* ,*114*,429-436.

Choi, S.-J., J.-M. Oh, et al. (2009). Toxicological effects of inorganic nanoparticles on human lung cancer A549 cells. *Journal of Inorganic Biochemistry***,** *103*, 463-471.

Christian, K. R., M. G. Nair, and J. C. Jackson. (2006) Antioxidant and cyclooxygenase inhibitory activity of sorrel (Hibiscus sabdariffa). *Journal of Food Composition and Analysis***,** *19*, 778-783.

Chu, Y., Y. Demin, P. Wang, J. Xu, D. Li, and M. Ding, M. (2010). Nanotechnology promotes the full-thickness diabetic wound healing effect of recombinant human epidermal growth factor in diabetic rats. *Wound Repair and Regeneration, 18*,499-505.

Chung, F. T., S. M. Lin, H. C. Chen, C. L. Chou, C. T. Yu, and C. Y. Liu. (2008). Factors leading to tracheobronchial self-expandable metallic stent fracture. *J Thorac Cardiovasc Surg, 136*,1328-1335.

Churchman, G. J., W. P. Gates, B. K. G. Theng, and G. Yuan. (2006). Clays and clay minerals for pollution control. *In Handbook of Clay Science*, ed. F. Bergaya, B. K. G. Theng, and G. Lagaly. Amsterdam: Elsevier Ltd.: 625-675.

Crossgrove, J., and W. Zheng. (2004). Review article: Manganese toxicity upon overexposure. *NMR Biomed, 17*,544-553.

Erne, P., M. Schier, and T. J. Resink. (2006). The road to bioabsorbable stents: reaching clinical reality? *Cardiovasc.Intervent Radiol., 29*,11-16.

Essa, M. M. and P. Subramanian. (2007). Hibiscus sabdariffa Affects Ammonium Chloride-Induced Hyperammonemic Rats. *eCAM ,4*, 321-325.

Essa, M. M. and P. Subramanian. (2007) .Hibiscus sabdariffa Affects Ammonium Chloride-Induced Hyperammonemic Rats.*eCAM., 4*, 321-325.

Feng, A., and Y. Han. (In Press). Mechanical and in vitro degradation behavior of ultrafine calcium polyphosphate reinforced magnesium-alloy composites. *Materials & Design* Corrected Proof.

Fujita, K., Y. Morimoto, et al. (2009). Gene expression profiles in rat lung after inhalation exposure to C60 fullerene particles. *Toxicology, 258,*47-55.

Gavin, A. (2002). Functional organization of the yeast proteome by systematic analysis of protein complexes. *Nature*, *415*,141-147.

Gerald, L. C., C. Y. Watson, R. Pender, K. Adler, J. Waterman. (2010) Oxidant stress in airway epithelial cells following swine confinement facility dust exposure. *American Journal of Respiratory and Criticial Care Medicine, 181*, A4695.

Gomez-Mejiba, S. E., Z. Zhai, et al. (2009). Inhalation of environmental stressors & chronic inflammation: Autoimmunity and neurodegeneration. *Mutation Research/Genetic Toxicology and Environmental Mutagenesis, 674*, 62-72.

Gourgoulianis, K. I., G. Chatziparasidis, A. Chatziefthimiou, and P. A. Molyvdas. (2001). Magnesium as a Relaxing Factor of Airway Smooth Muscles. *Journal of Aerosol Medicine*, *14*, 301-307.

Grassian, V. H., A. Adamcakova-Dodd, et al. (2007). Inflammatory response of mice to manufactured titanium dioxide nanoparticles: Comparison of size effects through different exposure routes. *Nanotoxicology*, *1*, 211-226.

Grimsrud, P. (2008). Oxidative stress and covalent modification of protein with bioactive aldehydes. *The Journal of Biological Chemistry***,** *283*, 21837-21841.

Grisanti, R. (2006). How to treat and prevent asthma attacks with nutritional medicine. *The American Chiropractor:* 20-22.

Hagens, W. I., A. G. Oomen, et al. (2007). What do we need to know about the kinetic properties of nanoparticles in the body? *Regulatory Toxicology and Pharmacology, 49*, 217-229.

Harju, T., M. Peltoniemi, et al. (2007).Glutathione S-transferase omega in the lung and sputum supernatants of COPD patients. *Respiratory Research***,** *8*, 48.

Hartung, J. (2003). Effects of Transport stress on health of farm animals. *Veterinary Research Communications***,** *27*,525-527.

Heublein, B., R. Rohde, V. Kaese, M. Niemeyer, W. Hartung, and A. Haverich. (2003). Biocorrosion of magnesium alloys: A new principle in cardiovascular implant technology? *Heart, 89*,651-656.

Hillegass, J. M., A. Shukla, et al. (2009). Assessing nanotoxicity in cells. *Wiley Interdisciplinary Reviews: Nanomedicine and Nanobiotechnology, 2*, 219-231.

Ho, Y. (2002) Systematic identification of protein complexes in Saccharomyces cerevisiae by mass spectrometry. *Nature*, *415*,180-183.

Hristovski, K. (2007). Selecting metal oxide nanomaterials for arsenic removal in fixed bed columns: From nanopowders to aggregated nanoparticle media. *Journal of Hazardous Materials***,** *147*, 265-274.

Inoue, K.-i. and H. Takano. (2010). Systemic Impact of Inhaled Diesel Exhaust Particles. *Toxicol. Sci.***,** *115*, 607-608.

Jill, A. P., A. W. Todd, et al. (2007). Repeat organic dust exposure induced monocyte inflammation is associated with protein kinase C activity. *The Journal of allergy and clinical immunology, 120*, 366-373.

Kirkham, P. and I. Rahman. (2006). Oxidative stress in asthma and COPD: Antioxidants as a therapeutic strategy. *Pharmacology & Therapeutics, 111*, 476-494.

Kosak, S. T. and M. Groudine. (2004). Gene order and dynamic domains. *Science*, *306*, 644-647.

Kowal, K., A. Bodzenta-Lukaszyk, A. Pampuch, M. Szmitkowski, M. B. Donati, L. Iacoviello. (2007). Plasminogen activator inhibitor-1 (PAI-1) plasma concentration in allergic asthma patients during allergen challenge. *Int Arch Allergy Immunol. 144*,240-246.

Krajangpan, S., J. Elorza, A. Bezbaruah, E. Khan, and B. Chisholm. (2007). Nitrate Removal by Zero-Valent Iron Nanoparticles Entrapped in Calcium Alginate. *Nanotechnology in Environmental Protection and Pollution*, ISNEPP: Ft. Lauderdale, FL.

Krijgsveld, J., and Albert J. R. Heck. (2004). Quantitative proteomics by metabolic labeling with stable isotopes. *Drug Discovery Today: TARGETS, 3*, 11-15.

Lebret, B., M. C. Meunier-Salaün, A. Foury, P. Mormède, E. Dransfield, J. Y. Dourmad. (2006). Influence of rearing conditions on performance, behavioral and physiological responses of pigs to preslaughter handling, carcass traits, and meat quality. *Journal of Animal Science, 84*, 2436-2447.

Lemaire, A., W. R. Burfeind, E. Toloza, S. Balderson, R. P. Petersen, and D. H. Harpole, Jr. (2005). Outcomes of tracheobronchial stents in patients with malignant airway disease. *Ann Thorac Surg, 80*, 434-438.

Li, L., J. Gao, and Y. Wang. (2004). Evaluation of cyto-toxicity and corrosion behavior of alkali-heat-treated magnesium in simulated body fluid. *Surface and Coatings Technology, 185*, 92-98.

Li, N., T. Xia, et al. (2008). The role of oxidative stress in ambient particulate matter-induced lung diseases and its implications in the toxicity of engineered nanoparticles. *Free Radical Biology and Medicine*, 44, 1689-1699.

Li, P. R., J. C. Wei, Y. F. Chiu, H. L. Su, F. C. Peng, and J. J. Lin. (2010). Evaluation on Cytotoxicity and Genotoxicity of the Exfoliated Silicate Nanoclay. *Applied Materials and Interfaces*, 2, 1608-1613.

Mann, M. (2003). Proteomic analysis of posttranslational modifications. *Nat. Biotechnol.*, 21,255-261.

Maynard, A. D., R. J. Aitken, et al. (2006). Safe handling of nanotechnology. *Nature, 444*, 267-269.

Mohammed S, S. Goodacre. (2007). Intravenous and nebulised magnesium sulphate for acute asthma: systematic review and meta-analysis. *Emergency Medicine Journal, 24*, 823-830.

Mueller, W. D., et al. (2007). Magnesium and its alloys as degradable biomaterials: Corrosion studies using potentiodynamic and EIS electrochemical techniques. *Materials Research, 10*, 5-10.

Nel, A. (2005). Air pollution-related illness: effects of particles. *Science*, *308*,804–806.

Neveu, W. A., J. L. Allard, D. M. Raymond, L. M. Bourassa, S. M. Burns, J. Y. Bunn, C. G. Irvin, D. A. Kaminsky, and M. Rincon. (2010). Elevation of IL-6 in the allergic asthmatic airway is independent of inflammation but associates with loss of central airway function. *Resp.Research*, *11*, 28.

Noppen, M., et al. (2005). Removal of Covered Self-Expandable Metallic Airway Stents in Benign Disorders. *Chest*, *127*,482-487.

Oberdorester, G., E. Oberdorester, and J. Obedorester. (2005). Nanotoxicology: An Emerging Discipline Evolving from Studies of Ultrafine Particles. *Environmental Health Perspectives*, *1131*,823-837.

Odigie, I., R. R. Ettarh, and S. Adigun. (2003). Chronic administration of aqueous extract of Hibiscus sabdariffa attenuates hypertension and reverses cardiac hypertrophy in 2K-1C hypertensive rats. *J Ethnopharmacol*, *86*,181-185.

Okasha, M. A. M., M. S. Abubakar, and I. G. Bako. (2008) Study of the effect aqueous Hibiscus sabdariffa l. seed extract on serum prolactin level in lactating albino rats. *Eur. J. Sci. Res., 22*, 575-583.

Olaleye, M. T. (2007). Cytotoxicity and antibacterial activity of methanolic extract of Hibiscus sabdariffa. *J Med Plants Research***,** *1*, 9-13.

Ong, S.-E., L. J. Foster, et al. (2003). Mass spectrometric-based approaches in quantitative proteomics. *Methods*, *29*, 124-130.

Owen, R. and M. Depledge. (2005). Nanotechnology and the environment: Risks and ewards. *Marine Pollution Bulletin, 50*, 609-612.

Oyabu, T., A. Ogami, et al. (2007). Biopersistence of Inhaled Nickel Oxide Nanoparticles in Rat Lung. *Inhalation Toxicology, 19*, 55-58.

Park, E.-J., J. Yoon, et al. (2009). Induction of chronic inflammation in mice treated with titanium dioxide nanoparticles by intratracheal instillation. *Toxicology,* 260,37-46.

Park, S.-J., et al. (2007). Anthocyanins inhibit airway inflammation and hyperresponsiveness in a murine asthma model. *Food and Chemical Toxicology, 45*, 1459-1467.

Purnama, A. (2010). Assessing the biocompatibility of degradable metallic materials: State-of-the-art and focus on the potential of genetic regulation. *Acta Biomaterialia***,** *6*, 1800-1807.

Reis, C. P., R. J. Neufeld, A. J. Ribeiro, and F. Veiga. (2006). Nanoencapsulation II. Biomedical applications and current status of peptide and protein nanoparticulate delivery systems. *Nanomedicine*, *2*, 53-65.

Rice-Evans, C. A., N. J. Miller, and G. Paganga. (1996). Structure-antioxidant activity relationships of flavonoids and phenolic acids. *Free Radic Biol Med., 20*, 933-956.

Robbins, S., V. Kumar, A. Abbas, N. Fausto, J. Aster. (2010). *Pathologic Basis of Disease* Saunders - Elsevier.

Romberger, D. J., V. Bodlak, et al. (2002). Hog barn dust extract stimulates IL-8 and IL-6 release in human bronchial epithelial cells via PKC activation. *J Appl Physiol*, *93*, 289-296.

Romberger, D., V. Bodlak, S. G. Von Essen, T. Matheisien, and T. A. Wyat. (2002). Hog barn dust extract stimulates IL-8 and IL-6 release in human bronchial epithelial cells via PKC activation. *J Appl Physiol*, 93, 289–296.

Rossi, A., I. Serraino, P. Dugo, R. Di Paola, L. Mondello, T. Genovese, D. Morabito, G. Dugo, L. Sautebin, A. P. Caputi, and S. Cuzzocrea. (2003). Protective effects of anthocyanins from blackberry in a rat model of acute lung inflammation. *Free Radic. Res., 37*,891-900.

Roussel, R. R., and A. Barchowsky. (2000). Arsenic inhibits NF-kappa B mediated gene transcription by blocking IKB kinase activity and IKBalpha phosphorylation and degradation. *Arch.Biochem.Biophys*, *377*, 204-212.

Sancha, R., J. Bajpai, and A. K. Bajpai. (2010). Designing of fullers-earth-containing poly(vinyl alcohol)-g-poly(2-acrylamido-2-methyl-1-propanesulfonic acid) nanocomposites: Swelling and deswelling behaviors. *Journal of Applied Polymer Science*, *118*, 1230-1239.

Sanvicens, N. and M. P. Marco. (2008). Multifunctional nanoparticles - properties and prospects for their use in human medicine. *Trends in Biotechnology*, *26*, 425-433.

Saris, N., (2000). Magnesium: An update on physiological, clinical and analytical aspects. *Clin Chim Acta*, *294*,1-26.

Schluger, N. (2005). The pathogenesis of tuberculosis: the first one hundred (and twenty-three) years. *Am. J. Respir. Cell Mol. Biol.*, *32*,251-256.

Seo, J. W. (2008). Magnesium Metabolism. *Electrolyte & Blood Pressure, 6*,86-95.

Sharma, A. K., et al. (2010). Genotoxicity of unmodified and organo-modified montmorillonite. *Mutation Research/Genetic Toxicology and Environmental Mutagenesis*, *700*, 18-25.

Shumilla, J. A., R. J. Broderick, Y. Wang, and A. Barchowsky. (1999). Chromium (VI) inhibits the transcriptional activity of nuclear factor-KB by decreasing the interaction of p65 with cAMP-responsive element-binding protein-binding protein. *J Biol Chem, 274*,36207-36212.

Sihvo, E. I. T., T. Sioris, O. Tynninen, and J. A. Salo. (2006). Fatal fistula between the trachea and the brachiocephalic artery: Late complication of a second-generation, self-expanding metallic tracheal stent. *J Thorac Cardiovasc Surg, 131*,1415-1416.

Singh, J., Schwartz, David A (2005). Endotoxin and the lung: Insight into the host-environment interaction. *Journal of Allergy, Asthma and Immunology*, *115*, 330-333.

Smit-de Vries, M. (2007). Resistance of quiescent and proliferating airway epithelial cells to hydrogen peroxide challenge. *European Respiratory Journal.,* 29, 633-642.

Song, G. (2007). Control of biodegradation of biocompatible magnesium alloys. *Corr. Sci.*, *49*: 1696-1701.

Staiger, M. P., et al. (2006). Magnesium and its alloys as orthopedic biomaterials: A review. *Biomaterials*, *27*, 1728-1734.

Strieter, R. M. (2002). Interleukin-8: a very important chemokine of the human airway epithelium. *Am. J. Physiol., Lung Cell Mol. Physiol, 283*,L688–L689.

Stroh, A., et al. (2004). Iron oxide particles for molecular magnetic resonance imaging cause transient oxidative stress in rat macrophages. *Free Radical Biology and Medicine*, *36*, 976-984.

Sutherland, E., and R. J. Martin. (2003). Airway inflammation in chronic obstructive pulmonary disease: Comparisons with asthma. *J Allergy Clin Immunol,. 112*, 819-27.

Talati, M., B. Meyrick, R. S. Peebles Jr., S. S. Davies, R. Dworski, R. Mernaugh, D. Mitchell, M. Boothby, L. J. Roberts II, and J. R. Sheller. (2006). Oxidant stress modulates murine allergic airway responses. *Free Radic Biol Med***,** *40*,1210-1219.

Thacker, E. L. (2006). Lung inflammatory responses. *Vet. Res.* 37,469–486.

Theng, B. K. G., G. J. Churchman, W. P. Gates, and G. Yuan. (2006). Organically modified clays for pollution uptake and environmental protection. *In Soil Mineral-Organic Matter-Microorganism Interactions: Fundamentals and Impacts*, ed. P. M. Huang, Q. Huang, and J.-M. Bollag. Springer: Heidelberg.

Valerio (2001). Induction of human NADPH: Quinone oxireductase (NQO1) gene expression by the flavanoll quercetin. *Toxicology Letters,* 119,49-57.

Valko, M. (2006). Free radicals, metals, and antioxidants in oxidative stress-related cancer. *Chemico-Biological Interactions, 160*, 1-40.

Vearick, S. (2007). Development and In Vivo Testing of a Nitinol Tracheal Stent. *Journal of Laparoendoscopic & Advanced Surgical Techniques*, *83B*, 216-222.

Verghese, M., M. S. C. Fullerton, (2008). Determination of Antioxidant contents in red sorrel and its anticarcinogenic potential in azoxymethane induced abberant crypt foci. *Research Journal of Phytochemistry***,** *2*, 69-76.

Verghese, M., M. S. C. Fullerton, (2008). Determination of antioxidant contents in red sorrel and its anticarcinogenic potential in azoxymethane-induced colonic aberrant crpyt focci. *Research Journal of Phytochemistry, 2*, 69-76.

Vinograd, I. (2005). Treatment of airway obstruction by metallic stents in infants and children. *J Thorac Cardiovasc Surg***,** *130*,146-150.

Von Essen, S. G. and B. W. Auvermann. (2005). Health effects from breathing air near CAFOs for feeder cattle or hogs. *Journal of Agromedicine,* 10, 55-64.

Vormann, J. (2003).“Magnesium: Nutrition and Metabolism. *Molecular Aspects of Medicine 24*,27-37.

Watlington, K. (2005). Emerging Nanotechnologies for Site Remediation and Wastewater Treatment. *U.S. Environmental Protection Agency-National Network for Environmental Management Studies*: Washington, DC.

Weinberg, M., J. Sandbank, Y. Flumeblit, B. Klin, and I. Vinograd. (2005). Tracheal Reaction to Three Different Intraluminal Stents in an Animal Model of Tracheomalacia. *Journal of Laparoendoscopic & Advanced Surgical Techiques,* 15,333-338.

Witte, F., et al. (2006). In vitro and in vivo corrosion measurements of magnesium alloys” *Biomaterials, 27*, 1013-1018.

Wyatt, T. A. (2007). Feedlot dust stimulation of interleukin-6 and -8 requires protein kinase C in human bronchial epithelial cells. *Am J Physiol Lung Cell Mol Physiol***,** *293*, L1163-L1170.

Yuan, G., and L. Wu. (2007). Allophane nanoclay for the removal of phosphorus in water and wastewater. *Science and Technology of Advanced Materials***,** 8, 60-62.

Zara, G. P., R. Cavalli, et al. (2002). Intravenous Administration to Rabbits of Non-stealth and Stealth Doxorubicin-loaded Solid Lipid Nanoparticles at Increasing Concentrations of Stealth Agent: Pharmacokinetics and Distribution of Doxorubicin in Brain and Other Tissues. *Journal of Drug Targeting***,** *10*, 327-335.

Appendix A

Supplemental Data

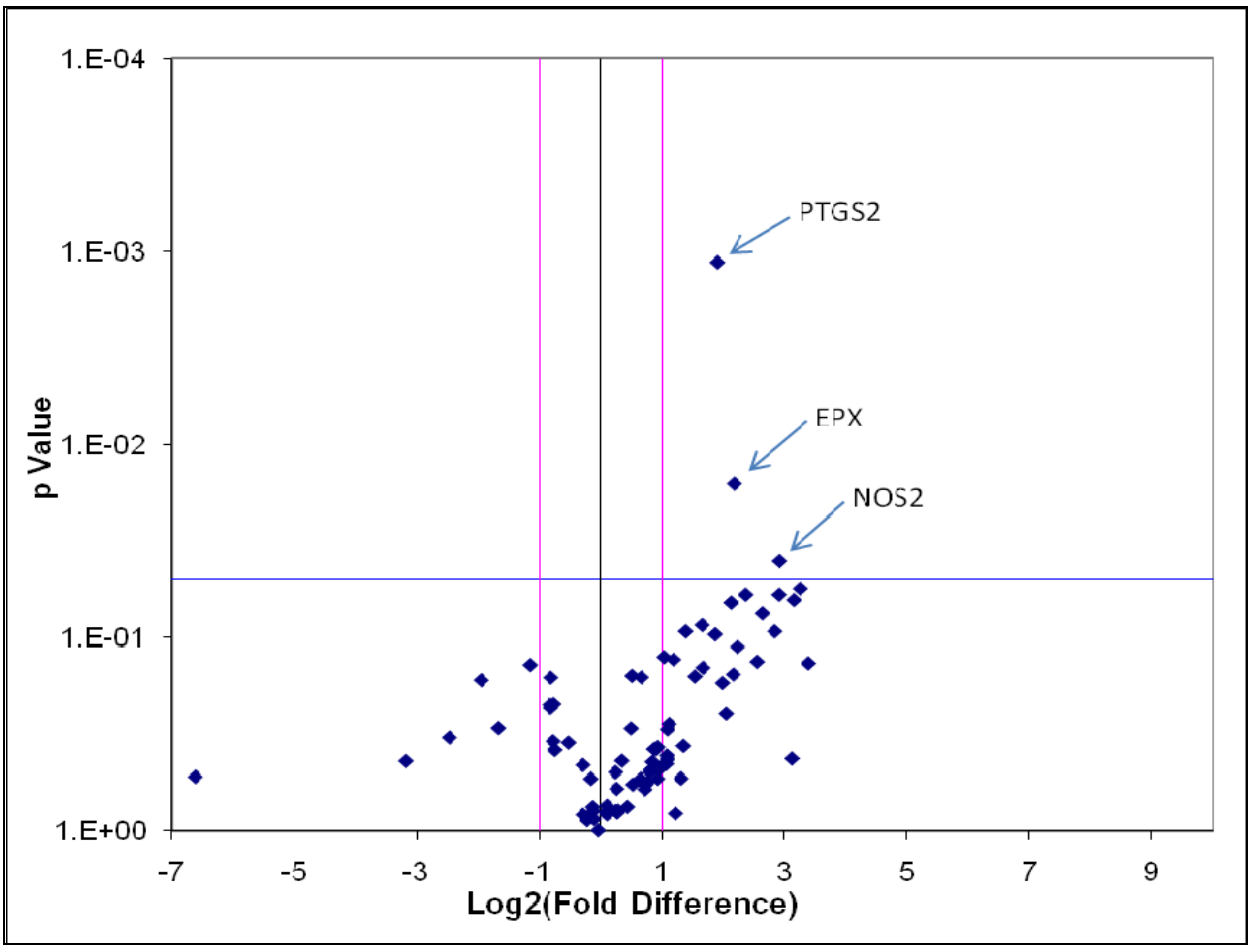

Figure 1. Gene expression patterns of NHBE cells treated with 10% aqueous sorrel extract for 4hr.

Table 1.

Modulation of gene expression of NHBE cells treated with 10% aqueous sorrel for 4hr.

Gene Name/RefSeq	Gene Symbol	Gene Function	p-value	Fold change
Prostaglandin endoperoxide (NM_000963)	PTGS2	Peroxidase and Oxidoreductase activity	0.0011	3.76
Eosinophil peroxidase (NM_000502)	EPX	Peroxidase activity	0.0160	4.55
Nitric oxide synthase 2, inducible (NM_000625)	NOS2	Superoxide metabolism	0.0401	7.59

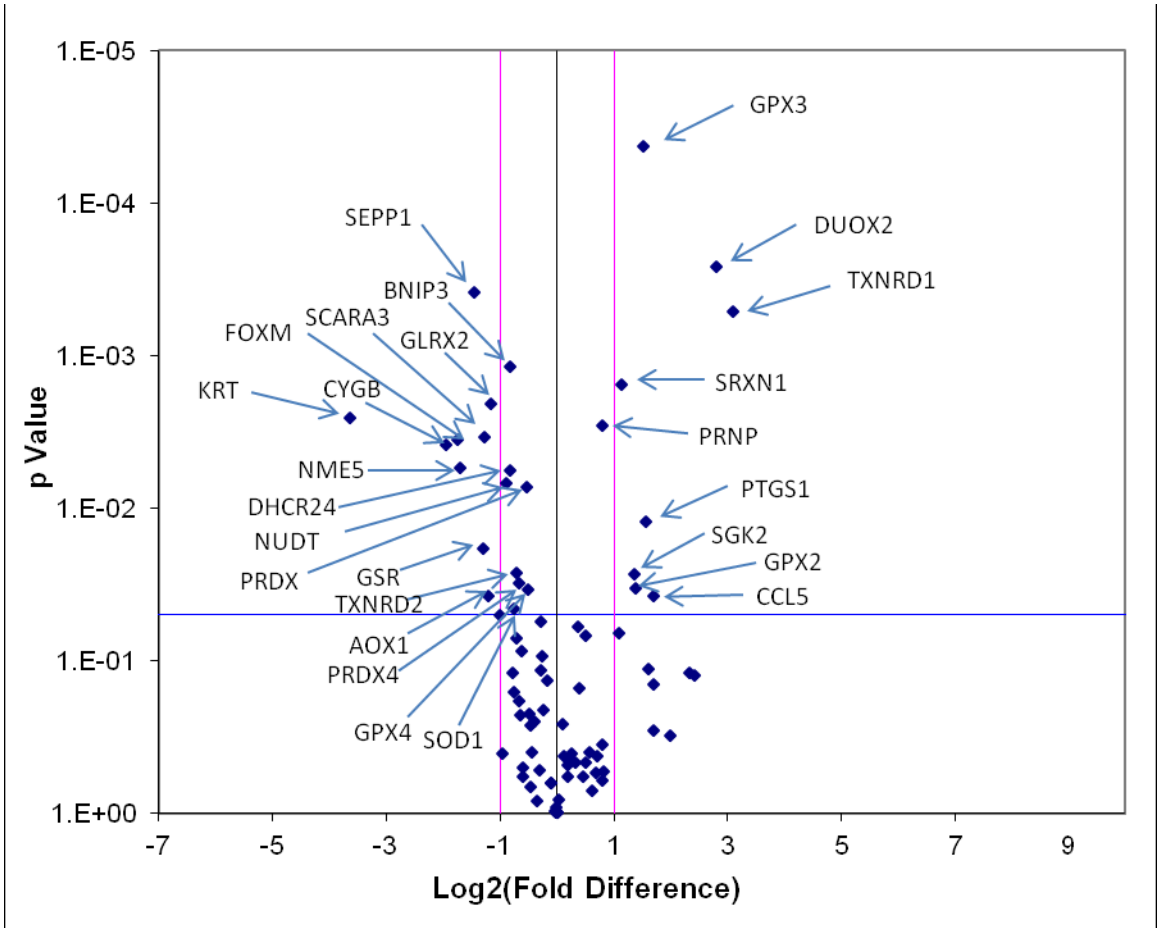

Figure 2. Gene expression patterns of NHBE cells treated with 10% aqueous sorrel extract for 24hr. Diamonds outside the pink lines indicate a fold difference greater than 2. Diamonds within the pink lines indicate fold difference of less than 2. P-values less than 0.05 are represented by diamonds above the blue line.

Table 2.

Sorrel alone (treatment) for 24hr mediated alterations in gene expression associated with oxidative stress and antioxidant defense in NHBE cells

Gene Name/RefSeq	Gene Symbol	Gene Function	p-value	Fold change
Dual Oxidase 2 (NM_014080)	DUOX2	-Superoxide release / metabolism -Peroxidase/ Oxidoreductase	0.0003	6.96
Forkhead box M1 (NM_021953)	FOXM1	-Cell division	0.0035	-3.35
Glutaredoxin 2 (NM_197962)	GLRX2	-Superoxide release/ metabolism -Apoptosis inducer	0.0021	-2.24
Glutathione reductase (NM_000637)	GSR	-Peroxidase activity -Oxidoreductase activity	0.0183	-2.46
Keratin 1 (NM_006121)	KRT1	-Oxidative stress	0.0026	-12.51
Non-metastatic cells 5, protein expressed in (nucleoside-diphosphate kinase) (NM_003551)	NME5	-Cell division	0.0054	-3.54

Table 2. (cont'd)

Gene Name/RefSeq	Gene Symbol	Gene Function	p-value	Fold change
Prostaglandin-endoperoxide synthase 1 (prostaglandin G/H synthase and cyclooxygenase) (NM_000962)	PTGS1	-Peroxidase activity	0.0123	2.95
Scavenger receptor class A, member 3 (NM_182826)	SCARA3	-Oxidative stress	0.0034	-2.41
Sulfiredoxin 1 homolog (S. cerevisiae) (NM_080725)	SRXN1	-Oxidoreductase activity -Oxidative stress	0.0015	2.19
Selenoprotein P, plasma, 1 (NM_005410)	SEPP1	-Oxidative stress	0.0004	-2.75
Thioredoxin reductase 1 (NM_003330)	TXNRD1	-Oxidoreductase activity	0.0005	8.55

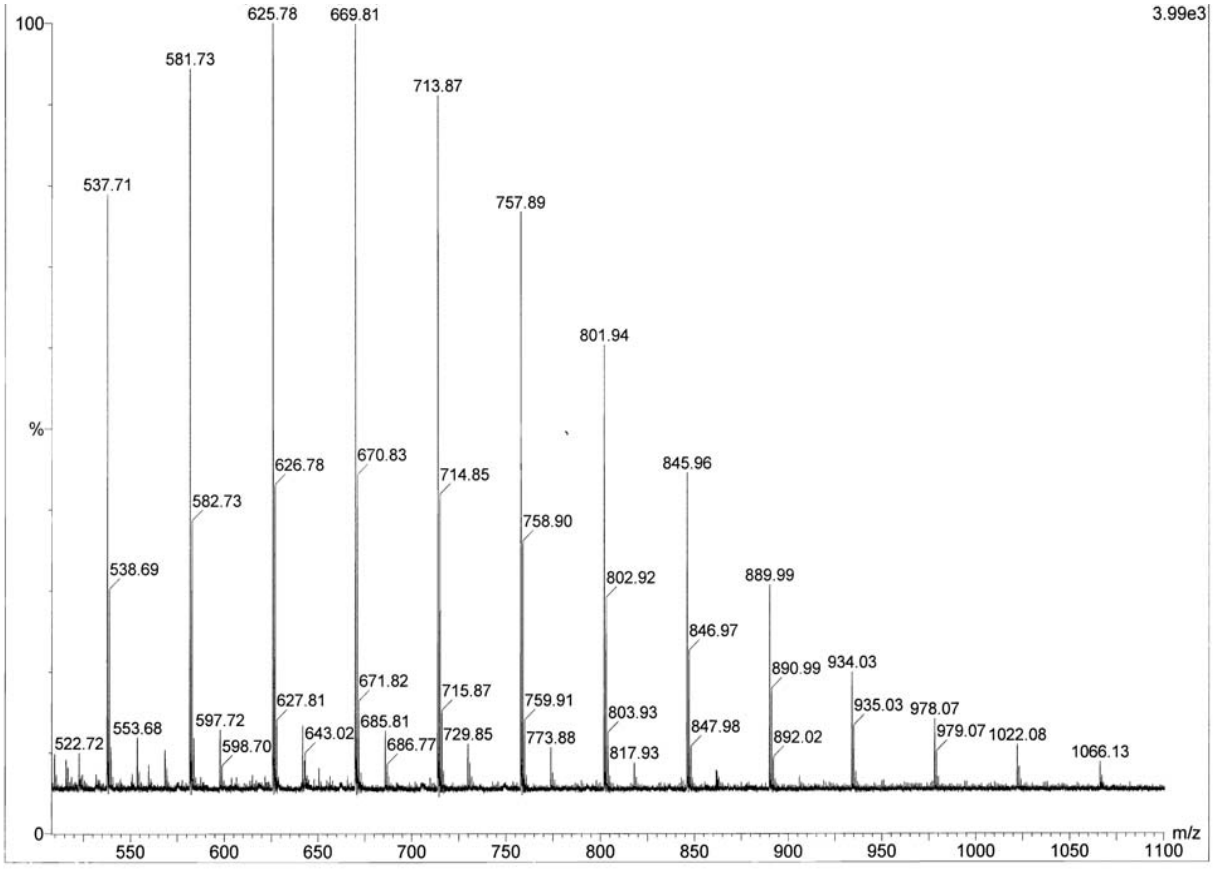

Figure 4. Mass spectra of protein lysates derived from dust and sorrel experiments. LC/MS indicates that protein signal was quenched due to large amounts of poly-ethylene glycol within samples. The cell lysis buffer used to extract protein lysates was found to be the source of polyethylene glycol source.

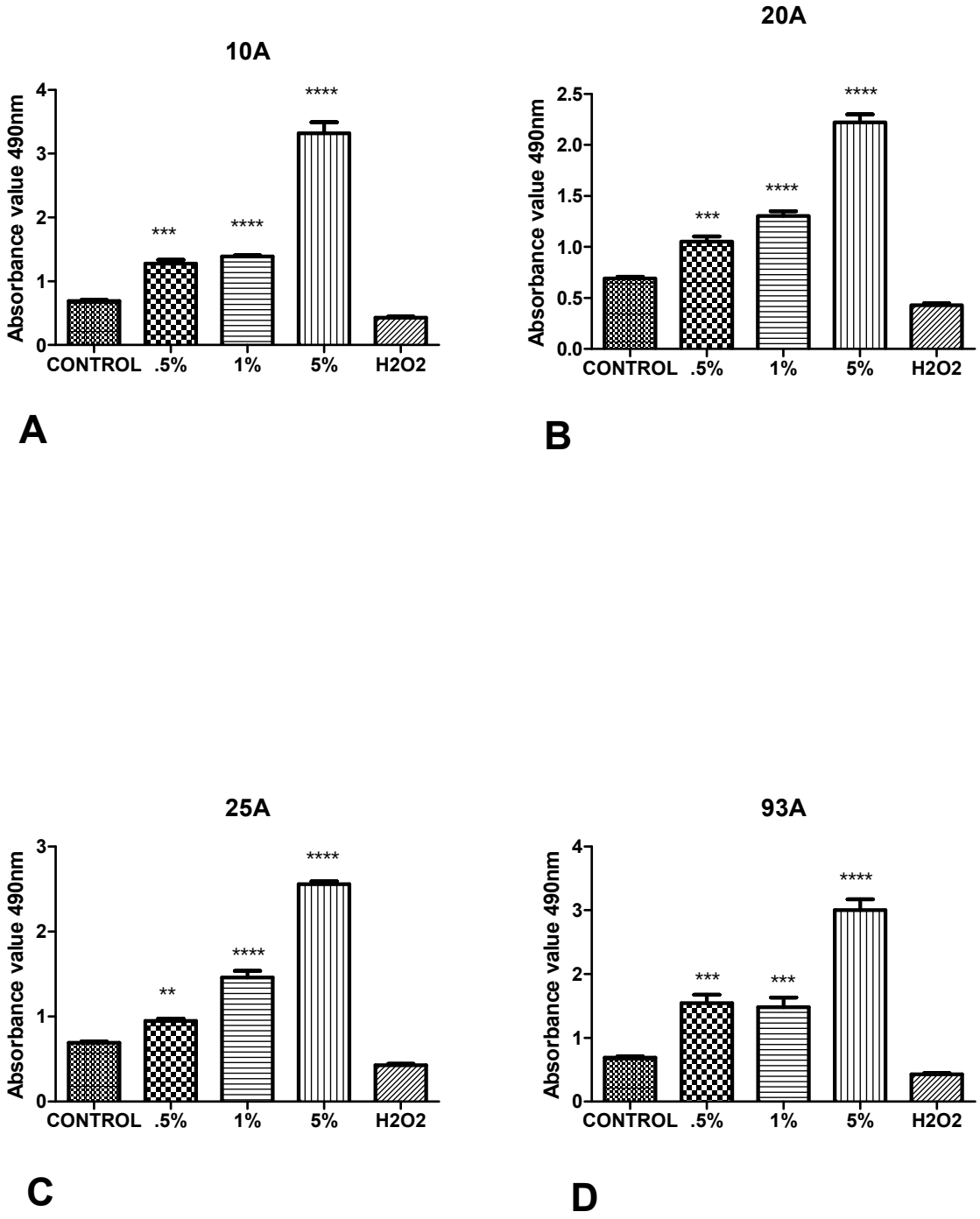

Figure 5. Cell viability determinations of hFOB 1.19 cells using MTT Assay at 4hrs. Osteoblast cells exposed to 10A, 20A, 25A, and 93A nanoclays for 4hrs revealed dose dependent relationship in response to increasing concentrations of nanoclay.

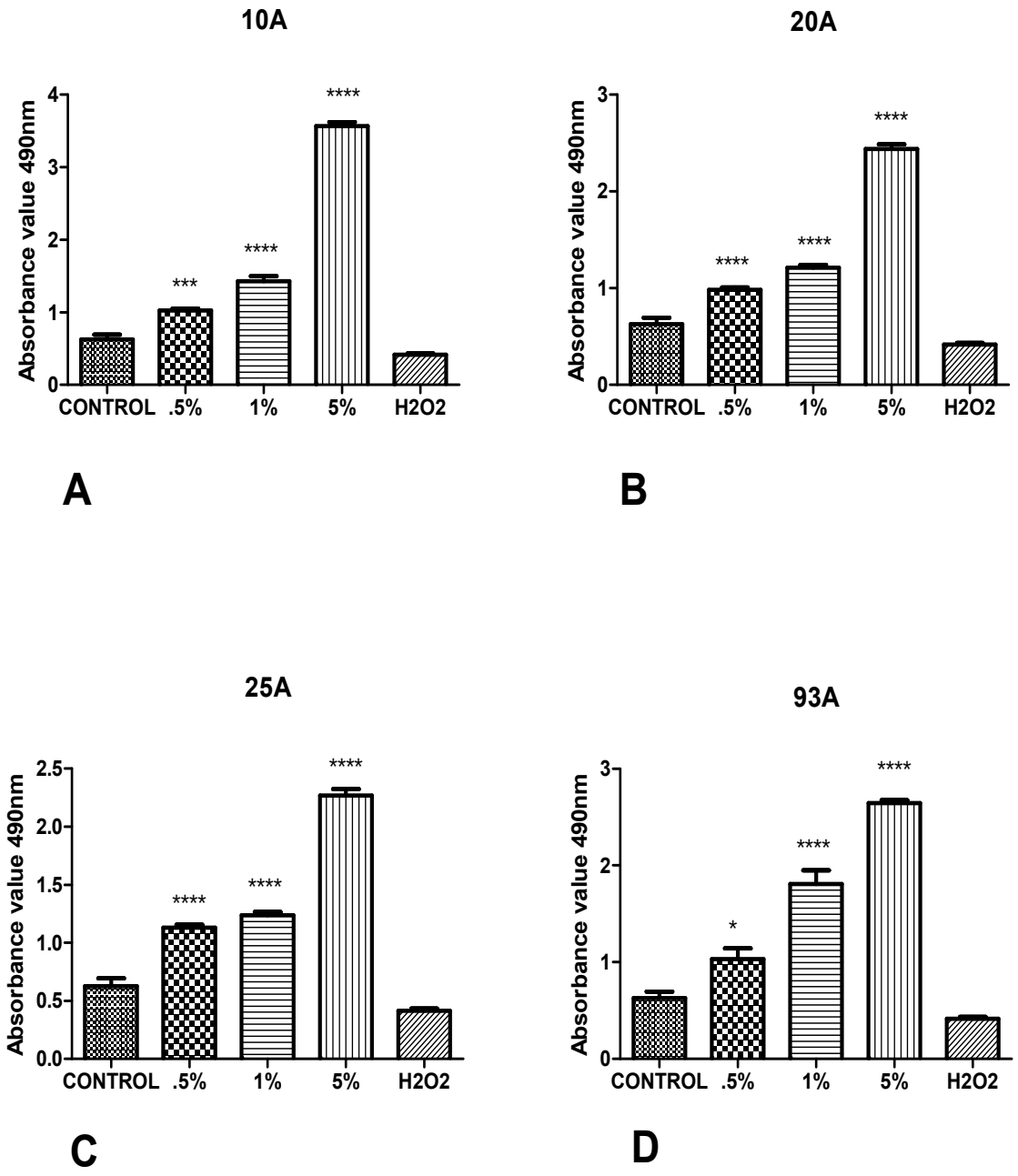

Figure 6. Cell viability determinations of hFOB 1.19 cells using MTT Assay at 24hrs. Osteoblast cells exposed to 10A, 20A, 25A, and 93A nanoclays for 24hrs revealed dose dependent relationship in response to increasing concentrations of nanoclay.

Appendix B

Laboratory Protocols

Protocol 1: Normal Human Bronchial Epithelial (NHBE) Culture

Day 1: Seeding Cells

1. Select plate type 6-well (plastic only/transwell insert-for going to air).
2. Label plate(s) with Name, Date, Plate # and donor (e.g. 5F0055).
3. **Make collagen** solution to coat wells by diluting collagen stock in 0.02 N Glacial Acetic Acid.
    a. Collagen Stock Solution: 3.13 mg/ml ≅ 3.13 μg/μl
    b. Desired final concentration = 50 μg/ml
    c. 50/3.13 = 15.97 ∴use 16μl collagen stock/1 ml acetic acid.
4. Add 0.5 ml/well and swirl plate to achieve complete well coverage.
5. Let stand at RT for 1 hour.
6. Vacuum-aspirate excess collagen solution and wash wells with 1 ml PBS for 10 min at RT.
7. Remove PBS and add 2 ml of conditioning media (50:50 without additives).
    a. Preparing 50:50 Media (viable for 6 weeks @ 4°C)
        i. Obtain a T-75 tissue culture flask (#3275)
        ii. Obtain BEBM & DMEM and mark fluid level in BEBM bottle
        iii. Pour 250 ml of BEBM into flask and 250 ml of DMEM into BEBM bottle.
        iv. Add 250 ml of BEBM from flask to DMEM bottle.
        v. Label accordingly with 50:50, initials, date and refrigerate.
8. Add 2 ml of conditioning media to wells and incubate @ 37°C/5% CO_2 for 1 hour.
9. Add "2 ml/well" in 50 ml tube and "1 ml/well" in a 50 ml tube (to reconstitute cells for distributing into wells) and warm both tubes in 37°C water bath for 15-30 min.
    a. Preparing Complete Media (viable for 6 weeks @ 4°C)

i. Get a "Clonetics BEGM Singlequots" pack (-20°C freezer in plastic bag).
ii. Remove BPE & Retinoic Acid from Singlequots pack and place in "Extras" container in -20°C freezer.
iii. Get Nystatin & BSA from -20°C freezer and BPE & Retinoic Acid (light sensitive, use small tubes) from the -70°C.
iv. Thaw components at RT.
v. Add all (11) components to 50:50 bottle, check them off on label from Singlequots pack and affix label to bottle, date, initial & refrigerate.

10. Determine how many vials of cells you will need (2.0×10^6 NHBE cells/vial) to seed the plates. Generally use ~ 1×10^4 cells/well (e.g., 3 6-well plates ≅ 18 wells = 13,888.88 cells/well). Record seed concentration.
    a. **Cells are kept in liquid nitrogen tank**.
    b. **Remember to mark log when you take cells**! (Box 5A)
        i. When retrieving LN_2-frozen cells get an ice bucket with lid. Tubes have been known to burst.
        ii. In hood, partially unscrew cap to make sure no LN_2 is in the threads of the vial. The close tightly again.
        iii. Quickly thaw cells for <u>1 min in 37°C</u> water bath.
        iv. Add cells to pre-warmed tube with "1 ml/well" volume. Pipet twice (gently) to mix.
11. Vacuum-aspirate conditioning media.
12. Add 2ml complete media to wells (use "2ml/well tube) first then add 1 ml cells to each well (or transwell chamber if "Going to Air").
13. Gently swirl plates to get even coverage of the wells. Incubate at 37°C/5% CO_2 ON.

Day 2: Feeding Cells

1. Pre-warm (37°C water bath) 3 ml/well complete media for <u>15-30 minutes.</u>
2. Vacuum-aspirate spent media.
3. Add 3 ml of media to each well (OR 2 ml to bottom + 1 ml transwell chamber if "Going to Air").
4. Gently swirl plates and place back in incubator.
5. Wait two days before feeding cells again. Then feed them daily/every other day until they reach 80-95% confluency (around ~Day 5-7 depending on initial seed concentration).

6. Proceed with experiments OR proceed to "Going to Air" protocol.

Day 7: Going to Air

1. Vacuum-aspirate media.
2. Add 2 ml pre-warmed media to the bottom of well only. Gently swirl plates and return to incubator.
3. **Cells must be fed every day at this point.**

50:50 Media with Additives ≅ Complete Media Components

Additive	*Stock Conc. (M/H)*	*Volume**	*Final Conc.*
Nystatin (in-house, -20°C)	**22,000 U/ml**	**0.5 ml**	**22 U/ml**
BSA (in-house, -20°C)	**1.5 mg/ml**	**0.5 ml**	**1.5 μg/ml**
Gentimicin (C.Sq.)	**50 mg/ml**	**0.5 ml**	**50 μg/ml**
BPE (in-house, -70°C)[€]	**13 mg/ml (65mg)**	**1 vial**	**0.13 mg/ml**
Insulin (C.Sq.)	**5 mg/ml**	**0.5 ml**	**5 μg/ml**
Triiodothyronine (C.Sq.)	**6.5 μg/ml**	**0.5 ml**	**6.5 ng/ml**
Hydrocortisone (C.Sq.)	**0.5 mg/ml**	**0.5 ml**	**0.5 μg/ml**
rhEGF (C.Sq.)	**0. 5 μg/ml**	**0.5 ml**	**0.5 ng/ml**
Transferrin (C.Sq.)	**10 mg/ml**	**0.5 ml**	**10 μg/ml**
Epinephrin (C.Sq.)	**0.5 mg/ml**	**0.5 ml**	**0.5 μg/ml**
Retinoic Acid (in-house, -70°C	**50 mM**	**0.5 ml**	**50 nM**

***Aliquots (Clonetics SingleQuot and in-house) are prepared such that adding the entire volume of 1 tube/vial will yield the correct final concentration in 500 ml of 50:50 DMEM/BEBM Media.**

[€]If no in house BPE is available, use 2.5 vials of BPE from SingleQuot Bullet Kit.

C.Sq. = Clonetics SingleQuot, stored at -20°C in plastic storage bag

Protocol 2: NHBE Cell Harvest & Cryopreservation

1. Aspirate media, rinse T-75 flasks with 8-10 ml PBS buffer.
2. Added 5-8 ml of warm trypsin (thaw in 37°C water bath) to each flask. Incubated at 37°C for 5 min, rocking flask every 1-2 minutes or until most of the cells have detached.
3. Immediately added 5-10 ml of cold Trypsin Neutralization solution to each flask.
4. Transferred cell suspension to a 50 ml conical tubes.
5. Rinsed flasks with 8-10 ml cold HBSS/ flask and add to conical tubes containing cell suspensions.
6. Spun at 4000 rpm for 5 minutes at 4°C.
7. Removed supernatant by vacuum aspiration.

8. Tapped tube to remove clumps prior to adding media to cells.
9. Used ice-cold Expansion media (with high EGF, 25 ng/ml) to resuspend and wash cells. Pool into one tube.
10. Spun cells again at 4000 rpm for 5 minutes at 4°C.
11. Determine cell concentration and viability using Trypan Blue Exclusion Dye (20 µl dye + 20 µl cell suspension). Count with hemacytometer.
12. Resuspended cells to a concentration of 2.0 x 10^6-2.4 x10^6 live cells/ml in Cell freezing Solution (80% BEBM expansion media, 10% DMSO; 10 % Heat inactivated FBS).
13. Made 1 ml cell aliquots. Using 2.0 ml cryotubes with internal threading and silicon gasket.
14. Placed cryotubes inside a Styrofoam cooler; place at -80°C, overnight.
15. Transferred cells to liquid nitrogen storage the next morning.

Protocol 3: Preparation of Swine Confinement Facility Dust Extract

Collecting Swine Unit Dust

1. Scraped or brushed settled dust from raised surfaces into zip lock bags. Collected several grams
2. Secure bags and transport to the laboratory immediately for further processing.
3. Dust must be used the same day it was collected

Preparing Swine Unit Dust Extract

1. Added 1 gram of dust to 10 ml Hank's Balanced Saline Solution without calcium.
2. Vortexed the mixture for 1 minute.
3. Let stand at room temperature for one hour.
4. Centrifuged for 10 minutes at 5,000 rpm at room temperature.
5. Transferred supernatant to a new tube.
6. Centrifuged again according to step 4.
7. Sterilized the final supernatant by filtration (0.22µm filter size).
8. The dust was used immediately.

Protocol 4: Aqueous Sorrel Extract Preparation

1. Add two milligrams of ground lyphollized sorrel calyxes to 20ml of deionized water.
2. Mix for 1hr at 4°C and centrifuge at 17000g for 15 minutes.
3. Remove supernatant and wash pellet with 5ml of deionized water.
4. Centrifuge pellet and wash water at 15,000g for 15minutes and remove supernatant.
5. Pool supernatants and evaporate at 30°C,
6. Store at 4°C until further use for up to two weeks.

Protocol 5: Preparing Mammalian Whole Cell Extracts

1. Placed cells on ice. Labeled microfuge tubes and place on ice.
2. Removed media from cells by vacuum-aspirating and washed gently with 1 ml cold PBS containing Phosphatase Inhibitor (1 ml aliquots at -20°C)
3. While on ice, add 100-200 µl ice-cold "Extraction Buffer" to each well (6 well plate)
    a. To make Extraction Buffer:
        i. Make 1X Cell Signaling Lysis Buffer
            1. Obtain 10X CS LB Stock (500 aliquots at -20°C) dilute with 4.5 ml deionized water.
        ii. Added 870 µl 1X CS Lysis Buffer prepared from (i.) to 100 µl 10X Roche® Complete Protease Inhibitor Cocktail Tablet aliquots (100 µl aliquots stored at -20°C, labeled "PIT").
        iii. Added 970 µl Pre-Extraction Buffer(ii.) to
            1. 10 µl Phosphatase inhibitor Cocktail 1(20 µl stored at 4°C)
            2. 10µl protease inhibitor cocktail 1(20 µl stored at -20°C)
4. Rocked plates on ice and work one plate at a time.
5. Used a cell scraper to scrape wells to one side of the well.
6. Transferred this lysate to the adjacent well. (Clean cell scraper in between samples with 70% ethanol and wipe with a kimwipe)
7. Transferred lysate to appropriate tube and return to ice
8. Sonicated 3 times for 7 second bursts with 1 minute incubations on ice
9. Pelleted debris at 15,000 rpm at 4°C for 15 minutes
10. Transferred supernatant to a clean tube.
11. Determined protein concentration via Bradford Assay

Protocol 6: Bradford Assay

1. Two sets of BSA standards (800, 400, 200, 100, 50, 0 µg/ml) stored at 4 C.
2. The Bradford Reagent Assay Dye (stored at 4° C) 1:4 in deionized water.
3. A 1:30 dilution of each unknown sample in triplicate was prepared using deionized water
4. Added 10 µl BSA standards, 10 µl of unknown sample dilutions
5. Added 190 µl diluted Bradford assay dye to each sample well
6. Read plate using Versamaxx Microplate Reader.

Protocol 7: Western Blot

SDS-PAGE Analysis

1. Added sample buffer to each extract (1/4 volume of 4X or ½ of 2X Laemmli Sample Buffer). Generally used 30-60 µg/ lane of cell extract for mini gels.
2. Boiled samples for 5 minutes.
3. Loaded samples onto SDS-PAGE gel.

4. Ran gel at 115 volts for 1 hour & 20 minutes at RT. (Run gels according to manufacturer's instructions).

Semi-Dry Transfer

1. Soaked 2 pieces of extra thick filter paper and one piece of nitrocellulose in Western transfer Buffer.
2. Made a sandwich (bottom to top) with 1 piece of filter paper, nitrocellulose, gel and 1 piece of filter paper. Place in semi-dry transfer apparatus and run at 10 V for 30-60 minutes.

Wet Tank Transfer

1. Presoaked 2 pieces of extra thick filter paper and one piece of nitrocellulose in ice cold transfer buffer.
2. Made sandwich with 1 filter pad, 1 piece of filter paper, nitrocellulose, gel, 1 piece of filter paper, 1 filter pad. Load into cassette and then into tank. Distribute ice around tank to keep temperature cool. Run gel at 100 V for 60 min.

Blocking

1. Nitrocellulose was removed from sandwich.
2. Blot was placed in 5% milk blocking solution and rocked at room temperature for one hour.
3. Blot was washed with TBS-T for 15 minutes with gentle agitation and washed twice for 5 minutes with gentle agitation.

Primary Antibody

1. Diluted appropriate antibody in TBS-T plus 0.5% BSA. Generally used 1:1000 (i.e. 10 µl antibody in 10 ml TBS-T/albumin).
2. Incubate blot overnight at 4ºC with agitation.
3. Blot was rinsed the following morning with TBS-T for 15 minutes once and washed twice for 5 minutes with TBS-T.

Secondary Antibody

1. Diluted secondary antibody in TBS-T plus 0.5% BSA. Generally used 5µl in 10 ml.
2. Incubated blot for one hour with agitation at room temperature.
3. Blot was washed with TBS-T for 15 minutes with gentle agitation and washed twice for 5 minutes with gentle agitation.

ECL Detection

1. Mixed equal amounts of ECL detection reagents (1-2 ml each per blot). It should come to room temperature before use.
2. Pipetted reagent over entire surface of membrane. Incubated for one minute.
3. Wicked excess liquid off by using dry edge of kimwipe.
4. Membrane was placed in sheet protector.
5. Exposed film to membrane. Exposure times vary depending on antibody and protein source.

Automated Film Development

1. Made developer and fixer. After use wrap container in foil.

a. Developer
    i. 800 ml warm tap water
    ii. 200 ml developer
    iii. Pour into flask and swirl
b. Fixer
    i. 720 ml warm tap water (16ºC to 27ºC)
    ii. 250 ml rapid fixer (solution A)
    iii. 30 ml hardener (solution B)
    iv. Pour into flask and swirl

2. After exposure, film was run through Hope Autovisualizer Processor.

Protocol 8: RNA Extraction from NHBE cells

Before starting

1. Ensure that 10 µl β-ME/1ml Buffer RTL has been added.
2. Ensure that ethanol has been added to Buffer RPE (before initial use).
3. If performing on column DNase digestion protocol, prepare DNase I stock solution. [10 µl DNase I Stock + 70 µl Buffer RDD = 80 µl/rxn]
4. During procedure, work quickly (at RT).

For animal cells grown in a monolayer (do not use more than 1 x 10^7cells). Cells grown in a culture dish may be lysed directly, but cells grown in a flask must be trypsinized and collected in a microfuge tube.

To Lyse Cells

1. Aspirate media.
2. Add Buffer RTL→ Dish diameter <6 cm^2 (12-well dish) = 350 µl; 6-10 cm^2 (6-well dish)= 600 µl
3. Collect cell lysate with a cell scrapper (rubber policeman).
4. Pipet lysate into a microfuge tube and vortex to remove clumps.
5. Homogenize cells by passing lysate at least 5 times through a 20-gauge (0.9 mm diameter) fitted RNase-free syringe (alternatively add lysate to a QIAshredder spin column fitted with a 2 ml collection tube and spin a max speed for 2 min).
6. Add 1 volume (usually 350 or 600 µl) of 70 % EtOH to the homogenized lysate and mix by pipetting.
7. Add up to 700 µl of the sample (including any ppt.) to RNeasy spin column fitted with a 2 ml collection tube. Close tube gently.
8. Spin for 15 sec at ≥8000g (≥10,000 rpm) to wash column. Discard flow-through and collection tube.

On-Column DNase I Digestion

D1. Add 350 µl RW1 to the column and spin 15 sec at ≥8000g (≥10,000 rpm) to wash column.

D2. Add 80 µl DNase mix to the center of each silica-gel membrane. Incubate at RT for 15 min.
D3. Add 350 µl RW1 to the column and spin 15 sec at ≥8000g (≥10,000 rpm) to wash column.

Wash and RNA Elution

9. Add 500 µl Buffer RPE onto column. Close gently.
10. Spin for 15 sec at ≥8000g (≥10,000 rpm) to wash column. Discard flow-through.
11. Add another 500 µl Buffer RPE onto column. Close gently. Spin for 15 sec at ≥8000g (≥10,000 rpm).
12. To dry column, spin at max speed for 1 min.
13. To elute, transfer column to a 1.5 ml microfuge tube and add 50 µl RNase-free water directly to the silica-gel membrane. Close gently.
14. Spin for 1 min at ≥8000g (≥10,000 rpm).

Determine RNA concentration and purity

1. Dilute RNA 1/50 (1 µl sample + 49 µl water).
2. Measure A_{260}.

$A_{260} = 1 \rightarrow 40$ µg RNA/ml

[RNA Sample] = 40 µg /ml x A_{260} x dilution factor

Store RNA at -70°C or proceed with cDNA synthesis.

---

iScript™ cDNA Synthesis Kit (BIO-RAD)

Component	Volume per reaction
5x iScript Reaction Mix	4 µl
iScript Reverse Transcriptase	1 µl
Nuclease-free water	x µl
RNA template* (100 fg to 1 µg Total RNA)	x µl
Total Volume	20 µl

Reaction Protocol
Incubate complete reaction mix:
Step 1 5 min @ 25°C
Step 2 30 min @ 42°C
Step 3 5 min @ 85°C
Step 4 Hold @ 4°C (optional)

*When using larger amounts of input RNA (> 1µg) the reaction should be scaled up, e.g. 40 µl for 2 µg, 100 µl for 5 µg to ensure optimum synthesis efficiency.

Protocol 9: cDNA Synthesis

1. Determine RNA concentration using Nanodrop (Thermoscientific)
2. For each RNA sample, combine the following in a PCR reaction tube:

Reagent	Amount	
5x iScript Reaction Mix	4 µl	→ 4 µl
Total RNA Template**	1 µg	→
iScript Reverse Transcriptase	1 µl	→ 1 µl
Nuclease-free water	q.s. 20 µl	→

3. After, RNA and samples are added run the following program on thermocycler (Biorad):

RT Reaction Protocol:
Step 1 5 min @ 25°C
Step 2 30 min @ 42°C
Step 3 5 min @ 85°C
Step 4 Hold @ 4°C (optional)

4. cDNA was stored at -80°C until further use.

Protocol 10: Gene Expression Profile Analysis

1. For each RNA sample complete the following chart:

Reagent	Amount	
Kapa Sybr Green	10 µl	→ 10µl
Total RNA Template**	1 µg (can use as little as .2µg)	→
Qiagen one-step RT-PCR reverse transcriptase+ cDNA amplifier	1 µl	→ 1 µl
Primer A	1µl	→1µl
Primer B	1µl	→1µl
Low ROX control	.4µl	→.4µl
High ROX control	.4µl	→.4µl
Nuclease-free water	q.s. 25 µl	→

2. Use the following program on a real time thermocycler:

RT Reaction Protocol:

Step 1	30 min @ 50°C
Step 2	16 min @ 95°C
Step 3	1 min @ 55°C
Step 4	11min @ 72°C

# of cycles = 40

*The maximum amount of the cDNA reaction that is recommended for downstream PCR is one-tenth of the reaction volume, typically 2 µl.

**When using larger amounts of input RNA (> 1µg) the reaction should be scaled up, e.g. 40 µl for 2 µg, 100 µl for 5 µg to ensure optimum synthesis efficiency.